Plant Protection Products in Sediments of a Swiss Pond: Breaking down PPP Contamination in Lobsigensee, Switzerland

Master thesis
Faculty of Science, University of Bern

handed in by

Emmanuel Schaad

2022

Supervisor:

Prof. Dr. Aurea C. Chiaia-Hernández R.

Co-supervisor:

Prof. Dr. Martin Grosjean

Emmanuel Schaad
Hopfenweg 23
3007 Bern, CH
emmanuel.schaad@students.unibe.ch
Matriculation Nr.: 17-105-388

Imprint

Acknowledgements

This thesis was only possible because of the immense support from numerous people, to which I would like to express my gratitude. First of all, many thanks to my supervisor Aurea Chiaia-Hernández; she introduced me to the topic of organic contaminants in aquatic ecosystem and I could profit and learn a lot from her vast knowledge on environmental pollution in connection with lakes and ponds. Many thanks also to my co-supervisor Martin Grosjean; it was him who got me into paleolimnology in the first place and who encouraged me to do a Master thesis in his group. His inputs and thoughts were of great importance throughout the project and I was able to grow my knowledge in this field of science. Then I would like to thank Giulia Wienhues, Paul Zander and Nayan Gosain for assisting me in the lab and introducing me to all the different paleolimnological methods. Further thanks go to Hendrik Vogel for conducting the X-ray fluorescence (XRF) measurements, Pascal Rünzi for the γ spectrometry measurements and Matthias Ruff for letting me measure my samples on the high resolution mass spectrometer (HRMS) at the water and soil protection laboratory Bern.

All data is available on the server of the Paleolimnology Group of the Institute of Geography, University of Bern, CH.

Abstract

In this thesis, I report on the temporal and spatial quantification of synthetic plant protection products (PPPs) and their deposition patterns in the sediments of Lobsigensee, a polytrophic Swiss pond under agricultural pressure. PPPs are widely applied in Swiss agricultural practices, with no holistic understanding of potential pathways and environmental fate of these chemicals. With a changing precipitation regime and longer lasting dry periods due to climate change, PPP transport from source to sink might also be altered. But unlike water, the sediments of lentic water bodies have been neglected in recent studies on potentially contaminated compartments. And while the ecological importance of ponds is undisputed, these smaller sites have been largely overlooked in monitoring programs and in-depth studies.

In my study, I applied a paleolimnological approach using hyperspectral imaging (HSI) and X-ray fluorescence (XRF) proxies coupled with organic pollution analysis using high-performance liquid chromatography coupled to a tandem mass spectrometer (HPLC-MS/MS) to track the temporal deposition patterns of PPPs in the sediments of Lobsigensee. For the first time in a Swiss pond, spatial samples are taken and analyzed in the context of catchment cultivation and artificial drainage to reveal main sources and pathways. In the sediment core of Lobsigensee, 26 contaminants including 24 PPPs and two transformation products (TPs) were detected throughout the last 70 years. Detected fluxes range from 10 pg/cm^{2}yr to 4200 pg/cm^{2}yr. Sediment description together with XRF and HSI proxies revealed the ongoing eutrophication of the pond. This process is accompanied with more PPPs being deposited in the sediments in recent years despite less input. Thus, in the catchment of Lobsigensee, reduced PPP fluxes are independent of clastic input but were found to correlate with bans and reduced sales of agents in Switzerland. Individual chemical properties such as low K_{oc} values of PPPs might lead to a higher mobility in the sediments or even resuspension due to sediment disturbance events.

Spatially, 26 substances including 23 PPPs and 3 TPs have been detected in samples taken across the whole pond, in the reed belt and at the outflow. The spatial analysis of PPP further revealed the importance of artificial drainage lines. The latter were found to short-circuit PPP from locations where PPP applications is assumed to be high (e.g. tree nurseries). The presence of such a drainage network might also undercut the protection effect of a natural reed belt around the pond, such as the one present at Lobsigensee. Correlation with land cultivation registers showed good agreement with applied chemicals and the findings in the sediments. This indicates the main sources to be within the catchment with little to no external atmospheric transport of PPPs.

Overall, my study showed the contamination of a neglected matrix of smaller aquatic ecosystems to be a reality, adding to findings of other Swiss sites. At the same time, my study showed the complex nature of PPP transport from agricultural practices to the deposition in the sediments. For Lobsigensee, it revealed the major constituents in the PPP transport scheme to be drainage lines and surface runoff. Preservation in the sediments was then attributed to prevailing anoxic conditions in the hypolimnion due to the strong eutrophication. Outflow locations of drainage lines were also found to induce peak concentrations of PPPs. I therefore highlight the need to impose further mitigation strategies to reduce PPP influx to these precious environments. Furthermore, my study shows the need to include sediments in risk assessment studies and subsequent approval processes of new substances.

Keywords:
sediments, ponds, plant protection products, high-performance liquid chromatography, tandem mass spectrometry, hyperspectral imaging, X-ray fluorescence

Contents

List of Figures vi

List of Tables vii

List of Abbreviations vii

1 Introduction 1
- 1.1 Problem Statement . . . 1
- 1.2 State of Research and Opening the Research Gap . . . 2
  - 1.2.1 Evolution of PPP Implementation . . . 2
  - 1.2.2 Classification and Applications . . . 2
  - 1.2.3 PPPs and TPs as Environmental Pollutants . . . 2
  - 1.2.4 On the Importance of Ponds . . . 4
- 1.3 Objectives and Research Questions . . . 5

2 Study Site 6
- 2.1 Location . . . 6
- 2.2 Geology . . . 6
- 2.3 Climate . . . 7
- 2.4 Land Use . . . 7
- 2.5 Hydrology, Bathymetry and Drainage . . . 9
- 2.6 Water Chemistry and Ecological State . . . 11
  - 2.6.1 Depth Profiles and Nutrients . . . 11
  - 2.6.2 Plant Protection Products and Transformation Products . . . 12

3 Material and Methods 14
- 3.1 Sampling Procedure . . . 14
- 3.2 Working Sequence of Sediment Core Analysis . . . 15
- 3.3 Non-destructive Analysis . . . 16
  - 3.3.1 Sediment Description . . . 16
  - 3.3.2 X-Ray Fluorescence Scanning . . . 16
  - 3.3.3 Hyperspectral Imaging . . . 16
- 3.4 Age-Depth Modelling and Core Correlation . . . 18
- 3.5 Destructive Analysis . . . 19
  - 3.5.1 Subsampling of Cores . . . 19
  - 3.5.2 Loss On Ignition . . . 19
  - 3.5.3 CNS Analysis . . . 20
- 3.6 PPP Analysis . . . 20
  - 3.6.1 Preparation of Sediment Core Samples . . . 20
  - 3.6.2 Detection by LC-MS/MS and HRMS . . . 20
  - 3.6.3 Quality Control . . . 21
- 3.7 Surface Sediment Analysis . . . 22
- 3.8 Data Analysis . . . 22
  - 3.8.1 Normalisation, PPP Fluxes and Hierarchical Agglomerative Clustering . . . 22
  - 3.8.2 Ecological Risk Assessment . . . 23

4 Results and Discussion 25
- 4.1 Sediment Description . . . 25
- 4.2 X-Ray Fluorescence Scanning . . . 26
- 4.3 Hyperspectral Imaging . . . 29
- 4.4 Age-Depth Modelling and Core Correlation . . . 30

4.5 LOI and CNS . . . 32
4.6 Temporal PPP Analysis . . . 32
4.6.1 Detected Compounds, Concentrations and Fluxes . . . 32
4.6.2 Hierarchical Cluster Analysis of PPPs . . . 34
4.6.3 Results from HRMS Peak Picking . . . 35
4.7 Temporal Ecological Risk Assessment . . . 37
4.8 Spatial PPP Analysis . . . 38
4.8.1 Detected Compounds . . . 38
4.8.2 Grain Size and Concentration Mappings of PPPs . . . 39
4.8.3 Correlation of PPPs and Cultivation Register . . . 41
4.8.4 Comparison of TPs in Sediments of Lobsigensee with previous Studies . . . 42
4.8.5 Comparison of PPPs in Sediments of Lobsigensee with other Ponds . . . 43

5 Conclusions **44**
5.1 Recent Catchment Development of Lobsigensee . . . 44
5.2 Temporal PPP Record and Sediment Quality . . . 44
5.3 Spatial Deposition Trends of PPPs . . . 45
5.4 Transformation Products - Friend or Foe? . . . 46
5.5 Proposed Mitigation Strategies of PPP Contamination . . . 46
5.6 Insights and Future Research . . . 47

References **48**

Appendices **55**

Appendix A Subsampling Procedure and Measurement Data **55**

Appendix B Dating, MAR, Age-Depth Modelling, Code of Core Correlation **61**

Appendix C Dionex ASE 350 Extraction Accuracy **66**

Appendix D Standard Operation Protocol: LOI **68**

Appendix E Standard Operation Protocol: CNS **75**

Appendix F Standard Operation Protocol: Extraction and Preparation of Samples for LC-MS/MS **81**

Appendix G Standard Operation Protocol: Grain-Size Distribution **114**

Appendix H R Code HCA, Flux Plots and Risk Assessment **118**

List of Figures

1 Important applications and major pathways for pesticide transport into surface waters . . . 3
2 Geographical location of the study site and aerial overview. . . . 6
3 Geological map of the study site. . . . 7
4 Catchment composition of Lobsigensee. . . . 7
5 Agricultural land use in the catchment of Lobsigensee. . . . 8
6 Cultivation Register of the catchment of Lobsigensee. . . . 9
7 Bathymetric map of Lobsigensee. . . . 10
8 Drainage grid at Lobsigen with additional inlet shafts. . . . 11
9 Concentrations of pesticides in the water column of Lobsigensee, 2013. . . . 12
10 Concentrations of transformation products in the water column of Lobsigensee, 2013. . . . 13
11 Coordinates of coring site and surface sediment samples. . . . 14
12 LOB21-3B core image. . . . 25
13 Summary diagram of the smear slide analysis. . . . 26
14 X-Ray fluorescence (XRF) data on clastic proxies. . . . 27
15 X-Ray fluorescence (XRF) data on organic proxies. . . . 28
16 Summary plot of hyperspectral imaging (HSI) data. . . . 29
17 Activity plots resulting from γ-spectrometry. . . . 30
18 Fitted activity of unsupported ^{210}Pb and fitted unconstrained CRS model. . . . 31
19 Composite CRS model of Master Core LOB21-2. . . . 31
20 Correlation of the master core LOB21-2 to core LOB21-3 used for PPP analysis. 31
21 Down-core results of loss on ignition (LOI) and carbon/nitrogen/sulphur (CNS) analysis. . . . 32
22 Down-core evolution of fungicide fluxes in sediments of Lobsigensee. . . . 33
23 Down-core evolution of herbicide fluxes in sediments of Lobsigensee. . . . 33
24 Down-core evolution of insecticide, metabolite and herbicide safener fluxes in sediments of Lobsigensee. . . . 33
25 Dendrogram resulting from Hierarchical Cluster Analysis performed on scaled PPP flux values. . . . 34
26 Vertical normalised fluxes sorted by hierarchical cluster analysis. . . . 35
27 HRMS peak picking done in QualBrowser showing the identifications used for nontarget analysis with desaminometamitrone as example. . . . 36
28 Summed up risk quotient for the three main pesticide types. . . . 37
29 Mean concentrations of PPPs detected in pond surface sediments. . . . 38
30 Mean concentrations of PPPs detected in reed belt sediments and outflow sediments. 38
31 Spatial grain size distribution at Lobsigensee. . . . 39
32 Interpolation of PPP concentrations of selected compounds together with grain size data and drainage entries to the pond. . . . 40
33 Maize and potato cultivation in the region of the pond based on the year 2021. . 42
34 Comparison of catchment composition of Lobsigensee to other ponds. . . . 43
35 MAR and definite CRS Models of core LOB21-2 with comparison of different constrained CRS models. . . . 61
36 Volume extract consistency of the Dionex ASE 350. . . . 66

List of Tables

1 Coordinates and lengths of sediment cores from Lobsigensee. 15
2 Terms used to calculate the relative absorption band depth (RABD). 17
3 Effect-based risk evaluation scheme of water quality from micropollutants. 24
4 Excerpt of detected PPPs together with applied plantation types. 41
5 Measurements taken during subsampling of the core for PPP Analysis. 56
6 Measurements and calculations from LOI and CNS for the core LOB21-3. 57
7 HPLC-MS Data from core LOB21-3. 58
8 Locations and measurements and calculations from LOI and CNS for the surface sediment samples. 59
9 HPLC-MS Data from surface sediment samples. 60
11 Solvent densities used for the calculation of extraction volumes. 66
12 Weight measurements and calculated values of extraction volumes. 67

List of Abbreviations

Bchl a	Bacteriochlorophyll-a
Bphe a	Bacteriopheoyphytin-a
CNS	Carbon, Nitrogen, Sulphur
GSD	Grain size distribution
HCA	Hierarchical cluster analysis
HPLC	High performance liquid chromatography
HRMS	High resolution mass spectrometry
HSI	Hyperspectral imaging
LOD	Limit of detection
LOI	Loss on ignition
LOQ	Limit of quantification
MAR	Mass accumulation rate
MEC	Mean environmental concentration
MESA	Metolachlor ethanesulfonic acid
MOA	Metolachlor oxanilic acid
PPP	Plant protection products
QQQ	Triple Quadrupole
QuECHERS	Quick, Eay, Cheap,Effective, Rugged, Safe
RABD	Relative absorption band depth
RQ	Risk quotient
RT	Retention time
TP	Transformation products
WWTP	Waste water treatment plant
XRF	X-ray fluorescence

1 Introduction

1.1 Problem Statement

Over the last 70 years, human population has increased from a little above 2.5 billion to 7.7 billion in mid-2019. It is projected to further increase to 10.9 billions by the end of the century (United Nations, 2019). In present days, the agriculture sector is under pressure to not only feed this ever-growing population but also meet cereal production demand for the increasing meat production. Furthermore the total food demand is accompanied by food loss and waste. Together with a change in dietary preferences, the agricultural sectors is pressured in keeping production rates high thus resorting to the usage of pesticides during cultivation of crops (Mateo-Sagasta et al., 2018). The population increase is accompanied by anthropogenic climate change affecting both humans and natural environments alike (IPCC, 2014). Lakes are thereby strongly affected as variable catchment processes and changes in climate may alter the ecological state of the reservoir. Effects of anthropogenic and climatic pressure may include eutrophication with subsequent algal blooms or hypoxia (Chislock et al., 2013), fish extirpations (Jeppesen et al., 1998) or changes in the mixing and stratification regimes (Woolway & Merchant, 2019). Changes in rainfall patterns including extreme weather events at higher frequencies are able to trigger rapid pesticide transport through preferential flow or surface run-off from fields to water bodies (McGrath et al., 2010; Schönenberger et al., 2022). Regarding aquatic reservoirs, plant protection products (PPPs) are among the major pollutants from agricultural activity further harming these ecosystems (Mateo-Sagasta et al., 2018, p. 45).

While the utilisation of chemicals to combat and control crop threatening organisms has been around for millennia, synthetic agents such as phosphate fertilisers have only emerged in the 1940s to sustain food production during the population increase in the 20th century (Carvalho, 2017; Gilland, 2015). At that time up until the 1980s little to no concerns were made about probable contamination of water sources through the application of such chemicals. But in the last few decades, it has been shown that PPPs do end up in the environment. They do so by primarily entering groundwater by seepage from agricultural fields after application (Postigo & Barceló, 2015), thus threatening drinking water resources, deteriorating water quality and losses in biodiversity of aquatic ecosystems (Kiefer et al., 2020; Sánchez-Bayo & Wyckhuys, 2019; Stehle & Schulz, 2015).

But while deposition processes of PPPs and their behaviour in different compartments (e.g. water (Doppler et al., 2017; Moschet et al., 2014), food or plants (Carneiro et al., 2013; Del Prado-Lu, 2015)) have been extensively studied in the last decades, lake sediments have been largely neglected in the consideration about possible contaminated matrices. It is primarily the limnic or fluvial water that is analysed in studies. Reason being the complex process of sediment analysis and the yet absent connection to paleolimnological methodology regarding chronology production and investigation on depositional patterns (Chiaia-Hernández et al., 2020). Previous work regarding PPP contamination of small lacustrine environments however have shown the urgent need to address the pesticide pollution in these biotopes (Chiaia-Hernandez et al., 2014; Chiaia-Hernández et al., 2020; Fahrni, 2021). Furthermore, the transformation products (TPs) resulting from degradation or sorption processes have been overlooked in studies due to insufficient analytical method, lack of of reference material or registration data of parent pesticides (Kiefer et al., 2020). This data is needed to assess pesticide transport from source to sink along with their fate including TPs and to help improve the ecological state of small but important aquatic environments providing ecosystem services. Additionally, effects of governmental legislation on pesticide types and usage can be studied by analyzing temporal trends.

Based on these observations, this thesis aims at adding knowledge on PPP and TP contamination in small lentic water bodies by examinating sediments of the pond Lobsigensee located in central Switzerland.

1.2 State of Research and Opening the Research Gap

1.2.1 Evolution of PPP Implementation

The concept of using pesticides to protect and control crops has been used before 2000 BC, when the Ancient Greeks and Mesopotamians applied sulphur as a fungicide (Mohaupt et al., 2020, p. 25; Srivastava et al., 2019). Before the 20th century, chemicals containing arsenic, mercury and lead were primarily being used to combat pest organisms (Srivastava et al., 2019). The rapid population increase in the 20th century was accompanied by the introduction of mineral phosphate fertilizers to sustain agriculture productivity (Gilland, 2015). Synthetic pesticides were introduced from the 1940s onwards, thereby further allowing an elevation of yield, coined "green revolution", and global pesticide production and application increased significantly (Carvalho, 2017).

Subsequently, studies were released reporting on the intoxication of farming personnel as a result of excessive exposure and unsafe handling of the toxic chemicals (Alavanja, 2009; Carvalho, 2017). Following these findings, the use of many of these early-stage persistent compounds (e.g. organochlorine crop chemicals such as DDT, HCH, toxaphene, aldrin) was discontinued and subsequently prohibited and superseded by more environmentally friendly products (Bouwman et al., 2013; Carvalho, 2017).

Depending on governmental regulations these chemicals are applied either manually by spraying on foot or by vehicles and aerial spraying by air planes. In Switzerland, PPPs are predominantly applied by mobile spraying units in the field. Aerial spraying is only possible after a specific approval from the Federal Office of Civil Aviation (BAFU, 2016).

1.2.2 Classification and Applications

The terms "pesticide" and "plant protection product" are often used as synonyms, however strictly speaking, PPPs are a subgroup of the more general expression "pesticides". The common use of the term pesticide however is mostly used to describe any type of vermin threatening crop yield in agriculture. The Food and Agriculture Organization of the United Nations (FAO) describes PPPs as pesticides "intended for preventing, destroying or controlling any pest causing harm during or otherwise interfering with the production, processing, storage, transport or marketing of food, agricultural commodities, wood and wood products" (Food and Agriculture Organization FAO, 2010, p. 7). The applications of PPPs therefore go beyond spraying in the fields but also include treatment of fruits and vegetables once harvested and stored to prevent premature expiration resulting from diseases.

1.2.3 PPPs and TPs as Environmental Pollutants

Pollution of aquatic ecosystems may originate from point sources and non-point sources, the latter also being called diffuse pollution. PPPs may stem from livestock farms, industries or private households entering the wastewater, which is then collected by a waste water treatment plant (WWTP), as described by ❹ to ❻ in Figure 1. From there the chemicals can be released into natural streams through the WWTP effluent. Since the entry point of the PPPs in this scenario can be identified, it is described as a point-source pollution (Mateo-Sagasta et al., 2018). On the contrary, diffuse sources (such as ❶ in Figure 1) include spray-drift from direct application, surface run-off during cleaning of equipment or leachate to field drains and groundwater and surface erosion (Mohaupt et al., 2020; Sandin, 2017). Some major pathways of PPPs into the environment are shown in Figure 1. Hereby, ❷ and ❸ can also be understood as diffuse source if the wastewater is not collected but rather introduced to the environment directly through surface run-off.

Whether the PPPs remain in the water is depending on their solubility, mobility and biodegradability (Mateo-Sagasta et al., 2018). Many early-generation PPPs (e.g. organochlorides

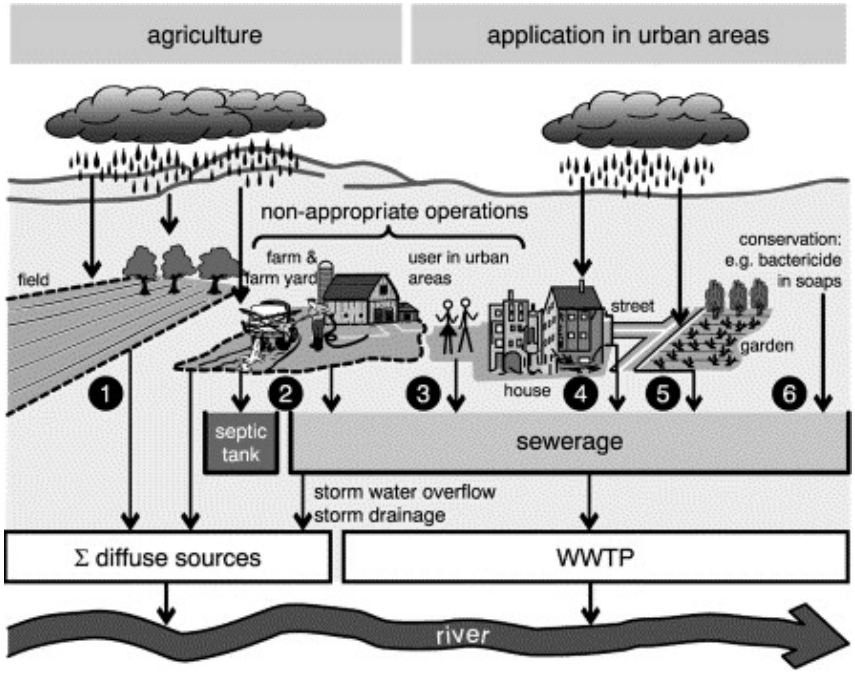

Fig. 1: Important applications and major pathways for pesticide transport into surface waters: ❶ Field: spray drift during application, surface run-off and leaching with subsequent transport through drainage channels during rain events. ❷ Farm and farmyard: improper operations (e.g., filling of sprayers, washing of measuring utilities, disposing of packing material, driving with seeping sprayers, cleaning of spraying equipment). These operations are done either at locations which are drained to the sewerage, to the septic tank or into surface waters. ❸ Like ❷ for pesticide users in urban areas. ❹ Pesticides in building material: leaching during rain events. ❺ Applications on lawns, streets, road embankments: run-off during rain events. ❻ Protection of materials: e.g. products containing antifouling ingredients that get into the sewerage (e.g. detergents, cosmetics) (Gerecke et al., 2002).

such as DDT, HCH, aldrin) have been denoted as environmentally persistent with residues remaining in soils and sediment up to weeks and even years (Carvalho et al., 2002).

Whilst these compounds have been banned several decades ago, traces of legacy compounds can still be detected hinting at the past applications (Carvalho, 2017). Once entered into water bodies, PPPs may remain suspended in the water, can be subjected to photodegradation, chemical or microbial degradation, adsorb to other particles or enter sediments through pore water transport (Eggleton & Thomas, 2004; Gavrilescu, 2005). While these processes suggest that aquatic ecosystems and sediments may act as permanent sinks of PPPs, this is not entirely the case. For example, it has been shown that PPPs can be remobilized by either a change in redox conditions in the sediment, through lakebed disturbance events or as a result of bioturbation (Eggleton & Thomas, 2004; Granberg et al., 2008). Hereby, solubility and adsorption behaviour - the latter being determined by pH, polarity and size - are among the most important physical-chemical properties determining the fate of these compounds in the environment (Gavrilescu, 2005; Pereira et al., 2016).

These characteristics are often described through partition coefficients, describing the preferred behaviour of the chemicals. One such measure of adsorption tendency is the so-called Soil Colloid Adsorption Coefficient (K_d), which is the ratio of the concentration adsorbed by the soil to the concentration of the compound present in water. The Organic Carbon-Water Partition Coefficient (K_{oc}) is a modified version of K_d and is normalised to the soil organic carbon content (dos Reis et al., 2013; Gavrilescu, 2005). Here, a higher K_d or K_{oc} implies a stronger adsorption of chemicals to the soil, whereas a low coefficient means that the compound is preferably present in the aqueous phase (Pereira et al., 2016).

Yet another measure is the n-octanol/water partition coefficient (K_{ow}) used to describe hydrophobic molecules. It is denoted as the equilibrium ratio of concentration in octanol to the concentration in water. K_{ow} is an indicator of hydro- and lipophilicity. The ratio describes the affinity of the compound towards the polar water phase or the non-polar octanol phase. Non-polar and lipophilic PPPs showing high K_{ow} values ($\log K_{ow} > 4$) have a greater tendency to be attached to lipids and are therefore more capable to bioaccumulate in organisms (Connell, 1988; Pereira et al., 2016). However, these characteristics are only one aspect of the prediction of PPP transport and pathways after application in the field. Other factors including catchment characteristics play an important role as well. These may include soil properties such as porosity, the presence of subsurface drainage systems but also precipitation patterns in the catchment, especially during the first subsequent days following the application (Leu et al., 2004a, 2004b).

While the use of PPPs in Switzerland is regulated and new chemicals undergo a specific admission procedure, their metabolites have been overlooked in monitoring studies. Three main reasons are listed by Kiefer et al. (2020): i) lack of reference material for TPs, ii) inappropriate analytical methods and iii) the difficulty to obtain pesticide registration data, which is either hard to get or not available at all. However, it has been shown that these TPs often are even more persistent in the environment and can be more mobile than the original compound (Buttiglieri et al., 2009). An example is the detection of the chlorothalonil TP R471811, which in Switzerland was detected for the first time in ground water samples in 2019 (Kiefer et al., 2020). From their work, its concentration is expected to increase due to its high persistence. Furthermore due to its chemical structure and high polarity, current advanced treatment methods may not be full able to degrade the compound. Additionally, the work done by Chiaia-Hernández et al. (2020) revealed several hundred unknown organic contaminants in a nontarget screening of sediments from Moossee in Switzerland which include TPs from pesticides. This stresses the need for a more comprehensive examination of the fate of PPPs in the environment by not only addressing the active substance but also the characteristics its metabolites including both persistency and ecotoxicity of these TPs.

1.2.4 On the Importance of Ponds

It has long been recognized that ponds are different from larger bodies of water in terms of ecological process due to the absence of the deep aphotic zone (Forel, 1904). There are numerous characteristics constituting to ponds, all connected to size, depth, formation, usage or water quality (Oertli et al., 2005). While there have been proposed size restrictions of 1 m^2 to 5 ha, the upper limit of total area is not distinctly defined (Meester et al., 2005; Oertli et al., 2005). In the work done by Oertli et al. (2000), a pond is specified as "a body of water with a maximal depth of 8 metres, which allows water plants to colonise the greater part of the pond floor"[1]. Ponds can be either man-made (e.g. by filling up construction pits, water storage) or naturally through various processes such as deglaciation, changes in river flow or land subsidence. Small lentic water bodies are especially prone to pesticide contamination, since they are often located in close proximity of agricultural soils and have a lower water volume and less discharge capacity. As a result, the reduced ability of small water bodies to dilute substances may lead to even higher pesticide concentrations in the water (Lorenz et al., 2017). These ponds however are ecosystems of great importance regarding biodiversity supporting overall more species and more unique species compared to other water-bodies (Williams et al., 2004).

While larger lakes are monitored and studied more frequently, the opposite is true for smaller lakes and ponds, where prioritization is needed due to the sheer number of water bodies (K. Guthruf et al., 2015). By selecting a pond as study sites rather than a larger lentic water body, this thesis aims at providing new data for ecosystems which substantially lack paleolimnological organic contamination data.

[1] Translated from French off Oertli et al. (2000, p. 31)

1.3 Objectives and Research Questions

In light of the scientific state on contamination in sediments of small lakes the work in the scope of this thesis focuses on providing a historical record of PPPs in down-core and spatial sediments to quantify PPP contamination in the pond Lobsigensee located on the Central Swiss Plateau. Furthermore, a focus is set on assessing TP occurrence and potential pathways of these compounds into the lake. The record is obtained by applying a multiproxy paleolimnological workflow which has already successfully been applied for a study at Lake Moossee (Chiaia-Hernández et al., 2020). Furthermore, the thesis done by Nicole Fahrni has successfully shown that this approach can equally be applied to pond sediments (Fahrni, 2021). By additionally exploiting the potential of high resolution mass spectrometry (HRMS), non-target suspect screening is applied to detect potential TPs in the sediments.

The personal goal of this thesis is to acquire the technical expertise to conduct a full-scale paleolimnological study from start to finish, whereas the scientific objectives are:

(a) To gain an understanding of appearance and implications of PPPs and TPs in small eutrophic ponds under agricultural pressure.

(b) To provide a historical record of PPPs in sediments to show that sediment studies are of great importance for the assessment of PPP distribution and contamination in smaller water bodies.

(c) To indicate the important ecological role of ponds in terms of exposure to PPPs.

The Research Questions of this Master Thesis are formulated as follows:

i. How do PPP concentrations extracted from sediments of Lobsigensee, CH, vary in the historical record?

ii. How are PPP concentrations spatially distributed in surface sediments of Lobsigensee, CH?

iii. How do the PPP profiles in the sediment compare with PPP sales in Switzerland and political measures?

iv. What are the ecological risks of the detected PPPs?

v. Do PPPs in the sediment reflect catchment use and what are their main entry paths into the lake?

vi. How findings in the sediment of Lobsigensee relate to previous results from studies done on the water column?

2 Study Site

2.1 Location

Lobsigensee (WGS 84: 47°01'50.18"N 7°17'52.79"E) is a polytrophic exorheic kettle hole lake located 14 km Northwest of the city of Bern between Lobsigen and Seedorf, as seen in Figure 2. It is situated at an elevation of 514 m.a.s.l. in a recessed plateau of the tertiary Molasse between the hill range of Frienisberg and a Würm moraine wall. The pond has a current surface area of $A = 1.73$ ha and a reported maximum depth of 2.5 m (J. Guthruf et al., 1999, p. 126). At present however, the depth was measured to be 3.9 m. Lobsigensee has no surface inflow and only one outflow stream called Seebach. Although naturally eutrophic, anthropogenic drainage of the catchment and subsequent agricultural activities led to over-fertilization and a polytrophic state (J. Guthruf et al., 1999, pp. 126 sq.). The landscape surrounding the lake is dominated by agricultural land followed by settlements with tree nurseries and isolated groves.

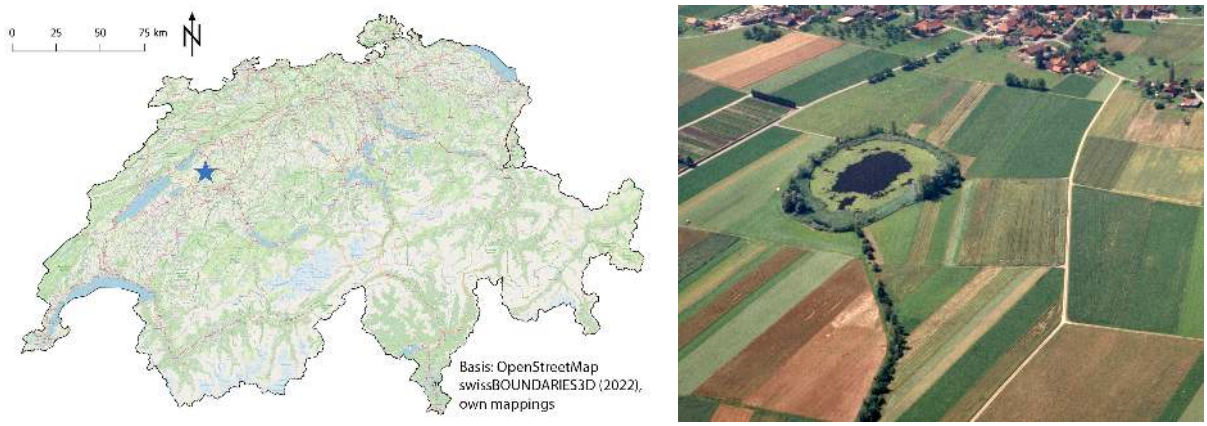

Fig. 2: Geographical location of the studysite and aerial overview (Source: own illustration backed with OpenStreetMap). Left: Location of Lobsigensee in CH. Right: Lobsigensee with outflow Seebach and the town of Lobsigen in the background, direction of view southwestwards. (Source: Zeh, 2003).

2.2 Geology

The pond is situated in a small tectonic depression of the Molasse basin North of the Alpine chain. This Molasse basin in general is composed of the Tertiary sequence consisting of Lower Marine Molasse, Lower Freshwater Molasse, Upper Marine Molasse and Upper Freshwater Molasse (Burkhard & Sommaruga, 1998). The Lower Freshwater Molasse assigned to the Aquitanian is hereby forming one of the main basal sediment containing sandstone and marl (Ammann & Tobolski, 1983). It is exposed along the slopes of the creek to the South of the lake and along the slope of the hill Southeast of the lake, as mapped in Figure 3. During the Würm glaciation, the study site was covered by the Rhone glacier, with its northeastern-most lobe extending up to the 27 km distant Solothurn. During the retreat of the ice masses, the lake developed in the depression from broken off pieces of the glacier. Alongside the development of kettle hole lakes, the landscape got covered by glacial till. Thus the main fraction of topmost sediment are ground moraines of the Würm period, as mapped in Figure 3. The hill separating the pond from the town of Aarberg is thereby shaped from piled up glacial till forming a moraine wall, denoted as brown dots in Figure 3. The depression in which the pond is situated is sealed from lower layers by glacial clays (von Büren & Leiser, 1961). The dominant soil type formed on the Bernese Central Plateau after de-glaciation are para-brown soils consisting of the characteristic sequences of A-E-Bt-C-Horizons of Cambisols and Luvisols (Veit & Gnägi, 2014). On the immediate surroundings of the lake and further downstream of the outflow, more recent alluvial

soils developed.

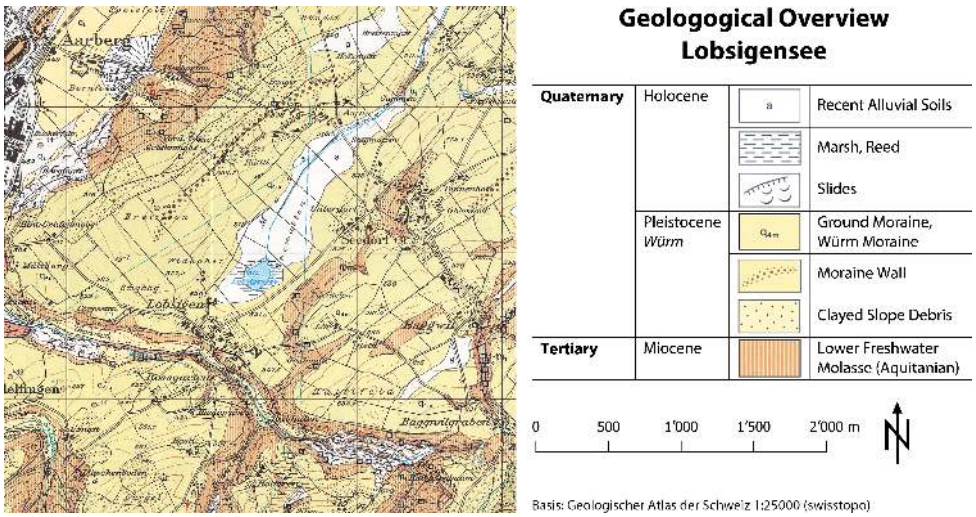

Fig. 3: Geological map of the study site. It shows the dominant type of sedimentary rocks to be moraine material from the Würm glaciation, with partly exposed Lower Freshwater Molasse on steeper slopes. Around the lake and the outlet alluvial soils developed. (Source: Kellerhals and Tröhler, 1981).

2.3 Climate

Switzerland lies in the temperate climate zone and the climate on the Swiss Plateau is strongly influenced by the Atlantic Ocean. Wind currents predominantly from the West transport mild humid air to Switzerland. This leads to a cooling in the summer and mild and damp winters (MeteoSchweiz, 2018). According to the classification of Köppen and Geiger, this type of climate is denoted as Cfb (marine west coast climate) (Beck et al., 2018). The mean annual temperature in Lyss, 6 km North of the study site, is 9.6 °C while average annual precipitation amounts to 1236 mm (Climate-data.org, 2021). Warmest month is July with 18.7 °C on average while the coldest temperatures occur in January with just 0.6 °C.

2.4 Land Use

With a share of 84 percent of the catchment area, agricultural fields make out the dominant fraction of land use around Lobsigensee, as shown in Figure 4. The remaining area is a mixture of unproductive land, settlements, groves or rocky terrain. Thereby the lake itself denotes only 2 percent of the whole catchment area.

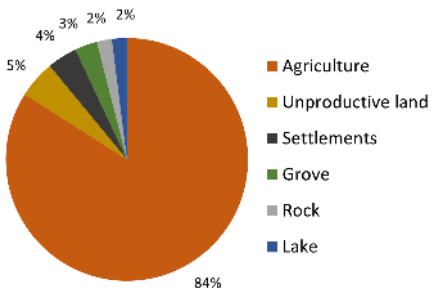

Fig. 4: Catchment composition of Lobsigensee. (Source: adapted from J. Guthruf et al., 1999)

The immediate surroundings of the lake are taken up by a wetland belt ranging from 10 to 40 m in width with a larger area around the outflow. Lobsigensee shows the typical sequence of a

floating leaf zone (*Nypmhaeion*) on the open water, followed by reeds (*Phragmition*) developing into tall sedge meadows (Ammann & Tobolski, 1983; J. Guthruf et al., 1999). There are single stands of black alder trees *Alnus glutinosa* located on the Northeastern edge of the lake, however field surveys have shown that the larger specimens have all died off, seemingly due to the prolonged high water stand in recent months. The lake and its belt around it have been protected since 1955 (Dubler, 2008). Accordingly, it is clear that the land is not cultivated with crops all the way to the shore. The adjacent area is exclusively used as permanent meadows, as seen in Figure 5. These meadows are mown at least once a year for forage production (Bundesamt für Landwirtschaft BLW, 2017). The agricultural land register further shows that the catchment of Lobsigensee is primarily cultivated arable fields, followed by orchards and permacultures.

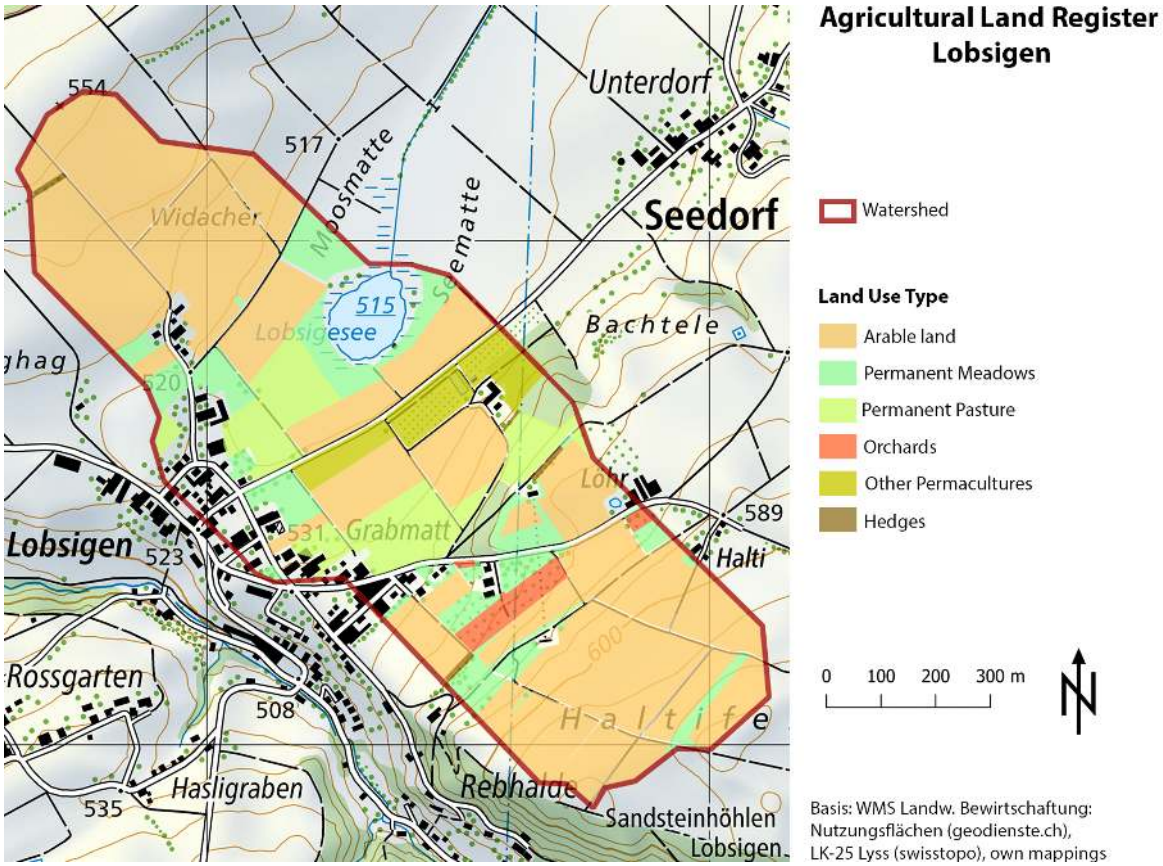

Fig. 5: Agricultural land use in the catchment of Lobsigensee. It shows that arable fields are the dominant type of land use around the small lake. A belt of uncultivated meadows surrounds the shoreline. (Landw. Bewirtschaftung: Nutzungsflächen WMS 2021 (geodienste.ch) backed with LK25 (swisstopo), own mappings).

The agricultural area is cultivated in a versatile fashion. Thus, in addition to root crops, there are also areas where cereals are grown with lesser-used meadows coexisting. This diversity of usable land is broken down in Figure 6. Thereby meadows make up the largest part regarding total area (18 %), followed by sugar beets (12 %), pastures (10 %) and wheat fields (9 %). The remaining land is shared among potatoes, pastures, orchards and other cereals, some of which used in forage production.

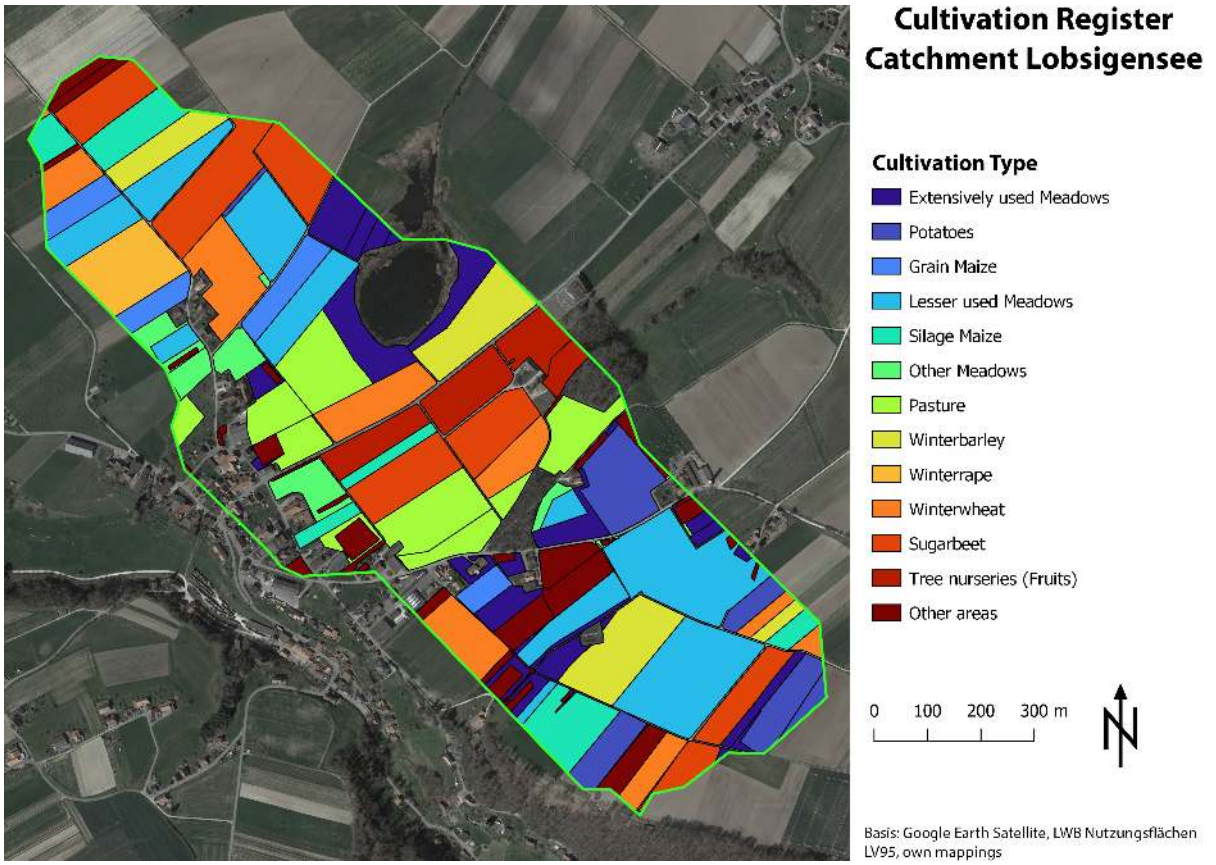

Fig. 6: Cultivation Register of the catchment of Lobsigensee. It shows the diversity of cultivated species on all agricultural fields with respect to the year of 2021. (Source: Landw. Bewirtschaftung: Nutzungsflächen 2021 (geodienste.ch) backed with Google Earth Satellite, own mappings).

Before the intense agricultural activity in the middle of the 19th century, the plane surrounding the lake was characterised as marshland. Starting in the 1860s this bog was subsequently drained for peat production and to gain agricultural lands (Staatsarchiv Kanton Bern, 1858). This led to the siltation process that continues to this day. According to K. Guthruf et al., 2015 the lake is threatened by further siltation and will transform into a wetland if countermeasures are not taken, including sediment removal or by artificially increasing the lake level.

2.5 Hydrology, Bathymetry and Drainage

The water body receives water and nutrient input from surface run-off and through drainage lines. It has no inflow, but one main outflow called Seebach which exits North of the lake shore. According to this configuration it can be classified as an exorheic lake with a certain flow-through. However, nutrients are accumulating due to dissolution from the sediments back into hypolimnic waters (K. Guthruf et al., 2015, p. 70).

At the time of formation, the lake surface was almost six times the current extent. This is confirmed by findings of lake marl in the surrounding soil (von Büren & Leiser, 1961). Alongside the greater size the maximum depth was about 17 m with prevailing meromictic conditions during the onset of the Holocene(Löffler, 1986). Subsequent formation of peat led to natural silting and concurrent eutrophication. These processes were enhanced by artificial lake level lowering phases in more recent decades and centuries: The Seedorf bog was drained in the 19th century and from 1928 to 1934 the lake level was further lowered by 1.2 m to about 3.5 m (Dubler, 2008; J. Guthruf et al., 1999). In May 1944 there was yet another lowering of 0.98 m through the construction of a channel, which initially was intended to include a sluice (von Büren & Leiser, 1961).

Field surveys in the scope of this thesis revealed the current maximum depth to be 3.9 m. This increase compared to measurements from K. Guthruf et al. (2015) of 2.5 m can be explained by the heavy precipitation during Summer 2021 and concurrent damming of the the small stream Seebach by beaver dams. In Figure 7 the higher resolution bathymetric map from J. Guthruf et al. (1999) is compared against the map created from the depth measurements of the surface sediment samples taken for this study. The latter is produced by interpolating the data points using Delauney triangulation in QGIS.

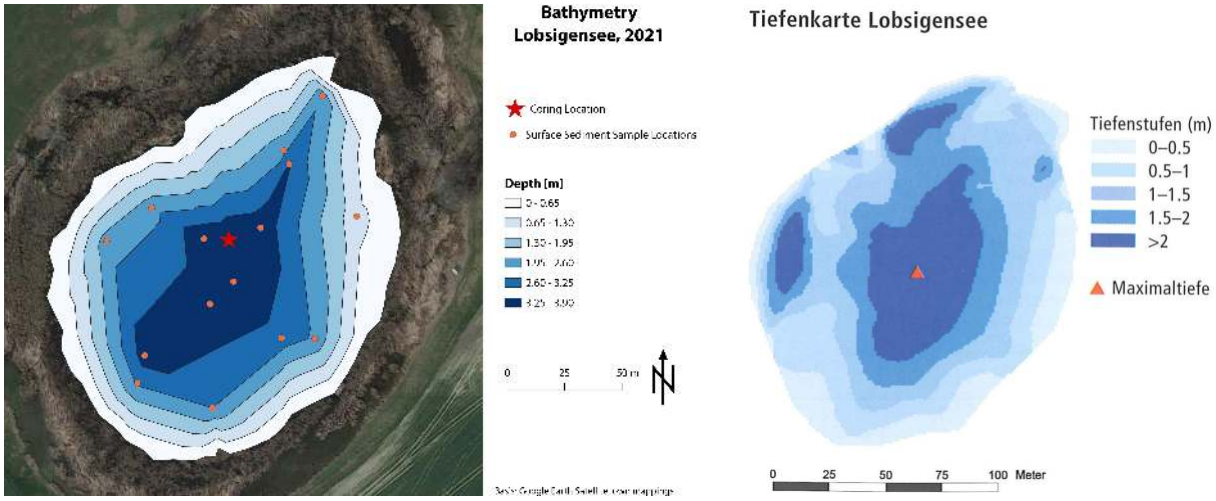

Fig. 7: Bathymetric maps of Lobsigensee. Left: Map created using depth measurements of the coring location (red star) and 15 surface sediment samples (orange points) using Delauney triangulation. Right: Bathymetric map from J. Guthruf et al. (1999), showing two small, deep sub-basins.

The map produced during the study at hand evidently does not show the same extent of lake bottom topography. Some 20 years ago, there seem to have existed two small, rather deep sub-basins on the Western and Northern shore, with the deepest point still being located in the very centre of the lake. The map from 2021 however does not reflect these topographical features of the lake bottom any more. This certainly has to do with the limited number of data points on one hand, but may also result from erosion into the lake filling up the two small sub-basins over the last twenty years.

The terrain downstream of the lake is rather plain with the slope of the outflow amounting to just 1.2 degrees over the first 3 kilometres. Therefore, both discharge volume and velocity can be assumed to be very low. Field observations confirm the slow flow velocity, which is also further reduced by the beaver dams. Due to its shallow depth, the lake is able to mix several times a year and thus can be categorised as polymyctic (J. Guthruf et al., 1999, p. 128). Predominant wind direction is south-west with speeds most commonly between 3.8 m/s and 4.4 m/s (Bundesamt für Landestopografie swisstopo, 2018). The mixing regime may be influenced by these winds due to the relatively even terrain and the low-growing vegetation around the lake.

The shoreline l_0 measured along the border of open water to closed reed growth amounts to 535 m. Using Equation 1 following the calculation of Håkanson and Jansson, 1983, p. 199, Lobsigensee is further characterised by a shoreline development of $F = 1.101$.

$$F = \frac{l_0}{2 \cdot \sqrt{\pi \cdot A}} \tag{1}$$

This corresponds to a rather low roughness of lake bottom topography, as determined by Håkanson (1974). In other words, it can be assumed that Lobsigensee has a uniformly even lake

bottom. This would need to be confirmed by taking depth measurements at a higher resolution than done in this thesis.

Since Lobsigensee is fed not only by surface run-off but also drainage pipes laid into the soil, the existence and layout of such a network may influence the load and deposition pattern of nutrients and solids to the lake (Gramlich et al., 2018). Figure 8 shows this network in the catchment and further beyond. It reveals that there are five artificial entry points at the lake shore from South to West with no direct drainage entries elsewhere. Furthermore, there is a plethora of sewer shafts connecting the surface with the drains.

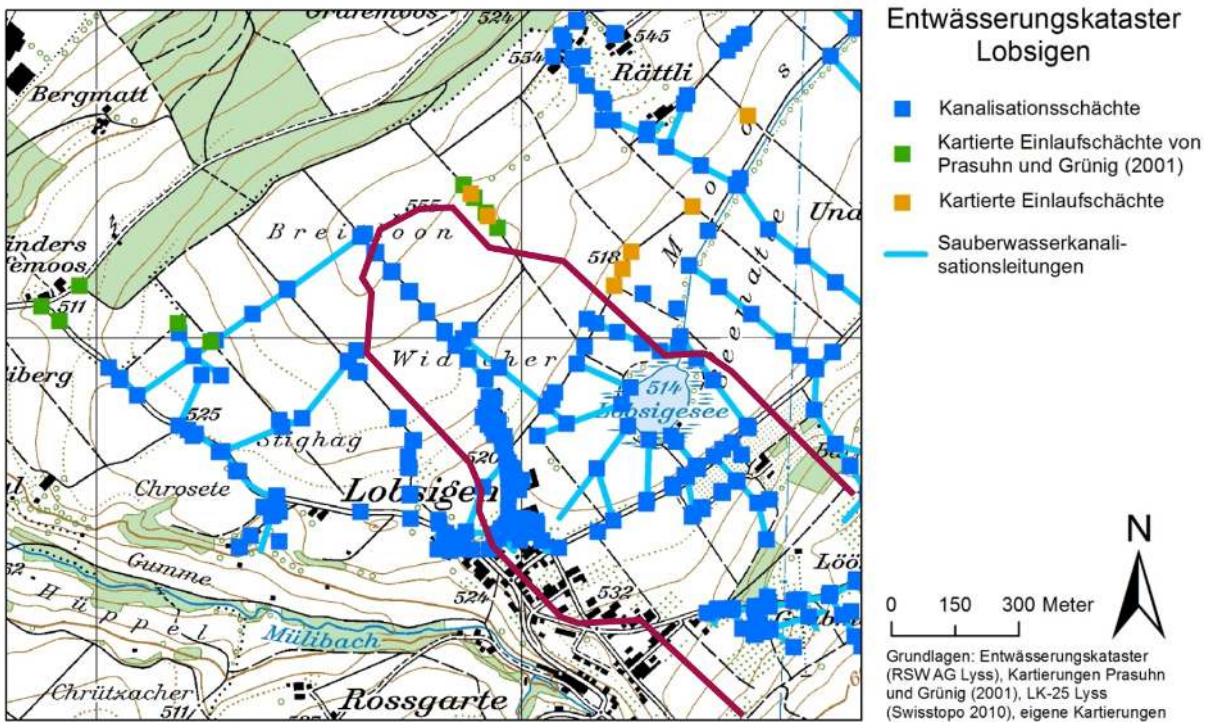

Fig. 8: Drainage grid at Lobsigen with additional inlet shafts. Blue lines: Clean water sewer lines. Squares: sewer shafts (blue), mapped inlet shafts from Grünig and Prasuhn, 2001 (green), other mapped inlet shafts (orange). The dark red outline denotes the watershed of the lake. (Source: Alder, 2012, adapted).

2.6 Water Chemistry and Ecological State

The water column of Lobsigensee, among other small lakes in the Canton of Bern, has been subject to an extensive sampling campaign regarding nutrient loadings, pesticide contamination, chemical depth-profiles and plankton biomass in the years 1993, 2003 and most recently in 2013 (K. Guthruf et al., 2015). Furthermore, the sediment was analysed regarding heavy metals and benthic species occurrence and composition. The following subsections summarise the key findings of this in-depth study.

2.6.1 Depth Profiles and Nutrients

Even though Lobsigensee is rather shallow and periodic mixing is to be expected, hypolimnic waters were found to be highly anoxic for prolonged periods of time, due to oxygen depletion through the decomposition of algal biomass. This is further shown in the one-sided and sparse colonisation of the sediment. According to K. Guthruf et al. (2015), short-term anaerobic conditions in the whole lake cannot be ruled out.

Phosphorus (P) concentrations were found to be increasing towards the lake bottom, hinting at re-dissolution from the sediment. Even though external phosphorus loading decreased, these

processes still promote internal fertilisation K. Guthruf et al. (2015). From 1993 to 2013, there seems not to be a reduction in total P in the lake water. pH was found to be higher at the surface in summer months (8.0 at the surface vs. < 7.5 in the hypolimnion) compared to a more homogenous situation in autumn and winter months ($7.75 <$ pH< 8). Electric conductivity shows a reverse behaviour, with lower values in the epilimnion during summer months than in the hypolimnion, indicating a stratified water column with increasing concentrations of dissolved solids towards the surface water (Holzner et al., 2009). However, it too shows a mixing water column in autumn months.

While naturally eutrophic, in 2013 the lake was again categorised as polytrophic, with no apparent improvement of the ecological state compared to the previous measurement campaign of 2003 (K. Guthruf et al., 2015).

2.6.2 Plant Protection Products and Transformation Products

Regarding pesticides, 12 origin compounds and 18 transformation products have been detected throughout the water column. The concentrations for the pesticides were found to be rather low. Figure 9 shows the detected parent compounds in the water column of the 2013 study as concentrations averaged over the sampling depths (0 m, 1 m, 2 m) and sorted by sampling month. Not shown are chloridazone and metalaxyl which were detected only once at one specific depth. It is important to note that some compounds show concentrations below the limit of quantification (LOQ), meaning these values show a great uncertainty but nevertheless reveal the occurrence of these chemicals in the lake water.

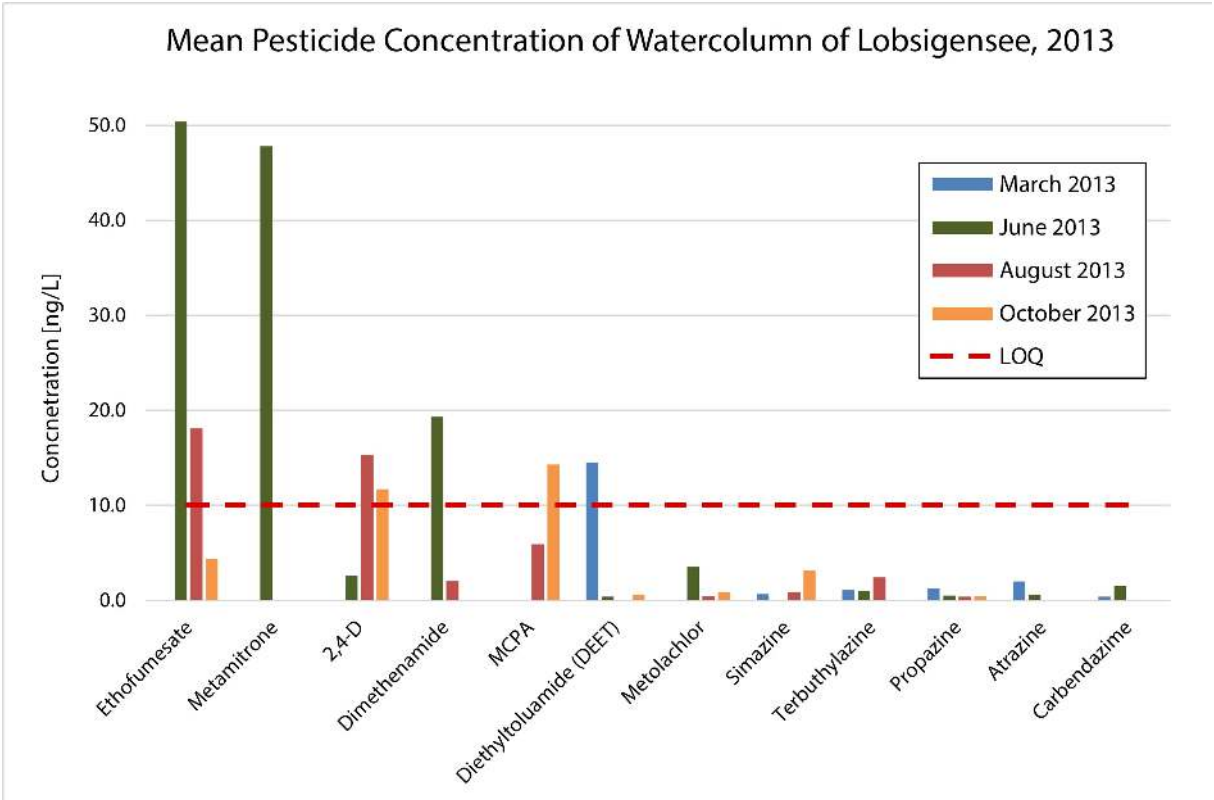

Fig. 9: Concentrations of plant protection products in the water column of Lobsigensee, 2013. Shown are the average concentration over the water column from measurements taken at depths 0 m, 1 m and 2 m in each given month. Note that some compounds show concentrations below the study's limit of quantification (LOQ). (Source: Data received from the project of K. Guthruf et al. (2015), own representation).

Transformation products (TP) were revealed to be present in much greater concentrations as

seen in Figure 10. It shows the 10 TPs with the highest concentrations measured. From the eight small lakes subject to this large campaign (among those being Grosser Moossee, Inkwilersee and Gerzensee), Lobsigensee showed the highest concentration values for these TPs. The major TP thereby was desphenylchloridazon, which has its origin in the herbicide chloridazon used in the cultivation of sugar beets. This discrepancy in occurrence is also observed in the recent work done by the BAFU on status and development of the groundwater in Switzerland (BAFU, 2019, p. 65). This contrast may be attributed to the rather short biodegradation time of chloridazon. It has been measured to degrade in soils at a DT_{50} of 31 days and in water at DT_{50} 51.5 days (Lewis et al., 2016).

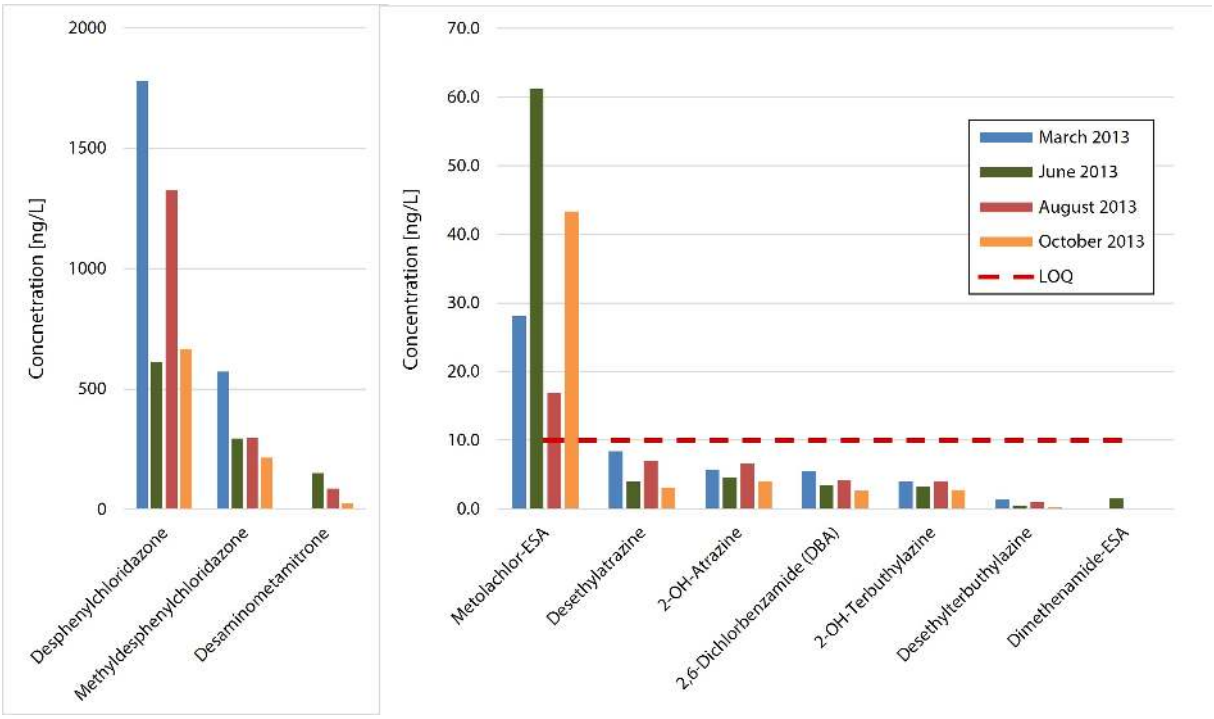

Fig. 10: Concentrations of transformation products in water column of Lobsigensee, 2013. Shown are the average concentration over the water column from measurements taken at depths 0 m, 1 m and 2 m in each given month. Note the different scales of the y-axis for two subplots and furthermore that some compounds show concentrations below the study's limit of quantification (LOQ). (Source: Data received from the project of K. Guthruf et al. (2015), own representation).

If considered as individual substance the measured levels of this compounds may be classified as ecotoxicologically harmless. The presence of these contaminants in the water of Lobsigensee however are contradicting the Appendix 1 of the Swiss Waters Protection Ordinance, which says that water quality should be such that human contaminants are only found in concentrations near zero (Gewässerschutzverdordnung GSchV)[2]. Moreover, this current situation contradicts the precautionary principle in Article 1 of the Federal Law on Environmental Protection[3]. According to this statement, chemicals should be prevented from appearing in these ecosystems in the first place whenever possible.

[2]Anhang 1, Ziffer 1, Abs. 3, Buchst. C GSchV: [3]Die Wasserqualität soll so beschaffen sein, dass:
c. andere Stoffe, die Gewässer verunreinigen können und die durch menschliche Tätigkeit ins Wasser gelangen können,
- im Gewässer nur in nahe bei Null liegenden Konzentrationen vorhanden sind, wenn sie dort natürlicherweise nicht vorkommen.
[3]Titel 1, Kapitel 1, Artikel 1, Abs. 2 USG: [2]Im Sinne der Vorsorge sind Einwirkungen, die schädlich oder lästig werden könnten, frühzeitig zu begrenzen.

3 Material and Methods

3.1 Sampling Procedure

Four sediment cores (LOB21-1 to LOB21-4) and a total of 21 surface sediment samples (LOB21surf-1 to LOB21surf-19) including two duplicates were retrieved from Lobsigensee (47°01'50.50" N, 07°17'53.35" E) during one sampling campaign in mid-September 2021. The cores were taken with a gravity core hammer (UWITEC) at the deepest part of the pond with a measured water depth of 3.9 m. The coordinates of the coring site were first approximated with the help of the bathymetric map shown in J. Guthruf et al. (1999, p. 127) and confirmed in situ by measuring the water depth with a digital depth sounder (Hondex™).

The surface sediment samples were planned to be taken along a transect from the outflow to the opposing shore and along a line perpendicular to this transect, crossing the deepest point, with additional spots near the shore. Due to the boat not being fully anchored and a slight West wind, the actual coordinates of these samples varied, as can be seen in Figure 11. Hereby, water depth ranged from 0.5 m near the shore to 3.9 m in the centre. Two additional samples were taken approximately 150 m down the outflow stream Seebach, as seen in Figure 11.

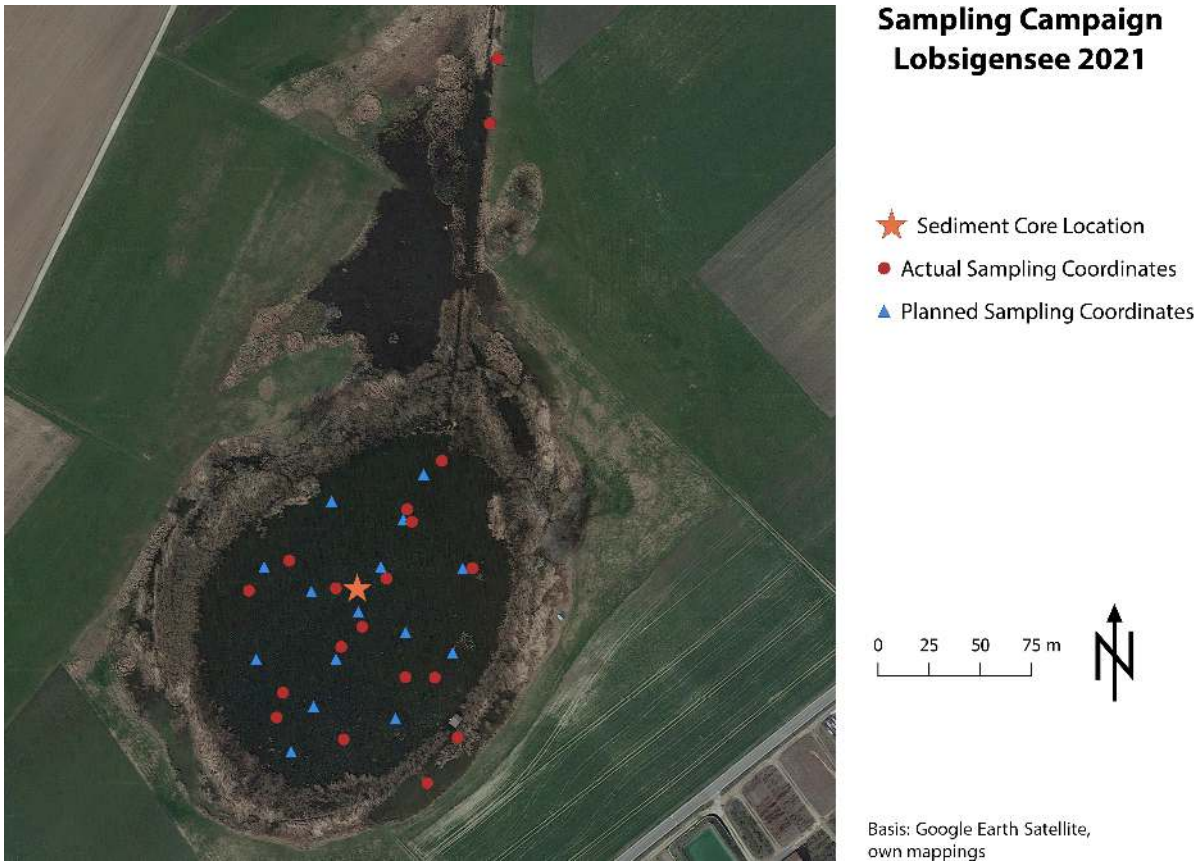

Fig. 11: Coordinates of coring site and surface sediment samples. It shows the discrepancy between planned and actual coordinates of the surface sediment samples taken for this study. Two samples were taken within the reed belt on the Southeastern shore and two samples were taken some 150 m from the outflow to the North. (Source: Own mappings backed with Google Earth Satellite Imagery).

The coordinates and length measurements of the sediment cores are listed in Table 1. The cores were then stored vertically in the dark at 4 °C until further use to inhibit microbial activity. The surface sediments were directly frozen down to -20 °C to avoid microbial degradation. For all subsequent analysis except sediment dating, core LOB21-3 was chosen as master core since

it was longest with 118 cm of sediment and showed no disturbances or broken sections upon opening. The core halve LOB21-3A was used for all non-destructive analysis and subsequent destructive analysis of loss on ignition (LOI), carbon/nitrogen/sulphur (CNS) and PPP analysis with the topmost samples being replaced with identical samples from the corresponding core halve LOB21-3B.

Core ID	Length [cm]	Lon	Lat	Analysis
LOB21-1	100	07°17'53.35"	47°01'50.50"	not used
LOB21-2	110	07°17'53.35"	47°01'50.50"	HSI, Dating
LOB21-3	118	07°17'53.35"	47°01'50.50"	HSI, XRF, LOI, CNS, PPP
LOB21-4	100	07°17'53.35"	47°01'50.50"	not used

Table 1: Coordinates and lengths of sediment cores from Lobsigensee. LOI: Loss on ignition. HSI: Hyperspectral imaging. XRF: X-ray fluorescence. CNS: Carbon/nitrogen/sulphur. PPP: Plant protection products

3.2 Working Sequence of Sediment Core Analysis

The multiproxy study of Lobsigensee is done on two different sample media: While sediment cores are used for the temporal analysis, surface sediments are used to reveal the current spatial PPP profiles along with geochemical analysis. When working with sediment cores, it is important to work on as few sediment cores as possible to keep the data consistent and homogenous due to possible variations even among cores taken from the same sampling location. If more than one core is used for the analysis, it is crucial to correlate all further cores used in the project to the master core and to match the chronology accordingly.

Based on this, the initial aim was to use core LOB21-3 for the whole analysis. In the present case however, due to very loose sediment in the top part of the core resulting in too little amounts needed for the destructive analysis and an operation error during PPP extraction, a second core was opened. This sediment core, LOB21-2, was subsequently correlated both visually and by comparing hyperspectral imaging (HSI) results and further subsampled for dating.

Sediment core halve LOB21-3A was first investigated with non-destructive methods including visual descriptions both macro- and microscopic, Hyperspectral Imaging (HSI) and X-ray Fluorescence scanning (XRF). With these methods, information on the geological and elemental composition of the sediment can be gained and possible catchment processes like floods or increased nutrient input can be identified. Additionally, past productivity within the pond can be studied. For further information see Section 3.3.

In a second step, the core halve was subsampled at 2 cm resolution until depth 60 cm. LOB21-3A was intended for PPP analysis and destructive geochemical analysis including loss on ignition (LOI) and CNS measurement. These measurements yield information on organic matter and carbonate content together with nitrogen and sulphur content of the sediment. Due to a technical failure during PPP extraction, the topmost six samples were replaced with identical samples from core halve LOB21-3B.

The PPP analysis of Lobsigensee was done according to an extraction protocol and subsequent detection using liquid chromatography tandem mass spectrometry (LC-MS/MS) and high-resolution mass spectrometry (HRMS).

3.3 Non-destructive Analysis

3.3.1 Sediment Description

The sediment description was performed on core half LOB21-3B immediately upon opening. If the sediment is exposed to air for too long, the surface layer is oxidised resulting in colour changes interfering with a consistent visual description. Thus, the surface was scraped evenly with a knife, which in addition reveals potential lithological features. Hereby it is important to move the blade in a horizontal fashion without moving it askew across different laminations to keep the chronology intact.

The initial core description was done according to the classification scheme proposed by Schnurrenberger et al. (2003). Thereby the sediment is described according to colour, bedding type and laminations and major and minor constituents. The sediment colour was determined using the Munsell® Soil Color Chart. While colour, beddings and structures can be identified by eye, the components making up the sediment matrix need to be determined by microscopic analysis. For this purpose, microscope slides at 5 cm resolution were prepared and evaluated according to the instructions from the Tool of Microscopic Identification (TMI) created by the Limnological Research Centre of the University of Minnesota (Myrbo et al., 2011).

To prepare a slide, a drop of deionised water is placed on a glass slide and a needle tip of sediment is evenly distributed on the glass. The water is left to evaporate and the sample is fixed with the addition of optical cement before adding the cover-glass. The classification thereby was made according to the four main groups presented in the TMI, those being organic matter, diatoms, siliciclastics and carbonates. Additionally the shape of the grains is noted and diatoms were counted to a total of 100 and the planktonic:benthic (P:B) ratio was calculated for every slide.

3.3.2 X-Ray Fluorescence Scanning

The elemental composition of the sediment can be determined by X-ray fluorescence (XRF) analysis. Certain elements can be used as proxies to describe catchment processes affecting the lake or process occurring within the water body itself. The principle of XRF lies on the behaviour of atoms when subjected to X-radiation. The energy uptake from X-rays leads to the ejection of inner shell electrons creating vacancies. These are filled by electrons from higher energy-state orbits resulting in the emission of fluorescence radiation. This radiation shows a characteristic wavelength spectrum for specific elements which allows the measurement of relative abundances (Weltje & Tjallingii, 2008).

The core halve was covered by a thin plastic film and scanned using an ITRAX™ XRF Core Scanner at the Institute of Geological Sciences of the University of Bern. In this study the instrument operated at a resolution of 5 mm using 30 kV, 50 mA and 30 s integration time. The device yields measurements of more than 30 elements in counts per second.

The observation of certain elements can be used as proxies for in-lake processes. In this case, the selection and interpretation were done according to Zander et al. (2021) which is based on Davis et al. (2003). The elements included in the analysis are K, Zr, Rb, Si and Ti as proxies for detrital input and Fe and Mn as indicators for redox conditions. Furthermore, Ca and Sr are used as proxies for carbonate input. P and S are used as proxies for nutrient input while the ratio of Si/Ti ratio is used to determine biogenic silica. Additionally, the ratio S/Ti is utilised to yield information about pyrite formation in the sediments.

3.3.3 Hyperspectral Imaging

Hyperspectral imaging (HSI) is an application of remote sensing where information about an object is obtained without the device being in direct contact with the sample. The measure-

ment principle is based on the reflectance behaviour of a material when being illuminated with electromagnetic radiation. The amount of reflected radiation at a given wavelength depends on its chemical composition as well as its surface structure. With the reflectance being recorded over a range of wavelengths, the compound can be characterised based on its spectral features. One such description is made by analyzing band ratios R_X/R_Y depicting slope changes between spectral bands. Another well-established index is the relative absorption band depth RABD describing an absorption feature at a specific wavelength.

In early years, marine sediments have been examined before using reflectance data in the visible spectrum (Schneider et al., 1995) but initial works also included mineral identification by using a broader spectrum ranging from NUV to NIR (Balsam & Deaton, 1996). However, these studies mainly focused on the lithogenic constituents of the sediment matrix. In the following decades, Rein and Sirocko (2002) introduced spectral indices for organic matter, characterising certain absorption features in the blue and red spectral region resulting from photosynthesis pigment produced by green algae. In recent years this analysis was extended to lake sediments, where the measurement of the relative absorption band depth (RABD) at different wavelengths in the 400-1000 nm range was used to determine the green pigments chlorophyll-a, -b, -c and derivates (Butz et al., 2015), the photopigment bacteriopheophytin-a BPhe *a* (Butz et al., 2017) or terrigenous clastic materials (Rein & Sirocko, 2002).

The pigments from algal remains are an important source of information on past primary production and lake mixing processes.BPhe *a* is produced through the degradation of Bacteriochlorophyll-a (Bchl *a*) from anoxygenic phototrophic bacteria. These organisms occur at the chemocline of a stratified water column and require reduced sulphur to photosynthesise (Van Gemerden & Mas, 1995). As consequence, the presence of BPhe *a* can be used to infer if the oxic/anoxic boundary existed within the photic zone (Sinninghe Damsté & Schouten, 2006). A presence of Bchl *a* indicates periods of meromixis with anoxic conditions in the hypolimnion (Butz et al., 2016). Sorrel et al. (2021) suggest that the RABD at 615 nm can be used to quantify phycocyanins commonly found in cyanobacteria, which indicate aerobic conditions.
Based on this research the following indices were selected and calculated from the spectral data:

1. RABD_{615} for phycocyanins (cyanobacteria)
2. RABD_{670} for green pigments (green algae)
3. RABD_{845} for BPhe *a* (anoxygenic phototrophic bacteria)
4. R_{570}/R_{630} for clastic materials

The RABD indices can be calculated according to Equation 2 as presented by Butz et al. (2015), with the components listed in Table 2.

$$\text{RABD}_{\text{FeatureMIN}} = \left(\frac{X \cdot R_{\text{Left}} + Y \cdot R_{\text{Right}}}{X + Y} \right) / R_{\text{FeatureMIN}} \tag{2}$$

Term	Meaning
$\text{RABD}_{\text{FeatureMIN}}$	relative absorption band depth at absorption feature minimum
R_{Left}	reflectance at start of absorption feature
R_{Right}	reflectance at end of absorption feature
$R_{\text{FeatureMIN}}$	reflectance at minimum of absorption feature
X	number of spectral bands between $R_{\text{FeatureMIN}}$ and R_{Right}
Y	number of spectral bands between $R_{\text{FeatureMIN}}$ and R_{Left}

Table 2: Terms used to calculate the relative absorption band depth (RABD). Adapted from Butz et al. (2015).

The cores LOB21-2A and LOB21-3B were scanned with a hyperspectral core scanner at the Institute of Geography, University of Bern. It contains a Specim PFD-CL-65-V10E VNIR camera with a Schneider Kreuznach Xenoplan 1.9/35 lens mounted above an illumination unit and a movable sample tray underneath. The scanner operated at a spectral resolution of 1.566 nm, spatial resolution of 75 μm, 160 ms exposure time, 6 Hz framerate and 0.45 mm/s scanning speed.

The raw reflectance data was processed in ENVI v. 5.4 (Exelis ENVI, Boulder Colorado). Normalisation was done to a white and dark reference taken immediately after the scan. Then the data was subset into two regions, one covering the core surface and another smaller, 2 mm transect down-core. A mask was applied to the small subset to remove pixels with R_{mean} outside the range 0.05-0.24. This removes very dark pixels and very bright pixels that produce noisy unreliable data. From the small subset the spectral indices were calculated based on the spectral end members.

3.4 Age-Depth Modelling and Core Correlation

To arrive at a meaningful interpretation of the data gained from the sediment, it is essential to know the specific age of the different laminations of the core. In environmental science this is predominantly done by detecting certain radionuclides. Depending on the timescale of the project, different radionuclides may be of interest. In the case at hand, ^{210}Pb-dating together with ^{137}Cs-chronomarkers is applied.

Due to its half-life of 22.3 years, ^{210}Pb dating is suited for a time-frame of at most two centuries. The principle of ^{210}Pb-dating lies in γ-counting of the 46.5 keV decay energy of ^{210}Pb. Hereby it is important to distinguish between so-called supported and unsupported ^{210}Pb activity: The supported ^{210}Pb describes the time independent fraction of ^{210}Pb originating from the continuos production by decay of ^{226}Ra present in the substance. It is the unsupported ^{210}Pb which is coming from the decay of atmospheric ^{222}Rn that can be used to determine the age of the sample. This is derived by subtracting the supported fraction of ^{210}Pb from the total ^{210}Pb activity, the former usually being measured from very deep sediment samples (Gäggeler & Szidat, 2016, pp. 147 sq.).

A way to constrain the age-depth model is by having specific horizons of which an exact year is known. One man-made radionuclide is ^{137}Cs which has its origin from nuclear fission produced by nuclear weapon tests or accidents in nuclear power plants. During these events, the volatile ^{137}Cs is emitted into the Earth's atmosphere and the subsequent fallout may be deposited in sediments (Gäggeler & Szidat, 2016, pp. 163 sq.).

The onset of ^{137}Cs in sediments is due to the aboveground nuclear weapons tests generally attributed to 1954 with a fallout peak in 1963 following the test-ban treaty. A more recent event includes the Chernobyl reactor accident in 1986, where another ^{137}Cs peak can be identified which allows for a precise dating (Last & Smol, 2001, p. 172).
The core LOB21-2 was sampled at a 2 cm resolution and the sediment was freeze-dried and homogenised for dating measurements. The radionuclide measurements were performed by gamma-spectrometry at the Department of Surface Waters Research & Management at Eawag, Zurich.

Since the PPP and geochemical analysis was done on core LOB21-3, the age-depth model resulting from core LOB21-2 needed to be adjusted to the master core. Both cores were first correlated visually by identifying specific coloured laminae and the different depths of these tie-points were noted. Additionally, both cores were scanned by means of HSI and the index signals were also compared to yield more tie-points. Then the age-depth relationship of these horizons was translated to core LOB21-3 and linear interpolation between two tie-points resulted in the adjusted chronology of LOB21-3.

3.5 Destructive Analysis

3.5.1 Subsampling of Cores

For the procedures of destructive geochemical analysis, PPP measurements and sediment dating, the selected core halves need to be subsampled at an appropriate resolution. This process compromises on workload and temporal resolution. If there is no age-depth model available for the site, it is of great importance to make reasonable assumptions, e.g. about sedimentation rate or with the help of descriptive sediment analysis, to arrive at a suitable sampling resolution. Subsampling the core halves involved cutting the sediment at the chosen intervals using a stainless steel slicer tool, which allows for precise vertical sectioning. The samples were then weighed and freeze-dried for at least 48 hours using a device consisting of a pump (Vacuubrand RZ 2.5) connected to a freeze-drier (Alpha 1-2LD). After freeze-drying, the samples were weighed again and subsequently homogenised using a mortar and pestle. It is crucial that all the tools used in this procedure are cleaned thoroughly with deionised water and ethanol after every sample to prevent sample carry-over and contamination.

Using the weight measurements at the different stages and neglecting mass and volume of gases the weight loss corresponds to the water content of the sample (Håkanson & Jansson, 1983, p. 74). Dry bulk density (DBD) is calculated according to Appendix A. From top to a depth of 60 cm, core halve LOB21-3A was sampled at a resolution of 2 cm. Due to very lose sediment in the upper 16 cm, two slices were combined to form one sample. From 60 to 75 cm, three 5 cm samples were additionally taken, assumed to be blanks. The sediment from 75 to 112 cm was pooled and used for calibration matrix. A total of 29 samples were used for CNS, LOI and PPP analysis and 11 pooled calibration samples. Six duplicates were taken from the other core half LOB21-3B at the respective depth.

The core LOB21-2 used for dating was sampled at 2 cm resolution and the samples were freeze-dried, homogenised and stored at room temperature until gamma-spectrometry analysis.

3.5.2 Loss On Ignition

Loss on ignition is conducted to obtain data on organic matter and carbonate content in lake sediments. This method is based on different oxidation temperature for organic matter and carbonates. A first combustion at 550 °C oxidises organic matter to ash and carbon dioxide which diffuses. A temperature increase to 900 °C yields again CO_2 and oxide. The weight loss after each step then correlates to the organic matter and carbonate content in the sample (Heiri et al., 2001).

To perform LOI, 200 mg of freeze-dried sediment were weighed into crucibles and heated to 550 °C and left for four hours to equilibrate. The weight loss measured after this step relates to the organic matter content. The samples were then heated to 950 °C and left for two hours at this temperature to reach equilibrium. This additional weight loss is due to the formation of CO_2 during a second oxidation where oxides remain and it corresponds to the carbonate content of the sample. LOI was performed for all of the 29 samples and six duplicates according to Appendix D.

3.5.3 CNS Analysis

CNS analysis is a measurement technique to quantify carbon, nitrogen and sulphur in a sample. In the process, the sample is combusted and the solids transform into gases, that is carbon dioxide CO_2, nitrogen gas N_2 and nitrogen oxide NO_2 and sulphur dioxide SO_2 or trioxide SO_3. These combustion gases are then separated using gas chromatography followed by detection via thermal conductivity measurements. CNS was performed for all 29 sediment samples and six duplicates according to Appendix E. It includes weighing 5 mg of freeze-dried, homogenised sediment into silver capsules, which are folded and then combusted using a Vario EL Cube CNS Analysed (© Elementar Analysesysteme GmBH, Germany).

3.6 PPP Analysis

3.6.1 Preparation of Sediment Core Samples

The samples of the sediment core undergo a sequence of extraction and clean-up steps, before being measured with the mass spectrometer. These steps include spiking with surrogate, extraction, spiking with internal standard, concentrating, clean-up and filtering.

In a first step, 4 g of freeze-dried, homogenised sediment were spiked with 70 μL surrogate solution of 2.5 mg/L Carbamazepine-D10 in acetonitrile. This is done to monitor extraction performance. Extraction was done using a Dionex ASE 350 Accelerated Solvent Extractor Operator (© Thermo Fisher). Thereby, pressurised liquid solvent is forced through a preheated sediment sample contained in an ASE cell. The analytes are subsequently filtered and collected in vials. Diatomaceous earth (Restek Corporation, U.S) was added to the sediment matrix to increase solvent channelling (Chiaia-Hernandez et al., 2013). Extraction followed the work of Chiaia-Hernández et al. (2020) which involves two successive extractions. First an extraction is applied to extract neutral compounds using 70:30 (v/v) ethyl acetate:acetone at 80 °C and 130 bar. The first extraction is then followed by a second extraction with 70:30 (v/v) acetone:1% phosphoric acid at 120 °C to extract acidic compounds.

The extracts were then spiked with 50 μL of a 2.5 mg/L mixture of 19 deuterated pesticides which allows to detect potential material losses during the subsequent preparation process and to quantify the matrix effect. To further clean up and concentrate the extracts, the samples were evaporated under a stream of N_2 using a TurboVap II Concentration Workstation (Biotage AB, Sweden). The extracts were then reconstituted with acetonitrile and further cleaned up using QuECHERS (Quick, Easy, Cheap, Effective, Rugged and Safe), according to (Chiaia-Hernández et al., 2020). This technique is applied to remove potential matrix interference such as lipids, proteins or pigments.
The resulting extracts were then evaporated with N_2 to a final volume of 500 μL and filtered directly into 2 mL HPLC vials. The exact procedure and specifications of the preparation process can be found in Appendix F.

3.6.2 Detection by LC-MS/MS and HRMS

Suspect screening of PPP compounds from the final extracts was performed using a coupled system consisting of a High Performance Liquid Chromatography (HPLC) System (Agilent 1260 II HPLC) connected to a Mass Spectrometer (6460 Agilent Triple Quad). All the measurements were done at the Institute of Geography at the University of Bern. 100 % ultra-pure water and methanol both with 4.5 mM ammonium formate, 0.5 mM ammonium fluoride and 0.1 % formic acid are used as mobile phase. 10 μL of sediment extract is then delivered to the LC-column (2.1 mm X 50 mm X 3.5 μm particle size XBridge C_{18}) before being injected to the Triple Quad using positive and negative electro spray ionisation (ESI, Jetstream) in different runs.

Additionally, the core samples and a selection of surface samples suspected to be highly contaminated were remeasured by High Resolution Mass Spectrometry (HRMS) at the Water and

Soil Protection Laboratory (GBL) of the Office for Water and Waste of the Canton of Bern (AWA Bern) to target additional PPPs and their transformation products (TPs). HRMS allows to detect suspect compounds based on exact mass acquisition without the need of reference standards (Schymanski, Singer et al., 2014). This analysis may result in a wider catalogue of PPPs and TPs. The system consists of a PAL Autosampler (CTC Analytics, Zwingen, Switzerland) and a Rheos 2200 quaternary low pressure mixing pump (Flux Instruments, Basel, Switzerland). The same XBridge C_{18} column was used in the chromatography. Mobile phase consisted of 100 % ultra pure water and methanol with 0.1 % formic acid. MS detection was done using a Q-Exactive Orbitrap (Thermo Scientific, San Jose, U.S.) operating at positive ESI. Details on detection and quantification including acquisition parameters and method performance are found in the supporting information of the work done by Chiaia-Hernández et al. (2020).

Suspect screening was performed based on the findings by the study of K. Guthruf et al. (2015), who detected 12 PPPs and 18 TPs in the water column of Lobsigensee. This was done to test if those compounds found in the water column, but which are not available in the target list of the QQQ, are also present in the sediment. The suspect screening was done by using exact mass filtering at 5 ppm and isotopic patterns as well as fragment simulation in Xcalibur ™Software (©Thermo Fisher Scientific Inc., 2019). Thereby, the simulated spectrum of a suspect compound is produced. Then the chromatogram data is filtered to this mass per charge ratio (m/z) to reveal the retention time (RT). This RT then is verified with theoretical RT as predicted from $\log K_{ow}$. The measured spectrum at this selected RT is then checked to coincide with the simulated spectrum. If the measured spectra of fragments also coincide with the theoretical mass spectrum, the suspect is considered as identified on level 2a according to the classification scheme proposed by Schymanski, Jeon et al. (2014). In addition, all PPPs detected with the Triple Quad were examined in the HRMS data for confirmation purposes.

3.6.3 Quality Control

The extraction and detection of PPPs in lake sediment has been already validated in previous studies (Chiaia-Hernandez et al., 2013; Chiaia-Hernandez et al., 2014; Chiaia-Hernández et al., 2020). To ensure consistent results and to monitor extraction methods and instrument performance as well as cross contamination, blank samples were introduced in the extraction process between sediment samples, consisting of either pure hydromatrix samples or sediment taken from the lower part of the core, which is assumed to be contaminant-free.

In order to arrive at the analytes' concentration based on the MS response during the measurement, a calibration curve has to be produced. The advantage of using sediment as substrate for the calibration instead of solvent is that matrix effects and PPP losses during the extraction can be directly translated to the sediment samples. These calibration samples consisted of homogenised sediment of the lower end of the core which was assumed to be free of any synthetic pesticides. These samples were then spiked with 50 μg/L of a mixture of 19 deuterated pesticides. A calibration curve was produced with final concentrations ranging from 0.5 to 300 μg/L by adding differently concentrated pesticide mixes stored in methanol and acetonitrile. More information regarding the calibration curve can be found in Appendix F. The samples were then subjected to the same extraction and clean-up procedure described in Section 3.6.1.

Furthermore, to survey the extraction accuracy of the Dionex ASE 350, the collection vials were weighed empty and after each extraction step such that the exact volumetric amount of extract can be calculated based on the density of the solvent mixtures to determine device accuracy. Details regarding solvents used, density and extract volume calculations together with the results can be found in Appendix C.

3.7 Surface Sediment Analysis

The 21 surface sediment samples were freeze-dried, homogenised and the same extraction process that was applied to the core samples was used to determine PPPs. All the samples were measured according to the SOPs in appendix F with the Triple Quad Mass Spectrometer operating at the settings given in section 3.6.2. Additionally, grain size distribution (GSD) analysis and LOI was conducted on the samples. GSDs including the abundance of the different size classes determined by this technique have been used as proxies for many different topics in environmental sciences (van Hateren et al., 2018). Based on end-member analysis of the GSDs, conclusions can be drawn regarding sediment transport mechanisms (Dietze et al., 2014), provenance (Shang et al., 2016) or flooding events (Parris et al., 2010). It has been shown that organic chemicals adsorb to suspended and dissolved materials such as fine-grained clay (Knezovich et al., 1987). Additionally, the sorption of these compounds by sediment correlates directly to the organic carbon content in the sediment. So with higher organic carbon content, more pollutants are scavenged from the water column and incorporated in the sediments. Based on this, GSD in connection to organic carbon content is applied to determine the spatial variability of sorption behaviour of detected PPPs and TPs.

The GSD analysis was performed on a Malvern Mastersizer 2000 at the Institute of Geography, University of Bern. In total 19 spatial grab samples including two duplicates were measured. One sample is estimated to contain sediments of the last five to ten years. The grain size analysis was done according to the SOP listed in Appendix G. The main steps during sample preparation include freeze-drying and subsequent removal of organic matter by oxidation with H_2O_2. Small amounts of H_2O_2 are added to the dry sediment until no more gases are produced. Then the H_2O_2 is replaced up to three times until no reaction was observed upon adding H_2O_2. The samples are put in a heated waterbath (60 °C) to accelerate the reaction. To preserve the grains for GSD, the sediment must not be ground with a pestle but only homogenised after freeze-drying. Biogenic silica from diatoms or chrysophytes is subsequently removed by heating the samples in NaOH to 90 °C for 3 hours to avoid clastic grain size alterations. The samples are then suspended in a dispersion solution and analysed in the Mastersizer by laser diffraction. Additionally, LOI is performed according to the procedure listed in Appendix D.

3.8 Data Analysis

3.8.1 Normalisation, PPP Fluxes and Hierarchical Agglomerative Clustering

The MS detection of PPPs yields concentrations in μg/L of extract, therefore, the concentrations are normalised as well as reported as fluxes. The values are first upscaled to kg of dry sediment. Then the values are normalised to kg of total organic carbon by dividing the concentration by the fraction of total organic carbon. This is done because these chemicals sorb to organic matter in the sediment. Furthermore, it makes findings from different sites more comparable instead of comparing the concentration to the dry weight of the sediment only. The concentration of PPPs in dry sediment is thereby divided by the organic carbon content in the dry sediment. To overcome relative concentration fluctuations due to the matrix-effect, PPP concentrations are converted to fluxes (denoted as μg cm^{-2}y^{-1}) by multiplying mass accumulation rate MAR (= DBD $\cdot$ sedimentation rate) with the normalised PPP concentration (which has unit μg/kg dry sediment).

PPP concentrations from surface sediment samples are only converted to µg per kg organic carbon, since there is no age date available for these samples. The data is then spatially interpolated across the lake surface using inverse distance weighing interpolation (IDW) implemented in QGIS (v. 3.16 Hannover). Thereby, the weighting coefficient p was set to 2 and pixel size was set to 1. A greater p value thereby describes a smaller effect of points far away from the unknown point during interpolation. Different p values were tested regarding output quality. Higher p values resulted in sharper boundaries between sample points whereas lower p values

produced a stronger bulls-eye effect which do not reflect physical deposition patterns. Therefore, a value of $p = 2$ was deemed reasonable. Kriging method was tested as well but disregarded because it predicted large concentration artefacts on the pond shore due to the limited number of sediment samples.

To examine similar temporal trends among detected compounds, hierarchical clustering analysis (HCA) is performed on the core samples in R v. 4.1.3. using the libraries `tidyverse`, `cluster` and `factoextra`. Flux values are first scaled to mean zero and standard deviation set to one using the `scale` function. HCA is then performed by calculating dissimilarity values using method `euclidian` and conclusively using Ward's minimum variance method `ward2.0`. With the help of a silhouette plot, the number of significant clusters is determined by applying the function `fviz_nbclust` together with method `silhouette`. Details including plots are found in Appendix H.

3.8.2 Ecological Risk Assessment

In addition to the sole quantification, another aim of this thesis is to examine the associated ecological implications of the detected pesticide compounds. To evaluate the ecological risks of PPPs in lake sediment, risk quotients (RQs) can be analysed. This procedure has been successfully applied before in the work of Chiaia-Hernández et al. (2020). The risk quotients show the relation between the mean environmental concentration (MEC) of a PPP and a corresponding quality standard (QS), as shown in Equation 3.

$$\mathrm{RQ} = \frac{\mathrm{MEC}}{\mathrm{QS}_{sed,EqP,dw}} \tag{3}$$

Hereby MEC is the measured concentration of a given PPP in μg/L as determined by LC-MS/MS and $\mathrm{QS}_{sed,EqP,dw}$ denotes the dry weight quality standard, which is a converted version of the wet weight quality standard $\mathrm{QS}_{sed,EqP,ww}$. The latter is obtained through the Equilibrium Partitioning Model and calculated with Equation 4. This conversion from values derived by freshwater organisms is necessary since not enough data exists yet for organisms residing in the sediment. This process is in accordance with the Technical Guidance For Deriving Environmental Quality Standards (European Comission, 2011, pp. 96 sqq.).

$$\mathrm{QS}_{sed,EqP,ww} = \frac{\mathrm{K}_{sed-water}}{\rho_{sed}} \cdot \mathrm{QC}_{fw,eco} \cdot 1000 \tag{4}$$

$\mathrm{K}_{sed\text{-}water}$ is the partition coefficient between sediment matter and water in $\mathrm{m}^3/\mathrm{m}^3$, ρ_{sed} the default value of bulk density of wet sediment (1300 $\mathrm{kg}_{ww}/\mathrm{m}^3$) and $\mathrm{QC}_{fw,eco}$ is the annual average concentration equality standard (AA-EQS). AA-EQS values are compiled for each PPP from existing literature such as Chiaia-Hernández et al. (2020) and Oekotoxzentrum (2022).

Since the PPP concentration measurements are done on dry sediment, a conversion needs to be done according to Equation 5 to obtain $\mathrm{QS}_{sed,EqP,dw}$ used to determine the risk quotients,

$$\mathrm{QS}_{sed,EqP,dw} = \mathrm{CONV}_{sed} \cdot \mathrm{QS}_{sed,EqP,ww} \tag{5}$$

where $\mathrm{CONV}_{\mathrm{sed}}$ is a conversion factor as described by Equation 6

$$\mathrm{CONV}_{sed} = \frac{\rho_{sed}}{\mathrm{Fsolid}_{sed} \cdot \rho_{solid}} \tag{6}$$

with Fsolid_{sed} being the fraction of solids in sediment (default value = 0.2), ρ_{solid} denoting the density of the solid phase (default value = 2500 kg/m^3) and ρ_{sed} as above.

The RQ can then be determined for every depth sample to get the down-core variability or if applied to the surface sediments, it reveals the current spatial variability. Together with the risk evaluation scheme shown in Table 3 a statement about the sediment quality can be inferred.

Evaluation		Description		compliance
colour	In words	RQ value	In words	
	Very good	RQ < 0.1	MEC is greater than or equal to one-hundredth of QS but less than one-tenth of QS	QC passed
	Good	0.1 < RQ < 1	MEC is greater than or equal to one-tenth of QS but less than QS	
	Moderate	1 < RQ < 2	MEC is greater than or equal to QS but less than two times QS	QC exceeded
	Insufficient	2 < RQ < 10	MEC is greater than or equal to two times QS but less than ten-times QS	
	Poor	RQ > 10	MEC is greater than or equal to ten-times QS	

Table 3: Effect-based risk evaluation scheme of water quality from micropollutants. (Source: Fahrni (2021), which is a translated version of German to English of the risk assessment done in the publication of Liechti (2010)).

More information regarding risk quotient calculations including parameters can be found in the supporting information of the work done by Chiaia-Hernández et al. (2020).

4 Results and Discussion

Since the study is done both on sediment cores and surface sediment samples, this section first shows the results from the multiproxy approach on the cores to understand the depositional context of PPPs. Because spatial samples reflect a single point in time, not all methods are applied to the spatial samples. The results of the surface sediment analysis are listed in a separate subchapter at the very end of this section.

4.1 Sediment Description

The core LOB21-3 shows a rather massif structure upon opening, with two Units separated by a distinct contact at depth 52 cm, as seen in Figure 12. Unit 1 is thereby characterised by dark olive brown sediments with high organic matter content and shows only few distinct laminae. There is a small bright lens visible at depth 30 cm. Contrastingly Unit 2 shows a much lighter brown-greyish colour with thin laminae and even horizontal beds with distinct contacts visible. Their thickness thereby ranges from a few millimetres up to 5 cm. In Unit 2 the colours vary from very light greyish brown over light greyish brown to light olive brown. The topmost sediment is very watery and is difficult to contain in the core opening process.

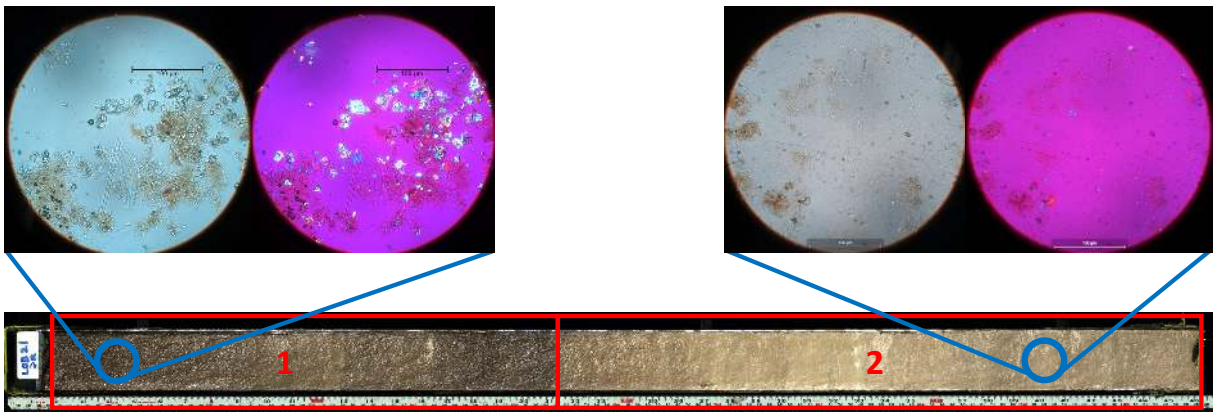

Fig. 12: LOB21-3B core image. Additionally, two microscope image excerpts (depth 10 cm in Unit 1 vs. depth 90 cm in Unit 2) are shown in both regular light (left) and in polarised light (pink). They are taken at locations indicated by the blue circles. This shows the contrasting grain size and organic matter content in both Units.

Testing the sediment by rubbing it between fingers reveals coarser grains in Unit 1 and much finer grains in Unit 2. This is further confirmed from microscopic analysis of the smear slides produced every 5 cm, an example shown in Figure 12. The two units become even more distinguishable based on the different fraction of siliciclastics and carbonates, with Unit 1 showing a fourfold calcite content compared to quartz or feldspar while the opposite is the case in the lower Unit 2, as can be taken from the summary diagram of Figure 13. The main carbonate mineral is calcite which is primarily present in polycrystalline form. The dominant grain shape of calcites in both Units is found to be sharp edged and well defined, hinting at chemical precipitation in the water column instead of external in-wash. Sorting shifts from poorly sorted in the top Unit to well sorted in the lower Unit for both siliciclastics and calcite. Grain size in Unit 1 is predominantly attributed to silt with a fraction of clay whereas in Unit 2 predominantly silty clay can be observed.

Furthermore, there seems to be an onset of pyrite at the interface of two Units, however sporadic observations of pyrite are also made in the lower section albeit in much smaller numbers. Regarding macrofossils an increased number of chitin fragments are observed towards the top of the core. Diatom counting reveals planktonic diatoms to be dominating the sediment, with only a slight increase in benthic species in the lowest part of Unit 1. The P:B ratio values mainly

range from 1.5 to 12 or even 32 with two depth samples showing a ratio of 49 and 99 respectively. This however may has to do with the total number of diatoms counted (100), which is certainly at the lower end of counts needed for a sound interpretation.

Organic matter content is found to be much higher in the upper Unit 1. The criterion of quantification hereby is the approximate area covered by brown amorphous algal material in a representative section of a given smear slide. Coverage ranged from 80 % to 90 % in Unit 1 whereas in the lower Unit 2 it sharply decreased where it amounts only between 10 % and 20 %. There are little to no remains of vascular plants in Unit 1, let alone in Unit 2.

The strong increase in precipitated calcite and algal organic matter indicates an increase in oxygen saturation of epilimnic waters, available nutrients and primary production, as already observed in J. Guthruf et al. (1999). The biogenically mediated calcite precipitation is the result of the disintegration of calcium-bicarbonate ($Ca(HCO_3)_2$), which may be present in solution due to high CO_2 content. However if CO_2 is consumed by photosynthetic activity of plants, the bicarbonate decays into water (H_2O), CO_2 and calcite crystals in order to reach equilibrium. These calcite crystals precipitate and are subsequently incorporated in the sediment. Among soil erosion and soil in-wash during heavy precipitation events this process significantly contributes to silting up of the lake (von Büren & Leiser, 1961).

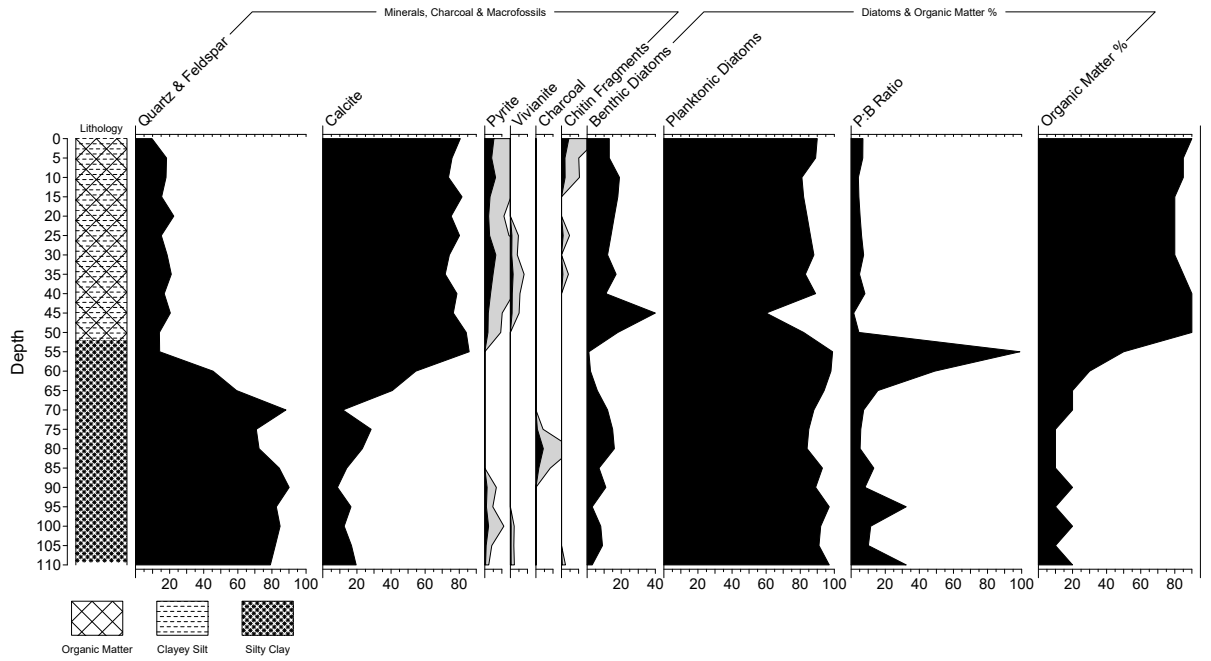

Fig. 13: Summary diagram of the smear slide analysis. The two Units are further distinguished by the contrasting quartz/feldspar and calcite fractions. The light grey background curves show the 5x exaggeration.

4.2 X-Ray Fluorescence Scanning

While a total of 36 elements are measured with XRF scanning, only a selection is used as proxies as discussed in Section 3.3.2. Figure 14 portrays a selection of elements and ratios describing lithogenic input. The elements K, Ti and Zr all show a very similar picture. Hereby there is an increased occurrence of these elements with over 80000, 75000 and 14000 cps respectively in the lower Unit 2 whereas numbers decrease in the more recently deposited sediments of Unit 1. A similar picture is shown by counts of Fe elements, hinting at the presence of Fe-Ti oxides as iron is commonly found in this configuration (Davies et al., 2015, p. 193). Unit 2 is thereby again characterised by very high values whereas in Unit 1 significantly less iron is observed.

Unit 1 is further characterised by a decrease of Fe/Mn ratios. This ratio often used as an indicator of changing redox conditions in the hypolimnion. However, in the case at hand iron seems to stem from detrital sources as shown by the similarity of the curves with K or Ti. This diminishes the significance of redox processes in relation to detrital input from the catchment, which can be revealed by looking at normalised values to Ti (Moreno et al., 2007). The right-most curve in Figure 14 confirms that the Fe/Mn signal in Unit 2 should not be over-interpreted as indicator of redox conditions in the sediments of Lobsigensee.

The strong decrease in allochthonous minerals may be the results of a drastic altering of the lake level. It is known that there have been multiple such interventions in the last century, which for a lake this size are extreme changes (J. Guthruf et al., 1999). Along with the development of a denser and more stable vegetation belt surrounding the lake this might have helped mitigate detrital input to the lake.

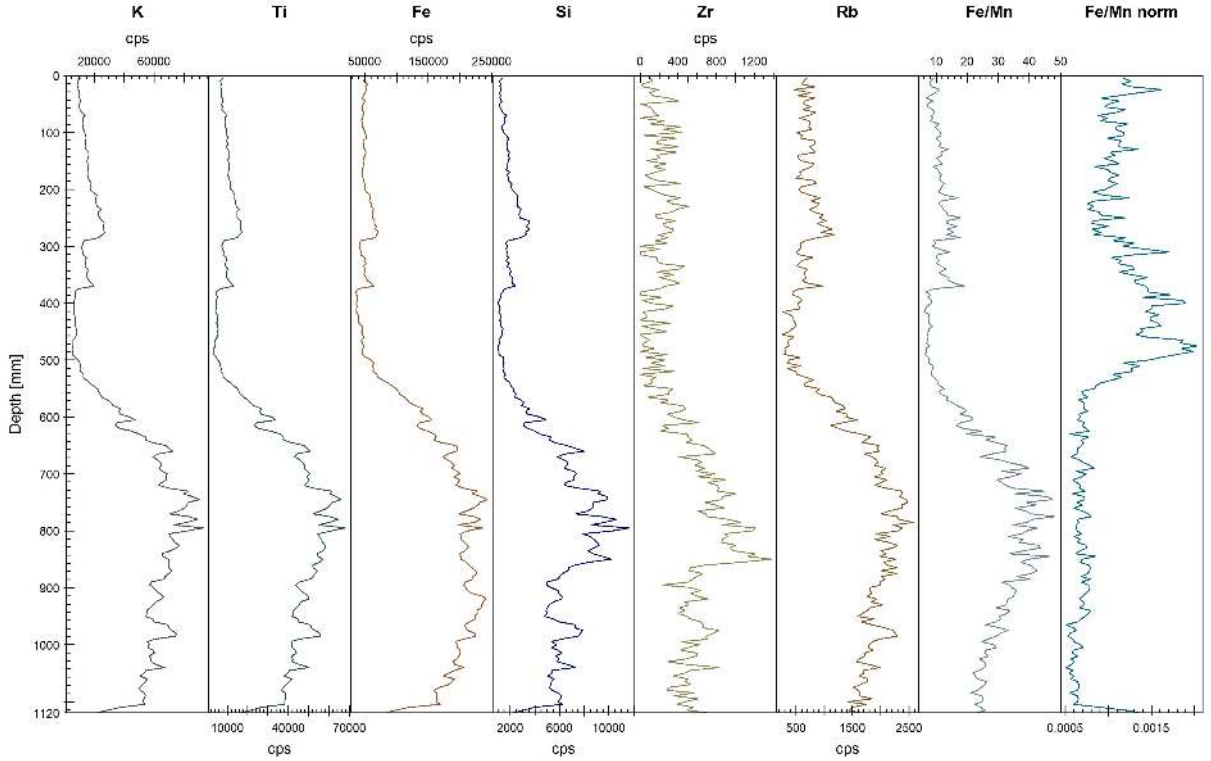

Fig. 14: XRF data on clastic proxies. Fe/Mn norm displays the Fe/Mn ratio normalised to Ti. Single elements are shown in counts per second (cps) whereas elemental ratios are without unit. It shows detrital input to the lake to be strongly increased in Unit 2 with less input towards recently deposited sediments.

Figure 15 shows the XRF data obtained regarding proxy elements and ratios related to organic matter and nutrient loadings to the lake. As portrayed phosphorus is only present in low amounts from 1 m up to 70 cm. In a great number of Swiss lakes, the decline in phosphorus in the 1970s and onwards has its origin in the implementation improved waste water treatment and banning of detergents containing phosphates (BAFU, 2020). However, while total phosphorus was measured to be declining in Lobsigensee in the last few decades, eutrophication is still high as there occurred merely a breakdown of excess phosphorus (J. Guthruf et al., 1999). In anoxic conditions in the hypolimnion sequestered phosphorus in the sediment may be recycled back into the water (Corella et al., 2012). With prevailing anoxic conditions in Lobsigensee as described by K. Guthruf et al. (2015) this may the reason that phosphorous is essentially absent in the sediment, but present in the water. Over the last two decades total phosphorus concentrations in the water column ranged between 0.05 and 0.2 mg P/L (K. Guthruf et al., 2015).

The element S shows stable values in both sections however with an inverse behaviour compared to the clastic proxy elements: It shows low, stable amounts in Unit 2 and high, stable amounts in Unit 1. This is attributed to a significant increase in nutrient input which is confirmed through smear slides by the high amounts of organic matter in the recent sediments. The ratio of S/Ti has been used before as a marker of pyrite (FeS_2), since the amount of sulphur reflects the occurrence of these mineral (Moreno et al., 2007). According to Figure 15 one can assume an increased presence of FeS_2 in the upper Unit 1. This is confirmed by the counts of pyrite from the smear slide analysis as shown in Figure 13. The presence of pyrite indicates anoxic conditions at the sediment-water interface of Lobsigensee in more recent times. This is because highly reduced conditions are necessary for the formation of sulphide minerals. These conditions are primarily found in productive lakes with a very low redox potential, which occurs in oxygen-free environments (Håkanson & Jansson, 1983, p. 112). Since the formation of FeS_2 requires iron sulphides, it can be assumed that FeS are also present in the sediment of Lobsigensee. These particles are highly insoluble and and are quickly incorporated in the sediment. The precipitation of FeS inhibits the sediments capacity to retain phosphorus since reactive and mobile Fe-ions are needed for phosphorus fixation (Håkanson & Jansson, 1983, p. 113). This may be an additional reason why phosphorus is completely absent in Unit 1.

With Si/Ti ratios, inferences about Si contribution from diatom frustules and therefore diatom abundance may be made (Peinerud, 2000). In the sediments of Lobsigensee however Si counts mirror those of Ti therefore it can be said that detrital sources make up the larger part of total silica. Even though diatoms were found to be more abundant towards the surface sediment, biogenic silica does not seem to contribute strongly to this element.

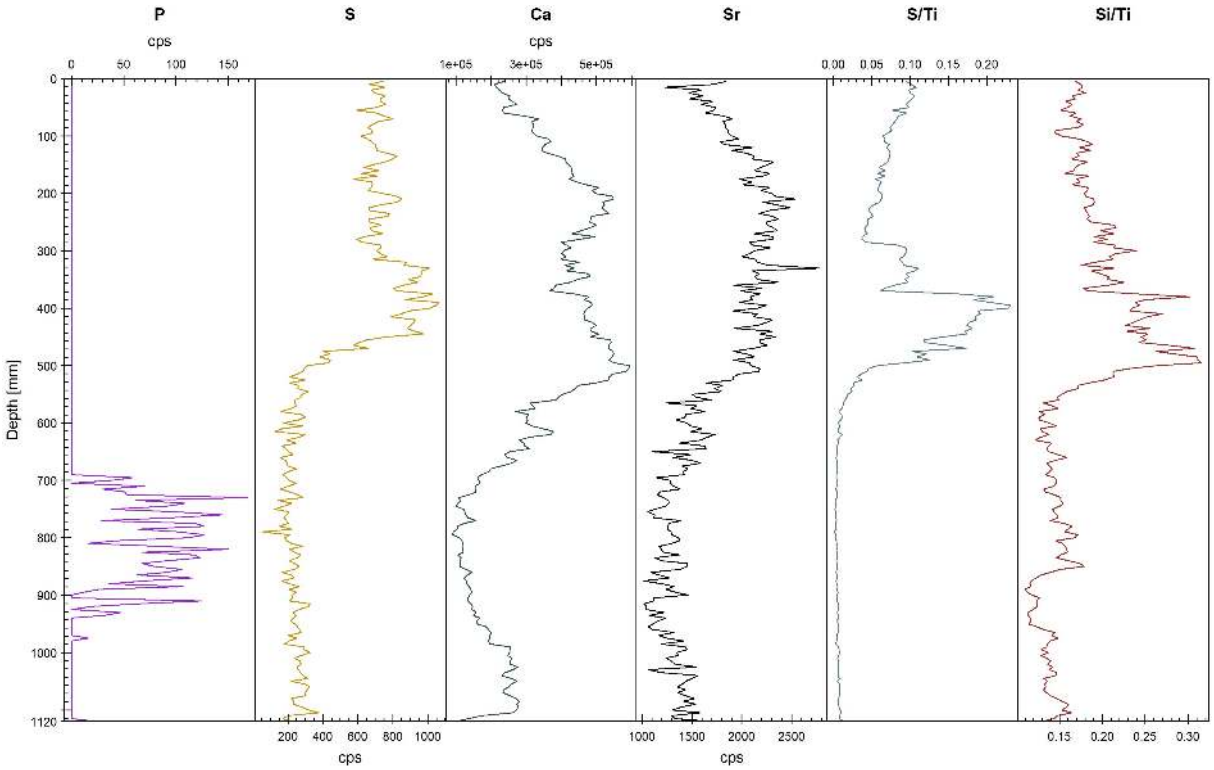

Fig. 15: X-Ray fluorescence (XRF) data on organic proxies. Single elements are shown in counts per second (cps) whereas elemental ratios are without unit.

4.3 Hyperspectral Imaging

Hyperspectral imaging was done on both cores. The spectral indices considered in this study are shown in Figure 16. Since the cores originate from the same location the signals are expected to show similar features. Indeed, all indices show a concurring signal between the two cores. Note the shift of certain features in core no. 2 compared to no. 3. This is further described in Section 4.4.

Erosional input to the lake seems to have decreased from depth 70 cm to about 50 cm in core no. 3 as suggested by the index R_{570}/R_{630}. Unit 1 then shows again a rather constant clastic input albeit slightly higher compared to lower Unit 2. In addition, Unit 2 is characterised by very low amounts of phycocyanins (RABD_{615}), green pigments (RABD_{670}) and BPhe *a* (RABD_{845}). This nutrient poor state of the lake is drastically altered towards more nutrient rich conditions in the last mid-century which continues to this day. Purple sulphur bacteria seem to have only appeared in the last few years shown by the significant increase of the index RABD_{845} near the top. Together with the increase in chloropigments this indicates more anoxic conditions in the lake with a concurrent increase in productivity in recent years.

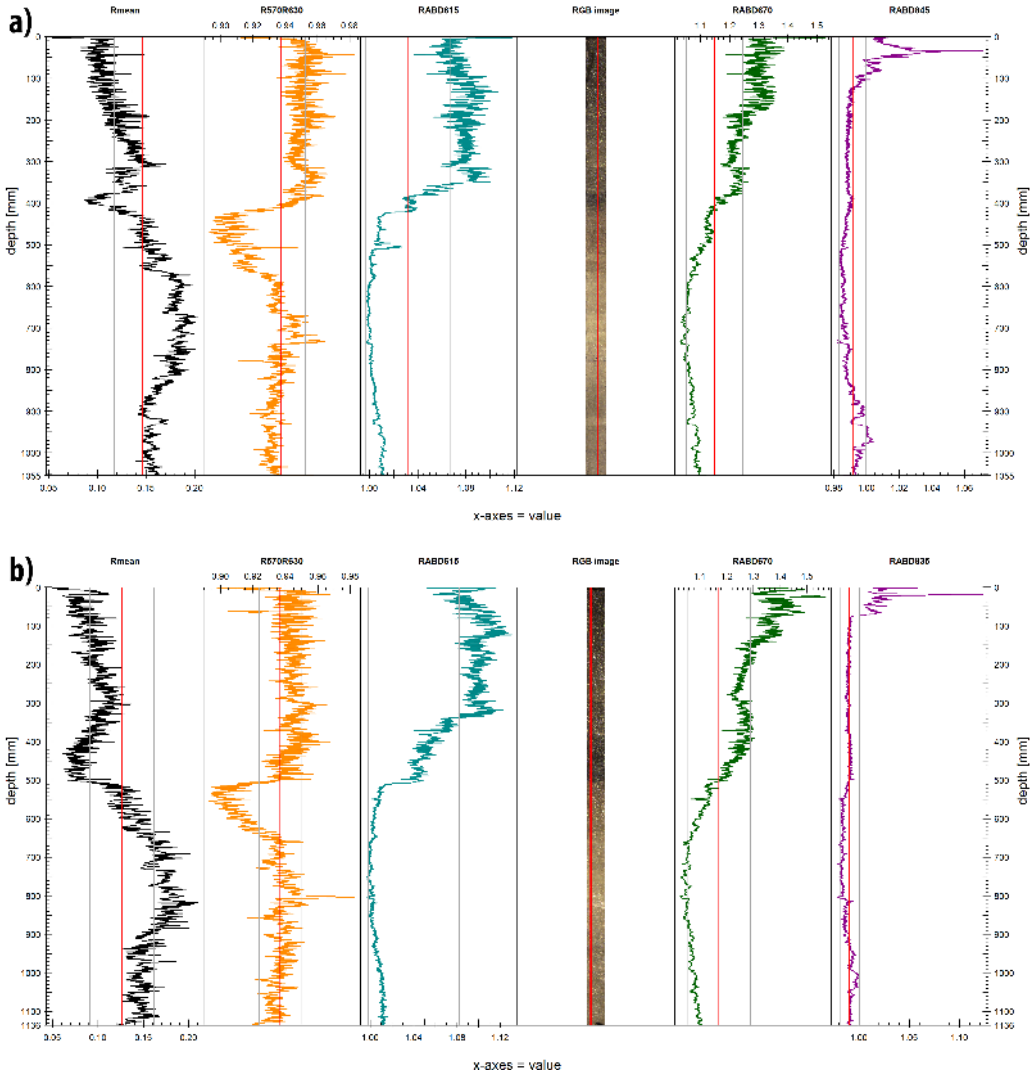

Fig. 16: Summary plot of hyperspectral imaging (HSI) data. a) Core LOB21-2. b) Core LOB21-3. All indices are calculated from the red subset shown in the RGB images. Black: R_{mean} (mean reflectance). Orange: R_{570}/R_{630} (clastic input). Cyan: RABD_{615} (phycocyanins from cyanobacteria). Green: RABD_{670} (green pigments from green algae). Purple: RABD_{845} (BPhe *a* from anoxygenic phototrophic bacteria).

4.4 Age-Depth Modelling and Core Correlation

The resulting activity plots from core LOB21-2 of ^{226}Ra, total ^{210}Pb and ^{137}Cs together with the determined unsupported fraction of ^{210}Pb are shown in Figure 17. From the ^{137}Cs activity, the ages 1954, 1963 and 1986 are attributed to mean depths 41 cm, 37 cm and 29 cm respectively, shown as vertical lines. Samples where ^{137}Cs activity was below the limit of detection are set to zero to indicate the onset of 1954. The unsupported fraction of ^{210}Pb shows a declining trend until depth 41 cm, from where on it shows a more erratic behaviour down-core. This coincides with the sudden variation in lithogenic input as shown by R_{570}/R_{630} in Figure 16a) from core 2 and the Ti record and sediment description of core 3 at the corresponding depth.

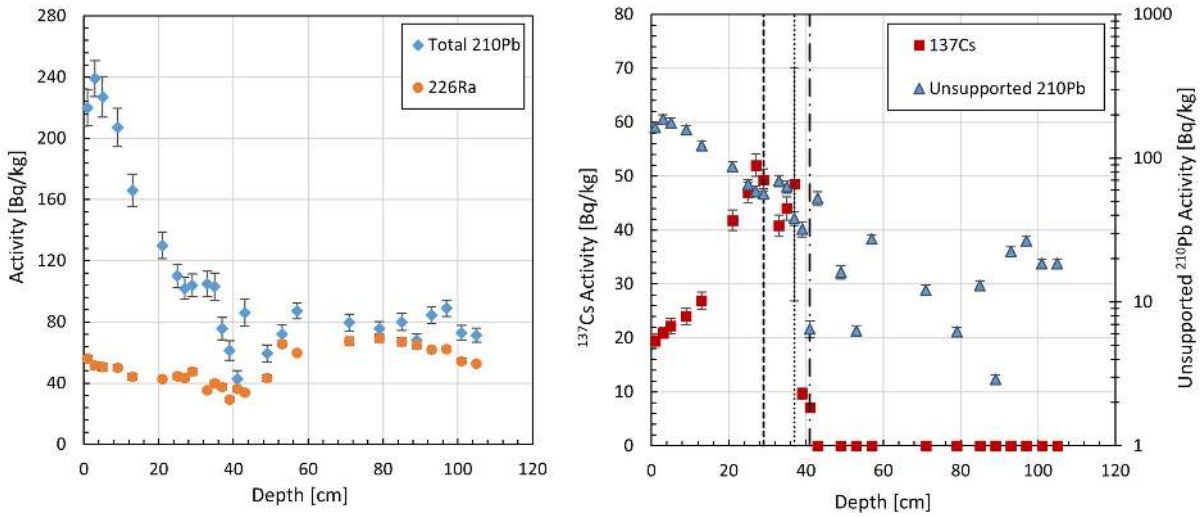

Fig. 17: Activity plots resulting from γ-spectrometry. Left: Total ^{210}Pb (diamonds) and ^{226}Ra (dots) activity. Right: ^{137}Cs activity (squares) together with the unsupported ^{210}Pb activity (triangles), the latter being shown in a semi-log scale. Samples where ^{137}Cs activity was below the limit of detection are set to zero to indicate the onset of 1954. Additionally, the three chronomarkers from ^{137}Cs are shown as vertical lines: 1954 (point-dashed), 1963 (dotted) and 1986 (dashed).

As these values cannot be reliably used to model the age-depth relation, the following procedure is used to build a CRS model which covers the depth of the PPP samples: Firstly, the ^{210}Pb data below 41 cm is disregarded. Then, until mean depth 41 cm, the measured activity is used to build a CRS model constrained to 1963 to date these samples. Constrains to 1954 and 1986 have also been tested but were disregarded. More information can be found in Appendix B. To extend the chronology beyond, an exponential fit is applied based on the unsupported ^{210}Pb values from 0 to 41 cm, which is then extended to depth 110 cm as shown in Figure 18 with the dotted line. With these extrapolated activity values, an unconstrained CRS model is built and the ages below 41 cm are then taken from this model for the final composite age-depth model. To avoid age inversions at the interface from measurement to extrapolation, half the age uncertainty is subtracted from the ages below 41 cm. The resulting age-depth model of core LOB21-2 is depicted in Figure 19. Sedimentation rate was calculated to be between 0.5 1.1 cm/yr, while mass accumulation rate (MAR) ranged from 0.1 g/cm^{2}yr to 0.2 g/cm^{2}yr for the period of interest.

The age-depth model is then translated to core LOB21-3 by linearly interpolating certain correlated layers both from visual and HSI analysis, as detailed in Figure 20. This is done by using the interpolation function `approx` with method `linear` in R v. 4.1.3 (R Core Team, 2021). It must be addressed that an ever increasing age uncertainty needs to be considered for all samples analysed where there is no measured ^{210}Pb data available. Since the PPPs are measured down to a depth of 60 cm in core LOB21-3, the age associated to these samples need

to be interpreted cautiously.

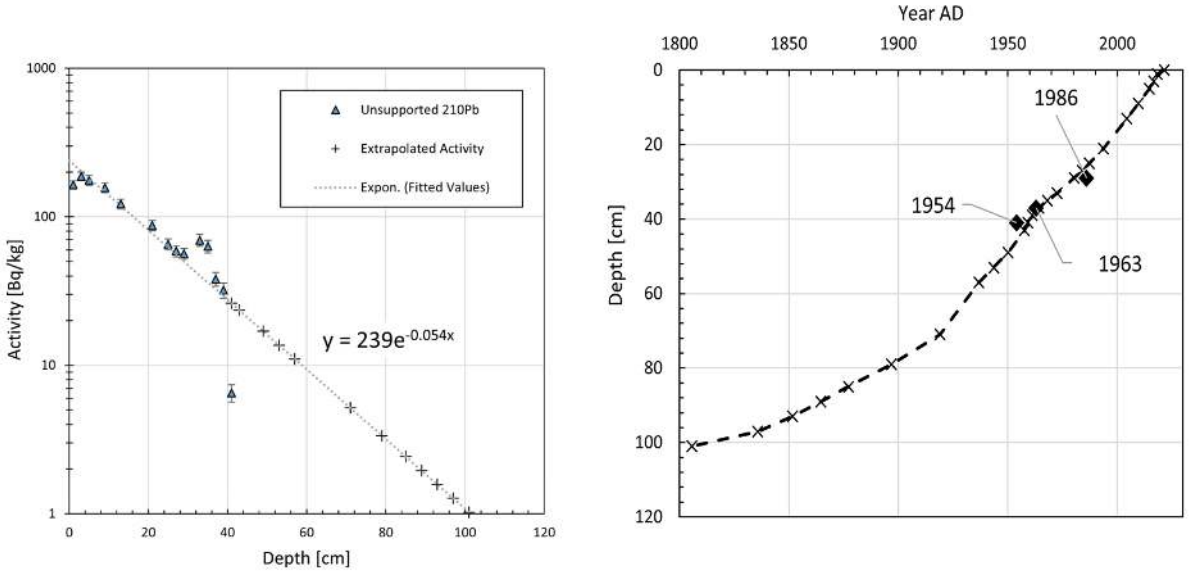

Fig. 18: Fitted activity of unsupported ^{210}Pb and fitted unconstrained CRS model. Left: Exponential activity fit (dashed line) based on unsupported ^{210}Pb activity from 0 to 41 cm (triangles) The crosses correspond to samples which showed unreliable Pb activity. Right: Unconstrained CRS model using activity values from the exponential fit.

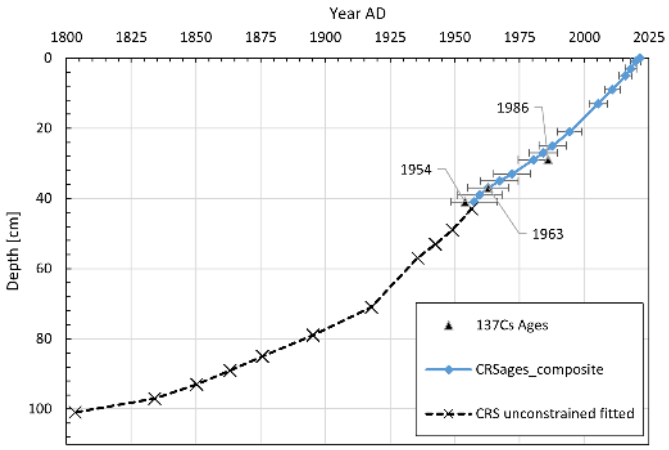

Fig. 19: Composite CRS model of Master Core LOB21-2. The blue line denotes the CRS model constrained to 1963 built from the measurements from 0 cm to 41 cm. The dashed line with onset 41 cm describes the unconstrained CRS model built from the extrapolated ^{210}Pb activity based on an exponential fit of the activity from 0 cm to 41 cm.

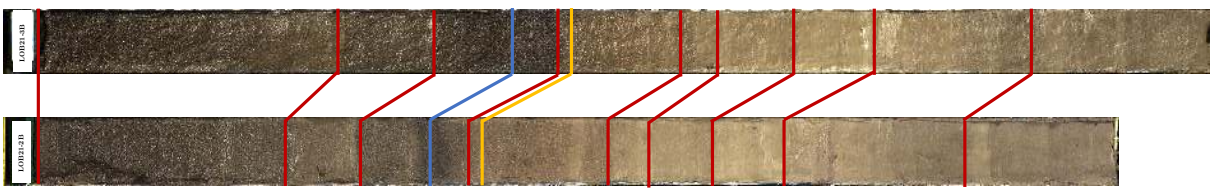

Fig. 20: Correlation of the master core LOB21-2 to core LOB21-3 used for PPP analysis. Visually correlated features are shown in red, blue denotes a feature identified from RABD$_{615}$, orange a feature correlated from R_{570}/R_{630}.

4.5 LOI and CNS

The down-core variability of carbon content in the sediments alongside the results from CNS analysis are shown in Figure 21. All the contents are given as weight percentage of the dry sediment weight. Inorganic carbon (IC) is determined from LOI_{950} whereas total organic carbon (OC) content results from IC being subtracted from total carbon (TC) as measured by CNS analysis. More information on the calculations is found in Appendix D.

Water content is found to decrease towards lower depths due to compaction of the sediment forcing out pore water and more lithogenic material in the sediment. The top is characterised by very porous and therefore watery sediment. LOI and CNS analysis further shows the lower part of the core being depleted in OC with increasing content towards the top. The same picture is drawn from total nitrogen and sulphur further revealing the increasing level of eutrophication of the pond in more recent years. From depth 55 cm on towards the top, the ratio of OC to nitrogen shows values consistently below 10 indicating organic matter predominantly originating from lake algae.

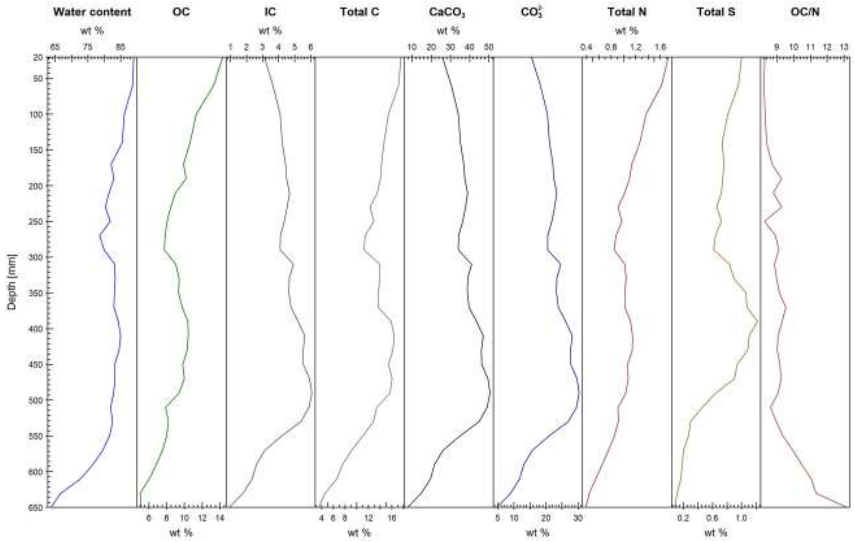

Fig. 21: Down-core results of loss on ignition (LOI) and carbon/nitrogen/sulphur (CNS) analysis. Further shown are water content in weight % (as measured from drying the sediment) as well as $CaCO_3$ and CO_3^{2-} content.

4.6 Temporal PPP Analysis

4.6.1 Detected Compounds, Concentrations and Fluxes

Of a total of 71 screened compounds, 26 chemicals are detected including 10 herbicides, 12 fungicides, two insecticides and one metabolite (terbutylazine-2-hydroxy). Additionally, the herbicide safener isoxadifen-ethyl is found, a chemical added to pesticide mixtures enhancing the resistance of crops to herbicides. Only the lowest depth examined (58-60 cm) is revealed to be pesticide-free.

When normalised to total OC, the PPP present at lowest concentration is bentazone (3 ng/kg_{oc} - 15 ng/kg_{oc}). In contrast, highest concentrations are measured for difenoconazole (19 ng/kg_{oc} - 4490 ng/kg_{oc}), tembotrione (19 ng/kg_{oc} - 1161 ng/kg_{oc}) and fenpropimorph (31 ng/kg_{oc} - 1085 ng/kg_{oc}). Fungicide fluxes range from as low as 10 pg/cm^2yr when first detected (azoxystrobine) to above 4000 pg/cm^2yr (difenoconazole). Regarding herbicides, fluxes are between 9 pg/cm^2yr (bentazone) and 1328 pg/cm^2yr (tembotrione). The two insecticides detected were found to be present at fluxes ranging from 30 pg/cm^2yr (thiamethoxam) to 238 pg/cm^2yr (chlorpyrifos).

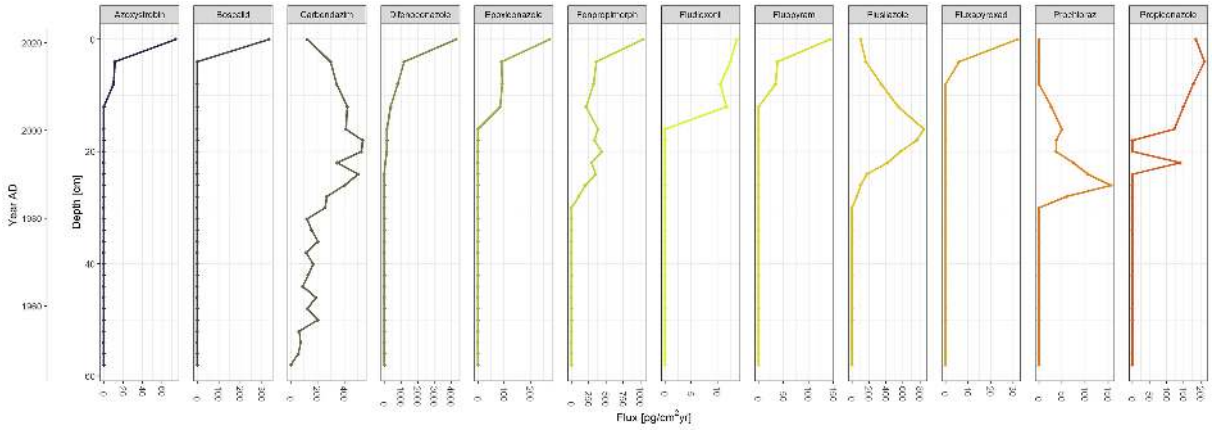

Fig. 22: Down-core evolution of fungicide fluxes in Lobsigensee. Shown are the fluxes of detected compounds classified as fungicides in picograms/cm^{2}yr. Note the different scales as the values show absolute fluxes.

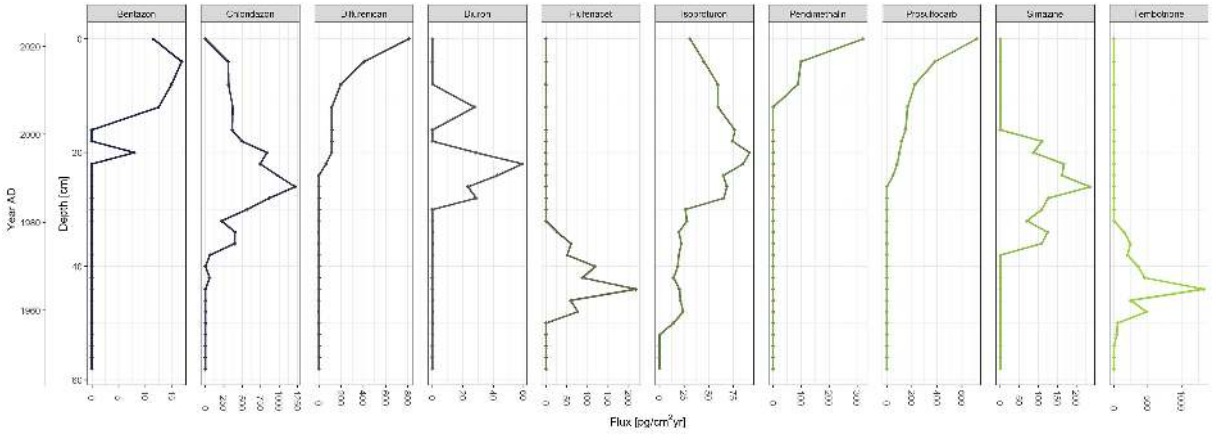

Fig. 23: Down-core evolution of herbicide fluxes in in sediments of Lobsigensee. Shown are the fluxes of detected compounds classified as herbicides in picograms/cm^{2}yr. Note the different scales as the values show the absolute fluxes.

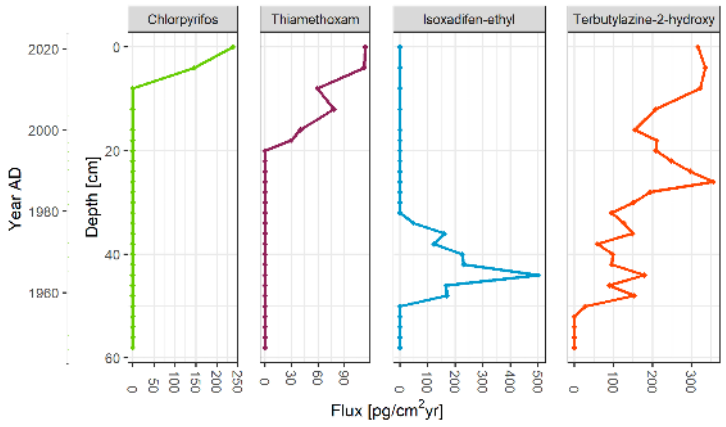

Fig. 24: Down-core evolution of insecticide, metabolite and herbicide safener fluxes in sediments of Lobsigensee. Left: Insecticides chlorpyrifos and thiamethoxdam. Right: herbicide safener isoxadifen-ethyl together with the metabolite terbutylazine-2-hydroxy. Note the different scales as the values show the absolute fluxes.

4.6.2 Hierarchical Cluster Analysis of PPPs

Hierarchical agglomerative clustering yields three significant clusters of PPPs when looking at average silhouette width taken from the skeleton plots as displayed in Figure 25. Additional summary plots regarding HCA are found in Appendix H.

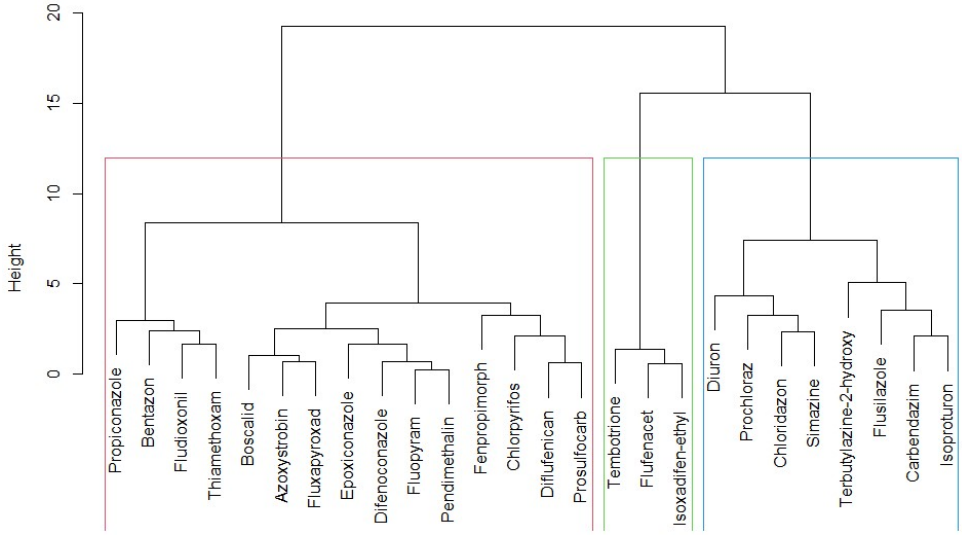

Fig. 25: Dendrogram resulting from Hierarchical Cluster Analysis performed on scaled PPP flux values. Three significant cluster are identified and framed in different colors.

If the normalised fluxes within these clusters are plotted together, these groups are distinguished by contrasting temporal deposition patterns, as seen in Figure 26. In cluster 1, the herbicides tembotrione and flufenacet together with the safener isoxadifen-ethyl are present. As the herbicide safener is used together with tembotrione, their concurrent occurrence in the sediment is expected. The cluster is characterised by an early occurrence of these chemical in the 1950s with sharply increasing fluxes and a subsequent decrease. However, these PPPs occur in a depth of which the attributed age is older than their initial introduction (occurrence vs. introduction: tembotrione: 1955 vs. 2007, flufenacet: 1959 vs. 2004, isoxadifen-ethyl: 1959 vs. 2002). A similar situation has been found in the sediments of the ponds Chly Moossee (Gosain, 2022) and Sängeliweiher (Fahrni, 2021). Therefore, this measurement can be regarded as robust. Even when taking into account the age uncertainty, the discrepancy between first occurrence and official introduction amounts to several decades. Chemical properties such as low K_{oc} and thus higher mobility may allow these compounds to infiltrate pore water and thus seep to lower sediment layers instead of being directly adsorbed and fixed to sediment particles. Tembotrione has a K_{oc} of 14 and according to this it is not expected to adsorb to suspended particles and sediments that well. Anaerobic conditions at the sediment-water interface during deposition may also explain that tembotrione was still above LOD, since its half-life in aerobic conditions in soils is reported to be 4 to 56 days (PubChem, 2022). Therefore, prevailing anaerobic conditions are needed for tembotrione to be persistent in the sediment, else it could degrade. Compared to all other detected PPPs, tembotrione exhibits the lowest K_{oc} value. For flufenacet, a K_{oc} value of 401 is determined, which is attributed to slight mobility and therefore the infiltration hypothesis might not be valid for this compound. However, chemically, they both have a trifluormethyl group, which might result in similar reactivity towards adsorption and post-depositional processes. Bioturbation of the sediment also may influence penetration depth of C_{org}, which is found to permeate into lower layers during such events (Aller & Cochran, 2019). If translated to core number 3, the highly variable 210 Pb activity from core 2 starts at depth 52 cm. The findings of the core description support the hypothesis of strong reworking of sediments during this time as the sharp contrast in sediment composition shows. This is in

phase with anthropogenic lake lowering phases from 1928 to 1934 and again in 1944, which may also have contributed to the disturbance of sediments.

Cluster 2 shows the most compounds with first occurrences of PPPs in the 1980s. All PPPs in this cluster have been detected in the most recent sediments revealing their ongoing application in the catchment. Some PPPs have just recently been banned (i.e. chlorpyrifos and epoxiconazole in 2021), the banning effect will only be observed in the years to come, as their current application remains high, shown by increasing fluxes in more recent sediments.

Cluster 3 is characterised by compounds being detected throughout the whole sediment core. It includes the herbicides chloridazon and simazine which show first appearances in the 1960s and 1970s, a few years after their introduction to the agricultural market in 1960 (simazine) and 1964 (chloridazon) (Lewis et al., 2016).

Similar to findings in Moossee produced by Chiaia-Hernández et al. (2020), reduced sale volumes of diuron and chloridazon and the ban of simazine in 2012 are shown as PPP concentrations near zero (< LOD). Further, the herbicide isoproturon shows a decreasing trend which is in phase with a decrease in sales of this chemical between 80 and 100 % in the last 13 years (Chiaia-Hernández et al., 2020). The ban of carbendazim in 2016 also shows with decreasing concentrations near the surface of the core.

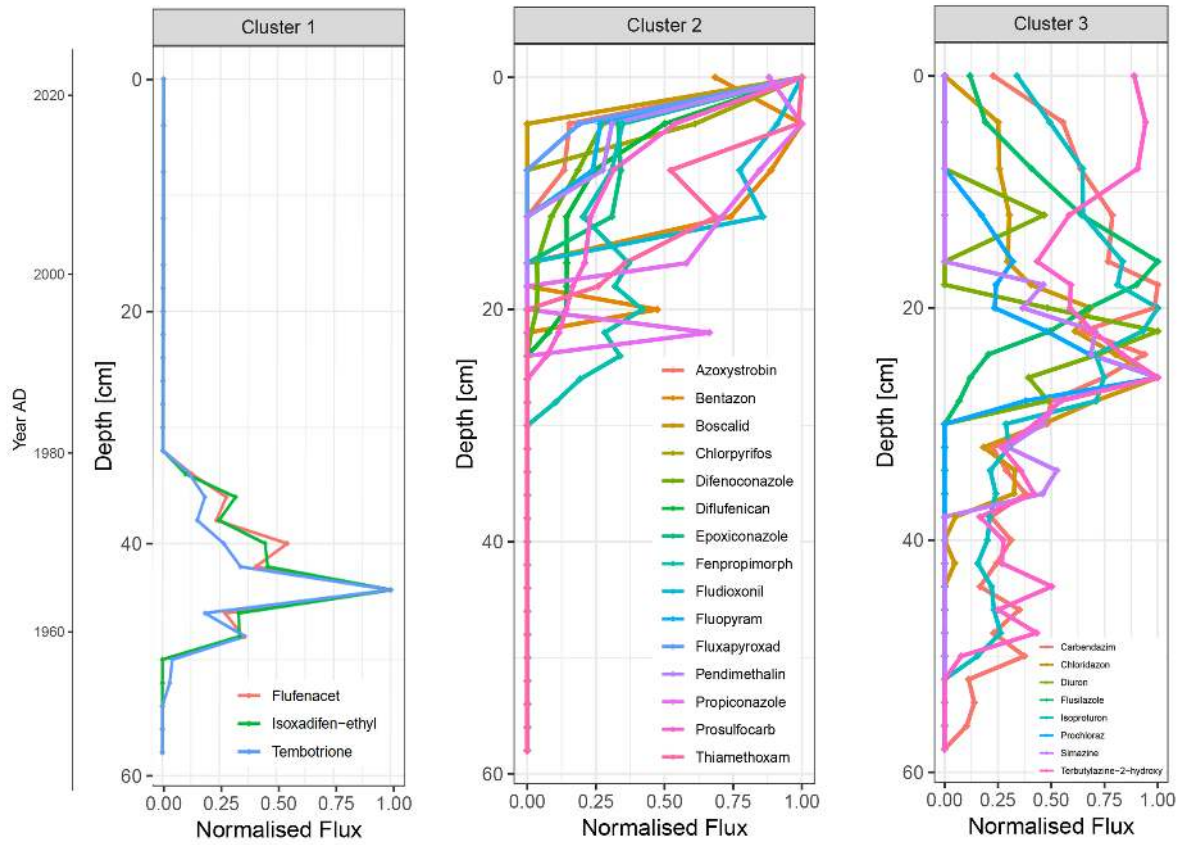

Fig. 26: Vertical normalised fluxes sorted by hierarchical cluster analysis. Shown are three distinct clusters with different occurrence patterns.

4.6.3 Results from HRMS Peak Picking

The data analysis from the Triple Quad revealed the TP atrazine-desisopropyl in one core sample only, albeit at very low concentration. With the help of HRMS data and peak picking in XCal Browser this was ruled out since there was no clear retention time (RT) signal and no matching m/z peak in the spectrum. Otherwise, all but six of the detected compounds have been verified in the core with HRMS data. Five out of these six are detected at m/z below 300 and were

found at low concentrations. Since the HRMS is less sensitive to lower concentrations, this may explain why the signals of these PPPs are not present in the high-resolution mass spectrometry data. Additionally, some compounds may have degraded due to the rather long storage time between the QQQ and HRMS measurements.

A total of 12 TPs have been detected in the water column in the 2013 study by K. Guthruf et al. (2015). Out of these, only two have been detected in the HRMS data from the sediment core: terbutylazine-2-hydroxy and desaminometamitrone. The process of detecting a compound is shown in Figure 27 with the example of desaminometamitrone. With isotope simulation, the exact m/z value is extracted by entering the chemical formula and choosing a single hydrogen atom as adduct (Figure 27, lower panel). Then the overall chromatogram is filtered to this m/z value. The measured chromatogram of some core samples thereby shows an effluent peak at around 6.6 minutes RT, which matches the predicted RT of desaminometamitrone based on $\log K_{ow}$ values. The spectrum at this RT is then analysed if it matches the simulated spectrum. Depending on the chemical, isotopic peaks are also seen in the spectrum, which further improves the identification. Additionally, measured fragment spectra can be compared to theoretical fragmentation. In the case of desaminometamitrone, the compound has been confirmed at level 1 according to the identification level proposed by Schymanski, Jeon et al. (2014). For true unambiguous identification, a reference standard would be needed. The process however confirms the presence of this TP in the sediments of Lobsigensee. However, it was not quantified, since it is not on the target list of the QQQ, in contrary to terbutylazine-2-OH for which quantification was possible.

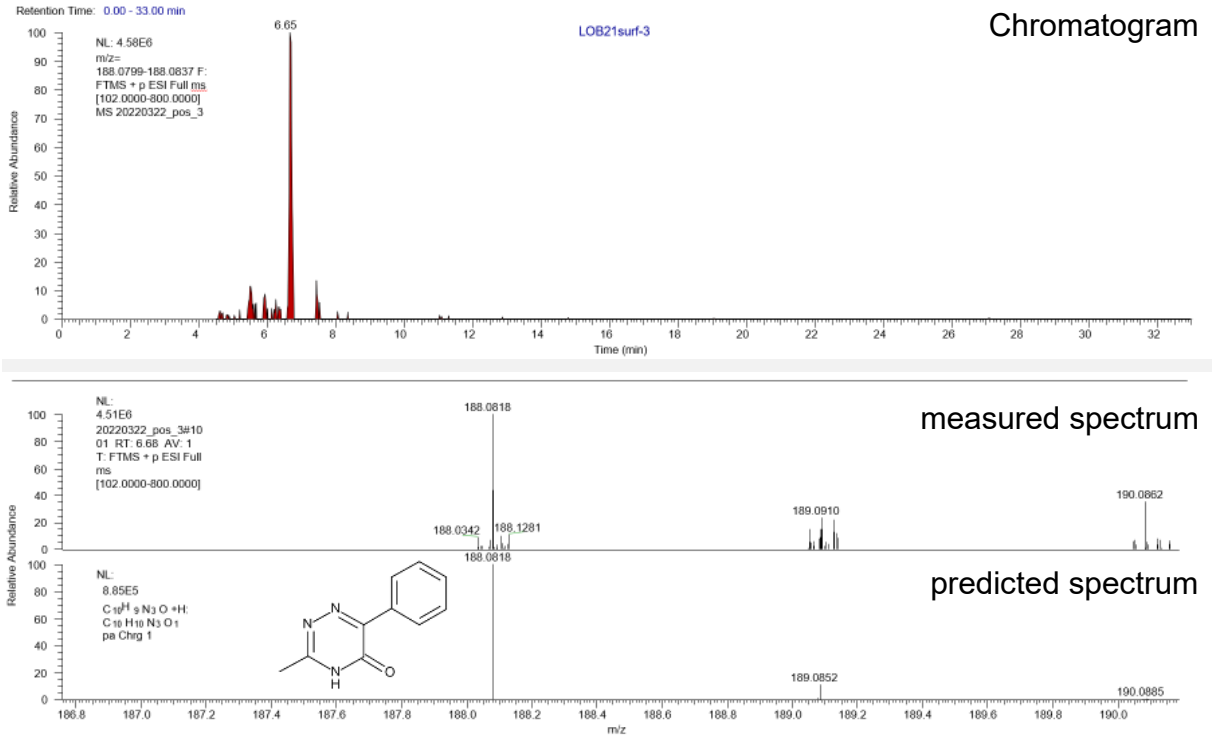

Fig. 27: HRMS peak picking done in QualBrowser showing the identifications used for nontarget analysis with desaminometamitrone as example. Top panel: Chromatogram (red curve) of surface sediment sample 3 showing a peak signal at retention time 6.65 minutes. Lower panel: measured spectrum with the simulated spectrum beneath. The simulation shows a signal at m/z = 188.0818. The sample matches this value to a precision of 4 decimals at a mass tolerance of 10 ppm. Isotopic peaks are also visible in the spectrum at m/z 189.0910 and 190.

4.7 Temporal Ecological Risk Assessment

The sediment quality for most PPPs can be considered very good to good if they are considered as single substances and RQ values are calculated individually. Some compounds show RQ values < 1, most even < 0.1. Some substances however exceed the quality control: The insecticide chlorpyrifos and the herbicide diflufenican show RQ values above 2, while thiamethoxam shows values close to 20, tembotrione even > 20. As a neonicotinoid insecticide, thiamethoxam has been shown to impose chronic responses for crustaceans and ostracods (Finnegan et al., 2017). However, organisms are not only exposed to single chemicals at a time but rather a cocktail of toxic PPPs. It is thus important to also consider cumulative risks, hereby assessed as worst-case scenario $\sum$RQ (Moschet et al., 2014). This results in a different picture, as Figure 28 suggests. Regarding herbicides, sediment quality was heavily impaired by tembotrione, dominating the cumulative RQ values. While after its disappearance from the sediment, RQ values remained low throughout the 1980s until the 2000s, cumulative risk assessment shows again a trend toward insufficient quality ($1 < \sum\text{RQ} < 10$). The same holds for fungicides, which show similar rising RQ values in more recent years. Regarding insecticides, only two compounds have been detected and the cumulative risk is dominated by thiamethoxam.

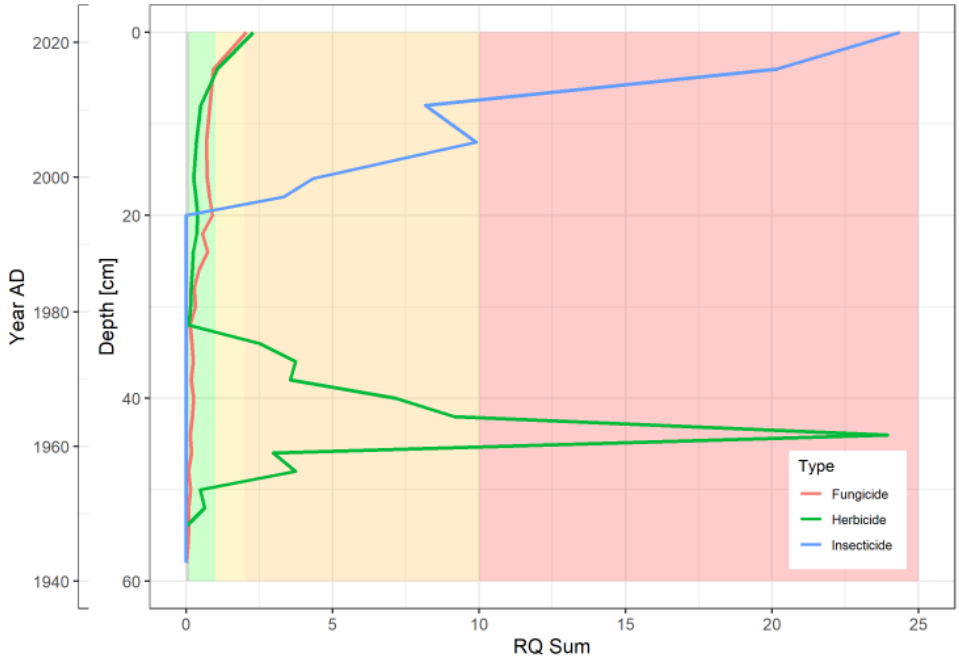

Fig. 28: Summed up risk quotient for the three main pesticide types.

4.8 Spatial PPP Analysis

4.8.1 Detected Compounds

In total 25 compounds have been detected across all surface sediment samples. The findings include 12 herbicides, 11 fungicides, one insecticide and two TPs. For presenting the overall results it was distinguished between mean concentrations of pond sediments and mean concentration of outflow and reed belt sediments. Figure 29 shows the mean concentrations of PPPs over all samples detected in the pond surface sediments. Concentrations range from as low as 0.1 µg/kg$_{oc}$ (fluazinam) to as high as 105.2 µg/kg$_{oc}$ (terbutylazine-2-OH). Even the lowest limit of these predicted concentrations is higher than the one of the temporal sediment core samples. The mean concentration of TP terbutylazine-2-OH in the surface sediment samples exceeds the concentration in core samples by a factor of 1159 (mean concentration in the surface sediments: 132132.4 ng/kg$_{oc}$ vs. mean concentration in the core: 114 ng/kg$_{oc}$). Even samples with a low OC content show high concentrations per kg dry sediment, which results in even higher predicted concentrations per kg OC.

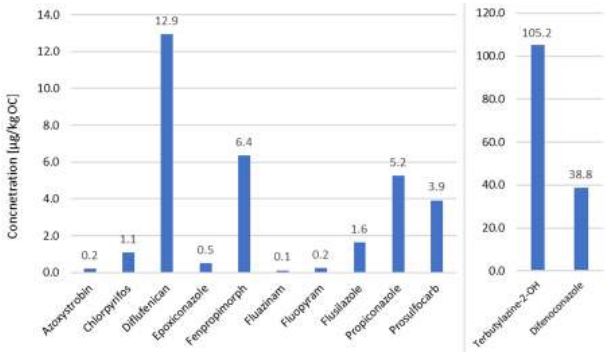

Fig. 29: Mean concentrations of PPPs detected in pond surface sediments. Shown are only 12 out of 25 PPPs, since not all compounds have been detected in the pond sediments. Note the different scale for terbutylazine-2-OH and difenoconazole.

On the contrary, Figure 30 shows the mean concentrations of compounds detected in the four samples taken at the outflow and the reed belt. Mean concentration within the pond sediments range from as low as 0.1 µg/kg$_{oc}$ (fluazinam) to as high as 105.2 µg/kg$_{oc}$ (terbutylazine-2-OH). In the outflow region and reed belt, mean concentrations range from 0.2 µg/kg$_{oc}$ (fluazinam) to 233.0 µg/kg$_{oc}$ (terbutylazine-2-OH). The concentration of terbutylazine-2-OH is thus more than double than within the pond.

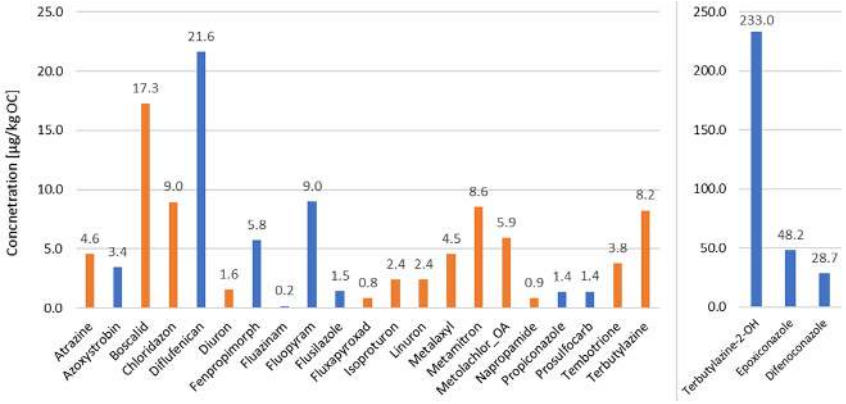

Fig. 30: Mean concentrations of PPPs detected in reed belt sediments and outflow sediments. The orange bars denote those PPPs which have been exlusively detected in these four samples. Note the different scale for terbutylazine-2-OH, epoxiconazole and difenoconazole.

13 compounds (orange bars in Figure 30) have only been detected in the samples taken within the reed belt at the southeastern shore or at the outflow, see Figure 11 as spatial reference. They include atrazine, boscalid, chloridazon, diuron, fluxapyroxad, isproturon, linuron, metalaxyl, metamitron, napropamide, tembotrione and terbuthylazine and the TP metolachlor-OA. All these chemicals have not been detected within the surface sediments of the pond itself. This discrepancy already indicates the importance of a vegetation belt being present around a surficial water body. Apparently, this belt may act as a sieve and sink for certain compounds. Others however might still be able to be washed through the reed into the pond where they are deposited.

Intriguingly, out of these 13 PPPs, four have also been detected in the topmost 10 cm of the core albeit in very low concentrations (up to 14.8 µg/kg$_{oc}$). These include boscalid, chloridazon, fluxapyroxad and isoproturon. However, these four compounds have been verified by HRMS data analysis to be real signals. These findings hint at very local anaerobic conditions at the sediment-water interface at the coring location, which favours PPP conservation. At other, less deep locations in the pond, more oxygenic conditions and different biodegrading organisms may lead to faster degradation. Near the shore, in the reed belt or the outflow area, oxic conditions needed for degradation are expected to be given. The reason that these PPPs are still present in these locations might be the recent application in the days or months prior to the sampling campaign. This is also reflected in the DT_{50} in water-sediment matrices of these four compounds: DT_{50} = 545 days (boscalid), DT_{50} = 137 days (chloridazon), DT_{50} > 847 days (fluxapyroxad) and DT_{50} = 149 days for isoproturon (Lewis et al., 2016).

4.8.2 Grain Size and Concentration Mappings of PPPs

The spatial distribution of grain size fraction is shown in Figure 31. The grain size analysis shows that silt makes up the dominant fraction of the lithogenic component in all sediment samples. Hereby percentages range from 70.5 % to 83.9 % within the pond, whereas the two samples from the reed belt show a smaller silt fraction with 63.6 % and 73.8 %. Sand then constitutes second most to the composition with fractions ranging from 10.3 % to 24.4 %. The reed belt samples show a greater sand fraction with 30 % and 47.3 % respectively. Clay shows the largest fraction in the two samples from the vegetation belt with 10 % and 10.4 %, otherwise it amounts to values ranging from as low as 3.8 % to 8 % within the pond itself. The two samples taken at the outflow Seebach show a greater sand fraction (30 % and 47.2 %). This is to be expected as they are more easily sedimented due to their increased size compared to fine-grained silt or clay. The latter is either transported into the pond or washed downstream, whereas sand particles are deposited along the shore or at the outflow.

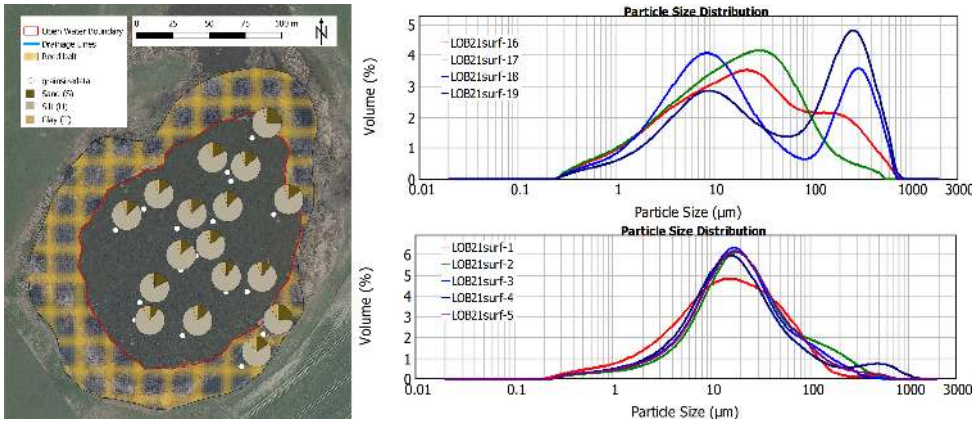

Fig. 31: Spatial grain size distribution at Lobsigensee. Left: Grain size pie charts showing the fraction of sand, silt and clay components in the grab samples. The yellow cross-hatched area shows the reed-belt, the red lines denotes the open-water boundary to the reed belt. Right: GSD plots for selected samples. The upper panel shows samples taken in the reed belt and outflow.

To show the spatial variability of PPP concentrations in the sediment around and within the pond, PPPs with non-zero concentrations in all spatial samples are shown in Figure 32. They include the TP terbutylazine-2-OH, the fungicides difenoconazole, fluazinam, fenpropimorph and propiconazole as well as the herbicide diflufenican. These chemicals all show elevated concentration levels towards the centre of the pond, except for propiconazole. However, regarding propiconazole, overall concentrations are very low and when compared to the other PPPs, this inverse concentration effect is strongly diminished.

This supports findings of PPP being persistent in the water column under anaerobic conditions (Ochsenbein et al., 2015). Coring in the center of the pond is indeed the best sampling location, since the compounds entering the water body are in fact preserved there. Lobsigensee is heavily influenced by anthropogenic activity and anoxic conditions in the hypolimnion are becoming more frequent. In summer months, epilimnic waters have been found to be depleted in oxygen or even totally anaerobic (K. Guthruf et al., 2015). Therefore, those PPPs scavenged from the water column in the centre of the pond are conserved. Near the shore however, oxygen and biodegrading organisms present at the sediment-water interface may be able to break the chemicals down, hence PPPs are detected at lower concentrations at these locations.

Fenpropimorph and propiconazole have been banned in Switzerland in 2020 and remaining stocks have been allowed to be used until beginning of 2022 (BLV, 2022c). DT_{50} in sediment-water compartments is found to be 38 days for fenpropimorph and 561 days for propiconazole (Lewis et al., 2016). The already low concentrations of these two PPPs indicate that fenpropimorph has probably been applied in the seasons before sampling or has been well preserved under anaerobic conditions. Otherwise it likely would have degraded to levels below detection, due to its moderate to low persistence (Lewis et al., 2016). Propiconazole however shows the effect of environmental persistence as reflected in the DT_{50}; even two years after a ban, it is still detected in the sediment.

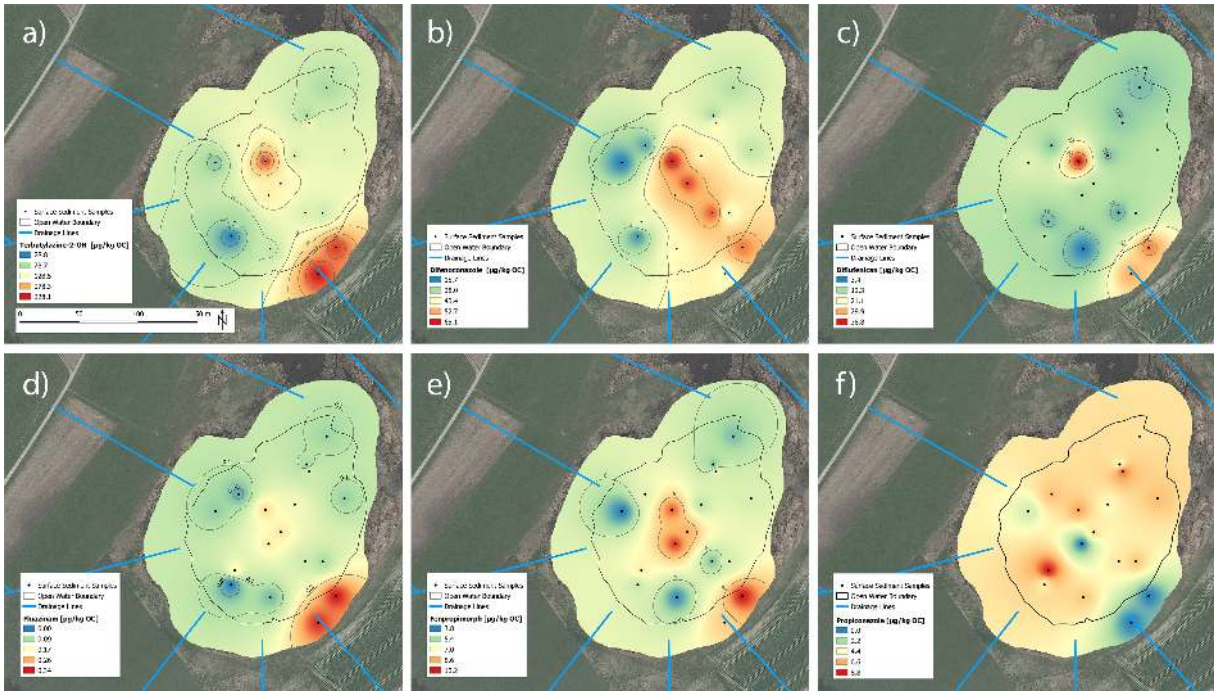

Fig. 32: Interpolation of PPP concentrations of selected compounds together with grain size data and drainage entries to the pond. a) Terbutylazine-2-hydroxy. b) Difenoconazole. c) Diflufenican. d) Fluazinam. e) Fenpropimorph. f) Propiconazole. PPP concentrations are shown in $\mu g/kg_{oc}$. The blue lines denote drainage lines which were georeferenced from (Alder, 2012).

Moreover, concentrations in the two samples taken in the reed belt have even been found to surpass the concentrations of those samples taken at the deepest point of the pond itself, see Figure 32 a) to e). A higher clay content in these samples may only partially explain this increase, as the concentrations are listed with respect to organic carbon. It is more likely the influence of drainage lines that drives concentrations up. These sample locations coincide with the approximate exit point of one of the drainage lines buried in the fields. Additionally, there is an orchard located in southeastern direction to the pond, which might act as an additional source of PPPs. Orchards may especially act as sources of PPPs, since an excess of chemicals might be applied because individual tree properties such as canopy size are neglected (Berk et al., 2016). The surface sediments taken at Lobsigensee in this study incorporate approximately the last 10 years because the scooping tool used sinks into the soft topmost sediment. Therefore, PPP applications from pre-organic farming years might be responsible for the concentration peaks at the Southeastern shore of Lobsigensee, even though the orchard is nowadays applying organic farming practices.

Additionally, the herbicide terbutylazine together with its metabolite terbutylazine-2-OH was detected in the surface sediments. However, within the pond, only the TP was found, whereas the mother compound was only detected in the reed belt samples and at the outflow. The deposition is hypothesised to occur as follows: Apparently, after application of terbutylazine in the field, it gets washed out either by surface run-off or subsurface drainage flow, where it is deposited at the edge of the reed belt. There it starts degrading, producing the TP terbutylazine-2-hydroxy. Degradation might also occur in transit to the pond. And it is then this daughter compound that is able to be transported into the pond where it is finally sedimented. There may be a small fraction of terbutylazine being able to pass this vegetation barrier. However due to its rather short DT_{50} of 6 days in water (Lewis et al., 2016), terbutylazine may have already degraded to quantities below LOD before being sedimented. In the sediment, the metabolite then accumulates. It has been shown to be persistent up to 120 days in freshwater and groundwater systems (Velisek et al., 2014). However, anaerobic conditions may favour persistence even in the pore water of the sediment (Ochsenbein et al., 2015). In soils is has been found to be highly persistent with modelled DT_{50} of up to 1000 days (European Food Safety Authority, 2017).

4.8.3 Correlation of PPPs and Cultivation Register

Table 4 shows a non-exhaustive list of a selection of detected PPPs together with the type of plantation they are typically applied to. The latter are taken from the Swiss national register of plant protection products (BLV, 2022a). Included are the six PPPs detected throughout the whole pond sediments, whereas tembotrione and metalaxyl have only been detected in the reed belt and at the outflow.

PPP	Type	Detected in sediments	Plantation applied to
Difenoconazole	Fungicide	pond, reed belt, outflow	sugar beet, forage beet, wheat, potatoes
Fluazinam	Fungicide	pond, reed belt	potatoes, vines, decorative plants
Fenpropimorph	Fungicide	pond, reed belt, outflow	wheat, barley, rye
Propiconazole	Fungicide	pond, reed belt, outflow	sugar beet, forage beet, wheat, rye, barley
Terbutylazine	Herbicide	pond, reed belt, outflow	maize
Diflufenican	Herbicide	pond, reed belt, outflow	wheat, rye, barley
Tembotrione	Herbicide	reedbelt, outflow	maize, poppy
Fluxapyroxad	Fungicide	outflow only	potatoes, vines, fruits

Table 4: Excerpt of detected PPPs together with applied plantation types.

Compared to the cultivation register, all these plant types have been cultivated within the catchment in the most recent year except for rye, vines and poppy (see Figure 6). The largest fraction of the arable land is used for sugar beet production (12.6 %) followed by winter wheat (9.3 %) and winter barley (7.2 %). Another smaller fraction is used up by potato cultivation (6.1

%) and silage maize (5.6 %). It is thus reasonable to assume that the fungicides difenoconazole, fenpropimorph, propiconazole and fluazinam mainly stem from the most recent applications of PPPs in the year before sampling. An investigation of crop rotation in the last couple of years would reveal if applications in the years before also contribute to the concentrations found in the pond sediments. Depending on field slope and distance to the pond, concentrations might be lower as in the case of fluazinam.

Furthermore, according to the cultivation register of 2020 there have been a few more potato and maize fields outside the catchment in the direction of the outflow as shown in Figure 33. They have also been closer to the stream than those within the catchment in relation to the pond. Spray drift, direct surface runoff to the creek or drainage flow from these field might have resulted to the deposition of tembotrione and fluxapyroxad. This might explain why these two compounds have not been found in the pond sediments, but only in the reed belt and the outflow.

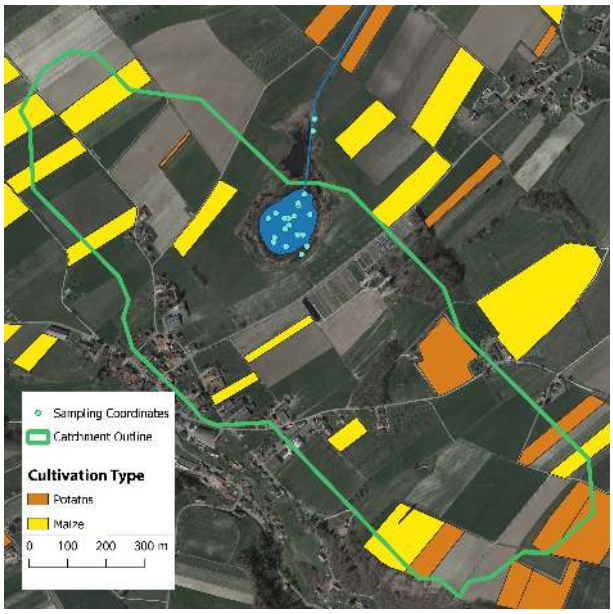

Fig. 33: Maize and potato cultivation in the region of the pond based on the year 2021. Three maize fields are relatively close to the two samples taken at the stream.

4.8.4 Comparison of TPs in Sediments of Lobsigensee with previous Studies

In the study performed by K. Guthruf et al. (2015), a total of 12 TPs have been detected in the water column. In the surface sediment samples analysed in the scope of this thesis, two TPs including terbutylazine-2-hydroxy and metolachlor-OA have been identified. For better comparison, concentration values of the final extracts are converted to predicted pore water concentrations. Additionally, from HRMS peack picking the TP desaminometamitrone has been identified to be present in the sediment as well, however no concentrations have been inferred.

While the ethanesulfonic acid (MESA) of metolachlor has been detected in the water phase together with its parent compound metolachlor, these two chemicals were not quantified in the surface sediments of the pond, since it is not on the suspect list of the mass spectrometer. However, metolachlor oxanilic acid (MOA), another metabolite of metolachlor, has been found to be present in the sediments of the outflow showing predicted concentrations of 1017 and 269 ng/L. Mean MESA concentrations found in the 2013 study ranged from 17.0 ng/L to 61.2 ng/L within the pond and 10.3 to 88.1 ng/L at the outflow. Therefore, MOA is present in much higher concentrations in the pore water of the sediment compared to MESA. But on the other hand it is only locally present in the sediment, as it is not found within the pond sediments. They both have very similar K_{oc} values ranging from 6.5 - 14.6 L/kg (MESA) and 2.7 - 13.7 L/kg

(MOA) (Brückner et al., 2017). Based on this, it is expected that also MESA is present within the sediments of Lobsigensee. Further measurements with enhanced suspect lists are needed to quantify these TPs. To the best of my knowledge there is no information on K_{ow} values on these two metabolites, so a statement regarding hydrophilia or lipophilia is difficult to make.

Additionally, the TP terbutylazine-2-OH has been detected in all surface sediments of the pond and at the outflow. Predicted pore water concentration in the sediment was determined to range from 93.2 ng/L - 821.3 ng/L, with highest concentrations found at the reed belt and the outflow. Concentrations in the pore water thus exceed those detected in the water column in 2013 by factors of 33 - 293. K_{oc} for terbutylazine-2-OH is found to be 192 (Lewis et al., 2016) while K_{ow} is determined to be 31.6 (Schuhmann et al., 2019). The comparison shows that once the metabolite enters surface waters, it is rapidly scavenged and accumulates in the sediment.

4.8.5 Comparison of PPPs in Sediments of Lobsigensee with other Ponds

Recently, a number of Swiss ponds located on the Swiss Plateau have been sampled for PPP analysis in the sediments using the exact same approach applied in this thesis. They include Sängeliweiher (Fahrni, 2021) and Chly Moossee (Gosain, 2022). Their relatively close location, similar size, same eutrophic state and mixing regime make them comparable to Lobsigensee. In the sediments of Lobsigensee, a total of 27 compounds (25 PPPs and 2 TPs) have been detected occurring over the last 70 years. Annual fluxes hereby range from 10 pg/cm^{2}yr to 4500 pg/cm^{2}yr. In Chly Moossee, 36 PPPs and one TP was detected with fluxes amounting from 10 pg/cm^{2}yr to 1700 pg/cm^{2}yr. And in the sediments of the pond Sängeliweiher, 34 PPPs and two TPs have been detected at yearly fluxes ranging from 5 pg/cm^{2}yr to 11000 pg/cm^{2}yr.

A comparison of the catchment composition shows that a higher share of agricultural activity in the catchment does not necessarily translate to an increase in total compounds and higher concentrations of contaminants in the pond sediments. Both Chly Moossee and Sängeliweiher have a smaller share of agriculture in their catchments, yet they are contaminated by more compounds. At Chly Moossee, the primary source of PPPs is hypothesised to be nearby the golf course, where predominantly fungicides are applied (Gosain, 2022). At Sängeliweiher, a rather large tree nursery might be a principal source of PPPs. Additionally, a study on topography and hydrology has revealed that erosion and artificial drainages might play a role in the deposition of PPPs into the pond of Sängeliweiher (Fahrni, 2021).

In agreement however, these studies all show the contamination of sediments of aquatic ecosystems by synthetic agrochemicals. Additionally, they show the complexity of identifying PPP sources, detecting pathways and analyzing the environmental fate of these PPPs.

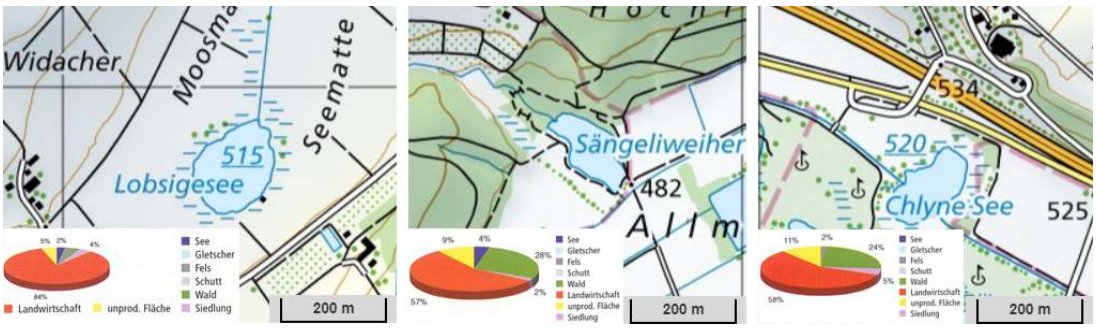

Fig. 34: Comparison of catchment composition of Lobsigensee to other ponds. While several characteristics such as size, trophic state or mixing regime correlate, the catchment composition is different. Red: Agriculture, yellow: unproductive lands, green: forest, pink: settlements. Share of agricultural area in the catchment: 84 % (Lobsigensee), 57 % (Sängeliweiher), 58 % (Chly Moossee). Pie charts are taken from J. Guthruf et al. (1999).

5 Conclusions

5.1 Recent Catchment Development of Lobsigensee

The catchment of Lobsigensee has undergone a lot of changes in the last few decades and even centuries. While the pond was surrounded by marshland before the 1950s, natural siltation enhanced through anthropogenic activities lead to a decrease in lake level and size. At the same time, much more nutrients were added to the lake as the surrounding fields were tilled. The only existing inflow to the pond has been closed sometime in the 1940s (von Büren & Leiser, 1961). Around the same time, surrounding lands were drained to gain more arable fields. While naturally eutrophic, human interference resulted in lake level lowerings, decrease in extent and strong eutrophication (J. Guthruf et al., 1999; K. Guthruf et al., 2015). In more recent decades, the pond can be classified as polytrophic, thereby revealing the consistent application of fertilisers in the catchment. The pond only has one small outflow, which together with the water body lies on a recessed plain. Together with low wind mixing and small discharge volume this leads to a longer resident time of the water in the pond (Ambrosetti et al., 2003). Therefore, dissolved substances are able to accumulate leading to a chemical altering of the water column and thus its environmental fate (Ambrosetti et al., 2003). In the case of Lobsigensee, this had consequences regarding the availability of oxygen in hypolimnic water leading to anaerobic conditions at the sediment-water interface. With the introduction of synthetic pesticides in the 1950s, a new class of chemicals started being transported to the water and sediment eventually. As a pond with a rather low water volume and slow outflow regime, these contaminants are expected to further accumulate in the pond, where the sediment may act as a sink.

This evolution is shown not only in studies done regarding the pond water by K. Guthruf et al. (2015), but it is also revealed in the sediment record produced in this thesis both visually and from different environmental sediment proxies. Sediment description reveals a strong increase in organic matter from a depth which is attributed to the year 1955. Before, the sediment seems to have been disturbed either by human activity, bioturbation or simply cattle traversing the shallower parts of the pond. This is revealed by the erratic ^{210}Pb measurements below the sharp change in sediment composition. Precipitated calcite indicates increased oxygenation of epilimnic waters and available nutrients in more recent decades. Oxygen measurements show significant O_2 depletion in the hypolimnion during stratification of the water column (K. Guthruf et al., 2015). At the same time, clastic proxies from XRF show a decrease thus hinting at less detrital input in the last few decades. This is attributed to the formation of e thick vegetation belt around the open water, including trees and reeds, which might stabilise the shoreline. Organic XRF proxies such as sulphur show a concurrent increase in concentrations. The pond eutrophication is further affirmed from green pigments detected by HSI.

As the pond is polymictic, nutrients from lower water layers are recycled back to the whole water column. J. Guthruf et al. (1999) predicts that even with a total suppression of nutrients entering the lake, primary production would remain high in the medium-term. While the lake has been under federal protection since 1955, there has been no sign of improvement regarding water quality and eutrophication (J. Guthruf et al., 1999; K. Guthruf et al., 2015).

5.2 Temporal PPP Record and Sediment Quality

The temporal PPP record that was produced in this thesis regarding the sediment of Lobsigensee revealed that these smaller lentic water bodies are indeed affected by contamination from agricultural practices. Out of 90 screened compounds, 26 have been identified, including 10 herbicides, 12 fungicides, two insecticides, one transformation products and a herbicide safener. The topmost 58 cm of sediment have been found to be contaminated by either single or multiple compounds. Three main deposition clusters of PPPs have been identified by HCA. There are some contaminants which stopped being applied at one point in time, while in another cluster

PPPs only start appearing from sediment depth 20 cm (1995) upwards. Some compounds such as tembotrione and flufenacet appear unexpectedly early in the sediment, at layers which are dated older than their original introduction. Reasons for this could be their chemical properties such as low K_{oc} values, which might allow these contaminants to infiltrate sediment pore water and seep to lower depths. Their K_{oc} are found to be lower than most other PPPs detected, tembotrione even shows the lowest value of all compunds detected. Bioturbation may enhance this process, as organic carbon has been found to permeate downwards during such events (Aller & Cochran, 2019). The findings from sediment description and XRF proxies support the theory of strong reworking of the sediment at depth 52 cm and lower, where tembotrione and flufenacet have been detected. In the third cluster are chemicals which are applied permanently, adding to the contamination of the sediment. Decrease in sales data correlates with a decrease in PPP fluxes as is the case for diuron, chloridazon or simazine. Total application bans of PPPs are also reflected in the sediment, as shown by a strong decrease in carbendazim fluxes, the compound was banned in 2016.

Based on the risk assessment performed in this thesis, sediment quality of Lobsigensee can be classified as good to very good for most isolated contaminates. Only three PPPs show RQ values above 2, with tembotrione even exceeding 20. The picture is worse if the cumulative RQ values are calculated. Thereby, sediment quality has to be considered moderate at best, with chlorpyrifos dominating the over all insecticide risk. Cumulative herbicide and insecticide show an increasing trend in risk quotient values. It is thus crucial to limit PPP influxes to the pond in order to restore sediment quality to levels before 1950. It has been shown that these contaminants are preserved under anaerobic conditions, which in Lobsigensee might become more frequent with increased eutrophication and enhanced primary production. Bundschuh et al. (2016) found that pesticides can be remobilised from the sediment. While they hypothesise that the quantity of remobilisation is too low to cause environmental effects, it shows that even an application ban of PPPs does not prevent these contaminants to be reintroduced into the water.

5.3 Spatial Deposition Trends of PPPs

The PPP analysis on sediments grab samples performed in this thesis has revealed a significant spatial extent of PPP contamination. The 19 spatial grab samples show contamination with a total of 25 compounds, including 12 herbicides, 11 fungicides, one insecticide and two TPs. Some of these chemicals have been detected in all samples, while a selection is only found in the samples taken at the reed strip and the outflow. The concentrations ranged from as little as 0.1 µg/kg$_{oc}$ for fluazinam to 105.2 µg/kg$_{oc}$ (terbutylazine-2-OH). As in the sediment core, the TP terbutylazine-2-OH showed highest concentrations of all PPPs measured. Spatial deposition analysis showed that the centre of the pond is indeed acting as a sink, as this coordinate has shown highest concentrations of contaminants within the pond sediment. The two samples from the buffer strip have shown higher contamination of PPPs. Their location coincides with the approximate entry point of one of the drainage lines, which have been mapped by Alder (2012). This strongly suggest that drainage lines from arable fields act as short-circuits for PPPs leading to increased contamination at the shoreline of the pond. The variation of detected compounds can be explained well by agricultural plantation types in the catchment. The main crops and vegetables cultivated in the catchment of Lobsigensee include sugar beet, wheat, barley, potatoes and silage maize. Those PPPs which show non-zero concentrations (> LOD) are all applied as either fungicides or herbicides in these plantations. Thus, the main entry pathways of PPPs to the pond can be attributed to surface runoff from fields and subsurface tile drain transport. It could be argued that for propiconazole, atmospheric deposition may play a role due to its even distribution within the spatial surface sediments. However, volatility of this compounds is low (Lewis et al., 2016), hence this PPP might just be applied on fields all around the pond leading to the even concentration profile.

5.4 Transformation Products - Friend or Foe?

One might think that once the active substance has degraded either through photolysis, biodegradation or chemical altering, it is no longer relevant in terms of persistence and environmental toxicity. However, these TPs have been found to pose risks to water sources due to their higher mobility and persistence (Kiefer et al., 2020). The findings of this Master thesis show that TP indeed must be included in contamination screenings, as their MEC may even exceed the concentrations of the parent contamination. This is shown in the case of terbutylazine-2-OH, which is able to accumulate in the sediment due to its environmental persistence. Kiefer et al. (2020) have also shown that these TP are relevant in groundwater screening with TPs of pesticides exceeding parental concentrations. The potential of mass spectrometry allows for the detection of more and more contaminants. However, there is a lack of reference standards which would allow for time-effective target-screening of TPs. To overcome this gap, suspect screening with HRMS data may be performed, however TP identification based on this becomes incredibly challenging and time consuming. This thesis shows that TPs are effectively detected by HRMS suspect screening as the findings of the TP desaminometamitrone shows. Contamination extent could further be revealed by non-target analysis, as Chiaia-Hernández et al. (2020) performed at Moossee. They have shown over 2000 unknown substances within the sediment of this pond. Therefore, TP loading in the pond of Lobsigensee is expected to be much higher. As a proof of concept however, HRMS suspect screening of pond sediment can effectively be used to detect TP based on RT, monoisotopic masses, isotopic patters and fragmentation.

5.5 Proposed Mitigation Strategies of PPP Contamination

It is crucial to limit PPP applications such that the level of contamination in aquatic surface waters remains low. Like this, also sediment quality can remain within the accepted levels of contamination. The risk assessment shows that despite bans of certain products, more and different compounds are being approved still contributing to the ecological risk potentially harming aquatic and sediment dwelling organisms. From 2016 to 2021, 67 chemical agents have been banned in Switzerland whereas 28 new PPPs have been approved for usage. Additionally, from the time of ban there is a period of up to three years during which the remaining stock is allowed to be used up (BLV, 2022b). Therefore, despite bans, PPPs may still pose a risk to the environment, more so in the case of persistent TPs such as terbutylazine-2-hydroxy. The environmental fate of these metabolites is often not studied well enough. While the mother compound might degrade within a couple days after being applied in the field, their TPs may be more persistent and more mobile (Buttiglieri et al., 2009).

To reduce PPP contamination from agricultural practices, an application ban would prove most effective. This will reduce PPP influx in the long-term, while sediment remobilisation might still lead to short-term increases in PPP concentrations. However, with a changing climate towards drier springs and summers, new weed species or plant diseases might occur, which would make pesticide spraying necessary again. Alongside increasing temperatures, strong precipitation events are becoming more frequent (IPCC, 2014). This increases PPP losses either through surface runoff or tile drainage (Kobierska et al., 2020), thereby threatening lentic water bodies within reach. A heavily drained catchment such as the one of Lobsigensee is thus directly affected by the changing climate. Therefore, it is crucial that PPP applications are limited to dry periods only such that runoff losses are diminished. A drainage system which is disconnected from aquatic environments might also help decrease PPP loadings to such ecosystems. Other mitigation strategies may include spraying from trailers with enclosed spraying nozzles or high-precision application with image-detection to limit spray drift and overall amounts used. Furthermore, PPPs might be replaced by using alternative crop combat methods such as local spraying of hot water or incineration by mobile gas-ignition units. A more natural approach would include the establishment of protected, unused vegetation around lentic water bodies

acting as natural sieves for PPPs. Today, a 6 m wide buffer strip of vegetation is already implemented in the Swiss federal application guidelines of PPPs. In the action plan for risk reduction and sustainable use of plant protection products released by the Swiss federal government in 2017, this measure is proposed to be increased in width wherever possible (Bundesamt für Landwirtschaft BLW, 2017). But while Lobsigensee is already protected by such a buffer zone, the findings of this Master thesis has shown that PPP contamination is still an ongoing process which needs to be diminished.

5.6 Insights and Future Research

The analytical procedure applied to sediments of Lobsigensee helped to qualify the temporal and spatial contamination extent of PPPs from agriculture. The findings of this thesis add to other studies performed on pond sediments in Switzerland, which are under agricultural pressure. They underline the fact that these contaminants are preserved even in smaller lentic water bodies which may mix several times a year and anoxic conditions are not always present. Green pigments detected by HSI and sulphur counts from XRF show the increase in eutrophication with concurrent increase of pesticide influx starting in the 1950s. XRF data is found to show decreased detrital input to the pond and, while endogenic calcite formation increased in the last few decades, all the while PPPs are consistently found in the sediment core. The contamination history is thus mainly related either to PPP sales or bans of specific compounds. Sediment remobilisation and bioturbation may only play a minor role for selected compounds such as tembotrione due to its high mobility in pore water. Pesticides started appearing in the sediment in the 1950s with fungicides and herbicides making up similar shares in compounds. The TP terbutylazine-2-OH has also been confirmed to be present throughout the core. With HRMS suspect screening, an additional TP (desaminometamitrone) has been confirmed in the most recent sediments.

Temporal risk assessment indicates that selected compounds such as chlorpyrifos and tembotrione may pose the greatest risk to sediment dwelling organisms. In recent decades, cumulative RQ values show a shift of sediment quality from good to moderate with a future trend towards insufficient. However there are no AA-EQS available for sediments. This study is thereby only an estimation. The true risk may well be elevated, as unknown substances are not detected in the target screening of the sediments.

The spatial contamination analysis indicates the presence of organic compounds across the whole pond. The ability of subsurface drainage lines to short-circuit PPP leachate shows in increased concentrations of PPPs near the entry points of these line to the pond. Correlation with the land cultivation register reveals that contaminants mainly originate from the application in the catchment itself with surface runoff and losses through tile drains being the major pathways. Spray drift from beyond the catchment may only weakly contribute to the contamination for selected compounds such as propiconazole.

Smaller water bodies such as Lobsigensee are important ecological systems and biodiversity hotspots in connection with the surrounding vegetation. The present study shows the importance of ponds being included in studies on environmental contamination of synthetic PPPs. The findings of this thesis call for continuing investigations on deposition processes to quantify the effect of tile drainage on PPP contamination. Furthermore, the example of tembotrione shows the possibility of compounds to be remobilised or being able to penetrate deeper sediment layers. Further studies on these seeping mechanisms are needed to better understand post-depositional effects. Ultimately there is an urgent need that findings of such studies reach policy makers such that a solid environmental assessment on PPPs is performed during the process of allowing new compounds. This ensures that these precious lacustrine ecosystems are better protected against anthropogenic pollution from agricultural practices.

References

Alavanja, M. C. R. (2009). Pesticides Use and Exposure Extensive Worldwide. *Reviews on Environmental Health*, *24*(4), 272–291.

Alder, S. (2012). Modellierung des Gewässeranschlusses potenziell erosionsgefährdeter Flächen im schweizerischen Mittelland. *Master Thesis*, (Institute of Geography), University of Bern, CH.

Aller, R. C., & Cochran, J. K. (2019). The Critical Role of Bioturbation for Particle Dynamics, Priming Potential, and Organic C Remineralization in Marine Sediments: Local and Basin Scales. *Frontiers in Earth Science*, *7*.

Ambrosetti, W., Barbanti, L., & Sala, N. (2003). Residence time and physical processes in lakes. *Journal of Limnology*, *62*(1s), 1.

Ammann, B., & Tobolski, K. (1983). Vegetional development during the late-Würm at Lobsigensee (Swiss plateau). Studies in the late Quaternary of Lobsigensee 1. *Revue de paléobiologie*, *2*(2), 163–180.

BAFU. (2016). Ausbringen aus der Luft von Pflanzenschutzmitteln, Biozidprodukten und Düngern. *Umwelt-Vollzug*, *1623*, 41.

BAFU. (2019). Zustand und Entwicklung Grundwasser Schweiz. Ergebnisse der Nationalen Grundwasserbeobachtung NAQUA, Stand 2016. *Umwelt-Zustand*, *1901*, 138. https://www.bafu.admin.ch/bafu/de/home/themen/wasser/publikationen-studien/publikationen-wasser/ergebnisse-grundwasserbeobachtung-schweiz-naqua.html

BAFU. 2020. Wasserqualität der Seen. https://www.bafu.admin.ch/bafu/en/home/topics/water/info-specialists/state-of-waterbodies/state-of-lakes/water-quality-in-lakes.html. (Last accessed 09.03.2022).

Balsam, W. L., & Deaton, B. C. (1996). Determining the composition of late Quaternary marine sediments from NUV, VIS, and NIR diffuse reflectance spectra. *Marine Geology*, *134*(1-2), 31–55.

Beck, H. E., Zimmermann, N. E., McVicar, T. R., Vergopolan, N., Berg, A., & Wood, E. F. (2018). Present and future Köppen-Geiger climate classification maps at 1-km resolution. *Scientific Data*, *5*(1), 180214.

Berk, P., Hocevar, M., Stajnko, D., & Belsak, A. (2016). Development of alternative plant protection product application techniques in orchards, based on measurement sensing systems: A review. *Computers and Electronics in Agriculture*, *124*, 273–288.

BLV. (2022a). Pflanzenschutzmittelverzeichnis, (Last accessed 16.5.2022). https://www.psm.admin.ch/de/wirkstoffe

BLV. (2022b). Zurückgezogene Pflanzenschutzmittel mit Ausverkaufs- und Verwendungsfristen. *Ausverkaufs- und Verwendungsfristen von Pflanzenschutzmitteln mit beendeter Zulassung*, (Last accessed 16.5.2022). https://www.blv.admin.ch/blv/de/home/zulassung-pflanzenschutzmittel/anwendung-und-vollzug/zurueckgezogene-pflanzenschutzmittel.html

BLV. (2022c). Zurückgezogene Wirkstoffe aus Anhang 1 der PSMV. *Zurückgezogene Pflanzenschutzmittel*, (Last accessed 16.5.2022). https://www.blv.admin.ch/blv/de/home/zulassung-pflanzenschutzmittel/anwendung-und-vollzug/zurueckgezogene-pflanzenschutzmittel.html

Bouwman, H., Bornman, R., van den Berg, H., & Kylin, H. (2013). DDT : fifty years since Silent Spring. In D. Gee (Ed.), *Late lessons from early warning: Science, precaution, innovation. lessons for preventing harm* (pp. 272–291). European Environment Agency.

Brückner, L., Kupfersberger, H., Klammler, G., Fank, J., Kah, M., & -Geoökologin, D. (2017). Sorption und Abbau von s-Metolachlor und dessen Metaboliten Metolachlor-OA und Metolachlor-ESA im Boden Höhere Bundeslehr-und Forschungsanstalt für Landwirtschaft Raumberg-Gumpenstein Einleitung, 33–38.

Bundesamt für Landestopografie swisstopo. 2018. Windgeschwindigkeit 50 m Höhe. https://map.geo.admin.ch/?lang=de%7B%5C&%7Dtopic=ech%7B%5C&%7DbgLayer=ch.swisstopo.pixelkarte-farbe%7B%5C&%7Dlayers=ch.swisstopo.zeitreihen,ch.bfs.gebaeude%7B%5C_%7Dwohnungs%7B%5C_%7Dregister,ch.bav.haltestellen-oev,ch.swisstopo.swisstlm3d-wanderwege,ch.bfe.windenergie-geschwindigkeit%7B%5C_%7Dh50%7B%5C&%7Dlayers%7B%5C_%7Dvis. (Last accessed 15.03.2022).

Bundesamt für Landwirtschaft BLW. 2017. Aktionsplan zur Risikoreduktion und nachhaltigen Anwendung von Pflanzenschutzmitteln. https://www.blw.admin.ch/blw/de/home/nachhaltige-produktion/pflanzenschutz/aktionsplan.html. (Last accessed 22.5.2022).

Bundschuh, M., Schletz, M., & Goedkoop, W. (2016). The mode of bioturbation triggers pesticide remobilization from aquatic sediments. *Ecotoxicology and Environmental Safety*, *130*, 171–176.

Burkhard, M., & Sommaruga, A. (1998). Evolution of the western Swiss Molasse basin: structural relations with the Alps and the Jura belt. *Geological Society Special Publication*, *134*, 279–298.

Buttiglieri, G., Peschka, M., Frömel, T., Müller, J., Malpei, F., Seel, P., & Knepper, T. P. (2009). Environmental occurrence and degradation of the herbicide n-chloridazon. *Water Research*, *43*(11), 2865–2873.

Butz, C., Grosjean, M., Fischer, D., Wunderle, S., Tylmann, W., & Rein, B. (2015). Hyperspectral imaging spectroscopy: a promising method for the biogeochemical analysis of lake sediments. *Journal of Applied Remote Sensing*, *9*(1), 096031.

Butz, C., Grosjean, M., Goslar, T., & Tylmann, W. (2017). Hyperspectral imaging of sedimentary bacterial pigments: a 1700-year history of meromixis from varved Lake Jaczno, northeast Poland. *Journal of Paleolimnology*, *58*(1), 57–72.

Butz, C., Grosjean, M., Poraj-Górska, A., Enters, D., & Tylmann, W. (2016). Sedimentary Bacteriopheophytin a as an indicator of meromixis in varved lake sediments of Lake Jaczno, north-east Poland, CE 1891–2010. *Global and Planetary Change*, *144*, 109–118.

Carneiro, R. P., Oliveira, F. A., Madureira, F. D., Silva, G., de Souza, W. R., & Lopes, R. P. (2013). Development and method validation for determination of 128 pesticides in bananas by modified QuEChERS and UHPLC–MS/MS analysis. *Food Control*, *33*(2), 413–423.

Carvalho, F. P. (2017). Pesticides, environment, and food safety. *Food and Energy Security*, *6*(2), 48–60.

Carvalho, F. P., Villeneuve, J.-P., Cattini, C., Tolosa, I., Montenegro-Guillén, S., Lacayo, M., & Cruz, A. (2002). Ecological risk assessment of pesticide residues in coastal lagoons of Nicaragua. *J. Environ. Monit.*, *4*(5), 778–787.

Chiaia-Hernandez, A. C., Krauss, M., & Hollender, J. (2013). Screening of lake sediments for emerging contaminants by liquid chromatography atmospheric pressure photoionization and electrospray ionization coupled to high resolution mass spectrometry. *Environmental Science and Technology*, *47*(2), 976–986.

Chiaia-Hernandez, A. C., Schymanski, E. L., Kumar, P., Singer, H. P., & Hollender, J. (2014). Suspect and nontarget screening approaches to identify organic contaminant records in lake sediments. *Analytical and Bioanalytical Chemistry*, 7323–7335.

Chiaia-Hernández, A. C., Zander, P. D., Schneider, T., Szidat, S., Lloren, R., & Grosjean, M. (2020). High-Resolution Historical Record of Plant Protection Product Deposition Documented by Target and Nontarget Trend Analysis in a Swiss Lake under Anthropogenic Pressure. *Environmental Science and Technology*, *54*(20), 13090–13100.

Chislock, M., Doster, E., Zitomer, R., & Wilson, A. E. (2013). Eutrophication: Causes, consequences, and controls in aquatic ecosystems. *Nature Education Knowledge*, *4*(4), 10. https://docplayer.net/34059863-Eutrophicati-on-causes-consequences-and-controls-in-aquati-c-ecosystems.html

Climate-data.org. 2021. Klima Lyss. https://de.climate-data.org/europa/schweiz/bern/lyss-10346/. Last accessed 17.02.2022.

Connell, D. W. (1988). Bioaccumulation Behavior of Persistent Organic Chemicals with Aquatic Organisms. In *Reviews of environmental contamination and toxicology* (pp. 117–154).

Corella, J. P., Brauer, A., Mangili, C., Rull, V., Vegas-Vilarrúbia, T., Morellón, M., & Valero-Garcés, B. L. (2012). The 1.5-ka varved record of Lake Montcortès (southern Pyrenees, NE Spain). *Quaternary Research*, *78*(2), 323–332.

Davies, S. J., Lamb, H. F., & Roberts, S. J. (2015). Micro-XRF Core Scanning in Palaeolimnology: Recent Developments.

Davis, B., Brewer, S., Stevenson, A., & Guiot, J. (2003). The temperature of Europe during the Holocene reconstructed from pollen data. *Quaternary Science Reviews*, *22*(15-17), 1701–1716.

Del Prado-Lu, J. L. (2015). Insecticide Residues in Soil, Water, and Eggplant Fruits and Farmers' Health Effects Due to Exposure to Pesticides. *Environmental Health and Preventive Medicine*, *20*(1), 53–62.

Dietze, E., Maussion, F., Ahlborn, M., Diekmann, B., Hartmann, K., Henkel, K., Kasper, T., Lockot, G., Opitz, S., & Haberzettl, T. (2014). Sediment transport processes across the Tibetan Plateau inferred from robust grain-size end members in lake sediments. *Climate of the Past*, *10*(1), 91–106.

Doppler, T., Mangold, S., Wittmer, I., Spycher, S., Comte, R., Stamm, C., Singer, H., Junghans, M., & Kunz, M. (2017). Hohe PSM-Belastung in Schweizer Bächen. *Aqua & Gas*, 46–56.

dos Reis, R. R., Sampaio, S. C., & de Melo, E. B. (2013). The effect of different log P algorithms on the modeling of the soil sorption coefficient of nonionic pesticides. *Water Research*, *47*(15), 5751–5759.

Dubler, A.-M. 2008. "Lobsigen", in: Historisches Lexikon der Schweiz (HLS), Version vom 30.01.2008. https://hls-dhs-dss.ch/de/articles/008340/2008-01-30/.

Eggleton, J., & Thomas, K. V. (2004). A review of factors affecting the release and bioavailability of contaminants during sediment disturbance events. *Environment International*, *30*(7), 973–980.

European Comission. (2011). *Guidance Document No. 27 Technical Guidance For Deriving Environmental Quality Standards* (tech. rep.).

European Food Safety Authority. (2017). Peer review of the pesticide risk assessment for the active substance terbuthylazine in light of confirmatory data submitted. *Journal*, *15*(23), 4868.

Fahrni, N. (2021). *A chronicle of plant protection product contamination in sediments of a Swiss pond: Target trend analysis of a sedimentary record from Sängeliweiher (MSc Thesis).* Institute of Geogaphy, Universität Bern.

Finnegan, M. C., Baxter, L. R., Maul, J. D., Hanson, M. L., & Hoekstra, P. F. (2017). Comprehensive characterization of the acute and chronic toxicity of the neonicotinoid insecticide thiamethoxam to a suite of aquatic primary producers, invertebrates, and fish. *Environmental Toxicology and Chemistry*, *36*(10), 2838–2848.

Food and Agriculture Organization FAO. (2010). International Code of Conduct on the Distribution and Use of Pesticides: Guidelines for the Registration of Pesticides. *Assessment*, (April), 42pp. http://www.who.int/whopes/resources/resources%7B%5C_%7D2010/en/

Forel, F.-A. (1904). *Le Léman : monographie limnologique*. F. Rouge.

Gäggeler, H., & Szidat, S. (2016). Nuclear Dating. In F. Rösch (Ed.), *Nuclear- and radiochemistry* (p. 133). De Gruyter.

Gavrilescu, M. (2005). Fate of pesticides in the environment and its bioremediation. *Engineering in Life Sciences*, *5*(6), 497–526.

Gerecke, A. C., Schärer, M., Singer, H. P., Müller, S. R., Schwarzenbach, R. P., Sägesser, M., Ochsenbein, U., & Popow, G. (2002). Sources of pesticides in surface waters in Switzerland:

pesticide load through waste water treatment plants—current situation and reduction potential. *Chemosphere*, *48*(3), 307–315.

Gilland, B. (2015). Nitrogen, phosphorus, carbon and population. *Science Progress*, *98*(4), 379–390.

Gosain, N. (2022). *Investigation of Temporal Variability of Plant Protection Products in a Small Pond in the Swiss Plateau*. Institute of Geogaphy, Universität Bern.

Gramlich, A., Stoll, S., Stamm, C., Walter, T., & Prasuhn, V. (2018). Effects of artificial land drainage on hydrology, nutrient and pesticide fluxes from agricultural fields – A review. *Agriculture, Ecosystems and Environment*, *266*(December 2017), 84–99.

Granberg, M. E., Gunnarsson, J. S., Hedman, J. E., Rosenberg, R., & Jonsson, P. (2008). Bioturbation-driven release of organic contaminants from Baltic Sea sediments mediated by the invading polychaete Marenzelleria neglecta. *Environmental Science and Technology*, *42*(4), 1058–1065.

Grünig, K., & Prasuhn, V. (2001). Evaluation Ökomassnahmen Phosphorverluste durch Bodenerosion. *AGRARForschung*, *8*(1), 30–35.

Guthruf, J., Guthruf-Seiler, K., & Zeh, M. (1999). *Kleinseen im Kanton Bern* (Amt für Gewässerschutz und Abfallwirtschaft des Kantons Bern, Ed.). Paul Haupt AG.

Guthruf, K., Maurer, V., Ryser, R., Zeh, M., & Zweifel, N. (2015). Zustand der Kleinseen. *Bau-, Verkehrs- und Energiedirektion des Kantons Bern*, (September), 112.

Håkanson, L. (1974). A Mathematical Model for Establishing Numerical Values of Topographical Roughness for Lake Bottoms. *Geografiska Annaler: Series A, Physical Geography*, *56*(3-4), 183–200.

Håkanson, L., & Jansson, M. (1983). *Principles of Lake Sedimentology*.

Heiri, O., Lotter, A. F., & Lemcke, G. (2001). Loss on ignition as a method for estimating organic and carbonate content in sediments: reproducibility and comparability of results. *Journal of Paleolimnology*, *25*(1), 101–110.

Holzner, C. P., Aeschbach-Hertig, W., Simona, M., Veronesi, M., Imboden, D. M., & Kipfer, R. (2009). Exceptional mixing events in meromictic Lake Lugano (Switzerland/Italy), studied using environmental tracers. *Limnology and Oceanography*, *54*(4), 1113–1124.

IPCC. (2014). *Climate Change 2014: Synthesis Report. Contribution of Working Groups I, II and III to the Fifth Assessment Report of the Intergovernmental Panel on Climate Change* (R.K. Pachauri and L.A. Meyer (eds.), Ed.).

Jeppesen, E., Søndergaard, M., Jensen, J. P., Mortensen, E., Hansen, A. M., & Jørgensen, T. (1998). Cascading Trophic Interactions from Fish to Bacteria and Nutrients after Reduced Sewage Loading: An 18-Year Study of a Shallow Hypertrophic Lake. *Ecosystems 1998 1:3*, *1*(3), 250–267.

Kellerhals, P., & Tröhler, B. (1981). *Geologischer Atlas 25, Blatt 76 Lyss (LK 1146)* (Erläuterun).

Kiefer, K., Bader, T., Minas, N., Salhi, E., Janssen, E. M., von Gunten, U., & Hollender, J. (2020). Chlorothalonil transformation products in drinking water resources: Widespread and challenging to abate. *Water Research*, *183*, 116066.

Knezovich, J., Harrison, F., & Wilhelm, R. (1987). The bioavailability of sediment-sorbed organic chemicals: A review. *Water, Air, and Soil Pollution*, *32*(1-2), 233–245.

Kobierska, F., Koch, U., Kasteel, R., Stamm, C., & Prasuhn, V. (2020). Plant protection product losses via tile drainage: A conceptual model and mitigation measures. *Agrarforschung Schweiz*, *11*(6), 115–123.

Last, W. M., & Smol, J. P. (2001). *Tracking Environmental Change using Lake Sediments - Volume 1: Basin Analysis, Coring, and Chronological Techniques* (W. M. Last & J. P. Smol, Eds.). Kluwer Academic Publishers.

Leu, C., Singer, H., Stamm, C., Müller, S. R., & Schwarzenbach, R. P. (2004a). Simultaneous Assessment of Sources, Processes, and Factors Influencing Herbicide Losses to Surface

Waters in a Small Agricultural Catchment. *Environmental Science & Technology*, *38*(14), 3827–3834.

Leu, C., Singer, H., Stamm, C., Müller, S. R., & Schwarzenbach, R. P. (2004b). Variability of Herbicide Losses from 13 Fields to Surface Water within a Small Catchment after a Controlled Herbicide Application. *Environmental Science and Technology*, *38*(14), 3835–3841.

Lewis, K. A., Tzilivakis, J., Warner, D. J., & Green, A. (2016). An international database for pesticide risk assessments and management. *Human and Ecological Risk Assessment*, *22*(4), 1050–1064.

Liechti, P. (2010). Methoden zur Untersuchung und Beurteilung der Fliessgewässer. Chemisch-physikalische Erhebungen, Nährstoffe. *Umwelt-Vollzug*, (1005), Bundesamt für Umwelt, Bern. 44 S.

Löffler, H. (1986). An early meromictic stage in Lobsigensee (Switzerland) as evidenced by ostracods and Chaoborus. *Hydrobiologia*, *143*(1), 309–314.

Lorenz, S., Rasmussen, J. J., Süß, A., Kalettka, T., Golla, B., Horney, P., Stähler, M., Hommel, B., & Schäfer, R. B. (2017). Specifics and challenges of assessing exposure and effects of pesticides in small water bodies. *Hydrobiologia*, *793*(1), 213–224.

Mateo-Sagasta, J., Zadeh, S. M., & Turral, H. (2018). *More people, more food, worse water? - a global review of water pollution from agriculture.*

McGrath, G., Hinz, C., & Sivapalan, M. (2010). Assessing the impact of regional rainfall variability on rapid pesticide leaching potential. *Journal of Contaminant Hydrology*, *113*(1-4), 56–65.

Meester, L. D., Declerck, S., Stoks, R., Louette, G., Meutter, F. V. D., Bie, T. D., Michels, E., & Brendonck, L. (2005). Ponds and pools as model systems in conservation biology, ecology and evolutionary biology. *Aquatic Conservation: Marine and Freshwater Ecosystems*, *15*(6), 715–725.

MeteoSchweiz. 2018. Klima der Schweiz. (Last accessed 15.02.2022).

Mohaupt, V., Jeanette, V., Rolf, A., Birk, S., Kirst, I., Kühnel, D., Küster, E., Semerádová, S., Šubelj, G., & Whalley, C. (2020). *Pesticides in European rivers, lakes and groundwaters – Data assessment* (tech. rep.). ETC/ICM Technical Report 1/2020.

Moreno, A., Giralt, S., Valero-Garcés, B., Sáez, A., Bao, R., Prego, R., Pueyo, J., González-Sampériz, P., & Taberner, C. (2007). A 14kyr record of the tropical Andes: The Lago Chungará sequence (18°S, northern Chilean Altiplano). *Quaternary International*, *161*(1), 4–21.

Moschet, C., Wittmer, I., Simovic, J., Junghans, M., Piazzoli, A., Singer, H., Stamm, C., Leu, C., & Hollender, J. (2014). How a complete pesticide screening changes the assessment of surface water quality. *Environmental Science and Technology*, *48*(10), 5423–5432.

Myrbo, A., Morrison, A., & McEwan, R. 2011. Tool for Microscopic Identification (TMI). http://tmi.laccore.umn.edu.

Ochsenbein, U., Berset, J.-D., & Scheiwiller, E. (2015). Mikroverunreinigungen in bernischen Gewässern. Belastungssituation und neue ökotoxikologische Beurteilung der Risiken — DORA Eawag. *Aqua & Gas*, *2*, 56–66. https://www.dora.lib4ri.ch/eawag/islandora/object/eawag%7B%5C%%7D3A8046

Oekotoxzentrum. 2022. Proposals for Quality Criteria for Surface Waters. https://www.ecotoxcentre.ch/expert-service/quality-criteria/quality-criteria-for-surface-waters/.

Oertli, B., Auderset Joye, D., Castella, E., Juge, R., & Lachavanne, J.-B. 2000. Diversité biologique et typologie écologique des étangs et petits lacs de Suisse. https://archiveouverte.unige.ch/unige:26123.

Oertli, B., Biggs, J., Céréghino, R., Grillas, P., Joly, P., & Lachavanne, J. B. (2005). Conservation and monitoring of pond biodiversity: Introduction. *Aquatic Conservation: Marine and Freshwater Ecosystems*, *15*(6), 535–540.

Parris, A. S., Bierman, P. R., Noren, A. J., Prins, M. A., & Lini, A. (2010). Holocene paleostorms identified by particle size signatures in lake sediments from the northeastern United States. *Journal of Paleolimnology*, *43*(1), 29–49.

Peinerud, E. K. (2000). Interpretation of Si concentrations in lake sediments: Three case studies. *Environmental Geology*, *40*(1-2), 64–72.

Pereira, V. J., Cunha, J., Morais, T., Ribeiro-Oliveira, J., & Morais, J. (2016). Physical-Chemical Properties of Pesticides : Concepts , Applications , and Interactions With the Environment Propriedades Físico-Químicas Dos Agrotóxicos : *Bioscience Journal*, *32*(3), 627–641.

Postigo, C., & Barceló, D. (2015). Synthetic organic compounds and their transformation products in groundwater: Occurrence, fate and mitigation. *Science of The Total Environment*, *503-504*, 32–47.

PubChem. 2022. Tembotrione. https://pubchem.ncbi.nlm.nih.gov/compound/Tembotrione%7B%5C#%7Dsection=Environmental-Fate-Exposure-Summary. (Last accessed 28.04.2022).

R Core Team. 2021. R: A Language and Environment for Statistical Computing. https://www.r-project.org/. R Foundation for Statistical Computing.

Rein, B., & Sirocko, F. (2002). In-situ reflectance spectroscopy - analysing techniques for high-resolution pigment logging in sediment cores. *International Journal of Earth Sciences*, *91*(5), 950–954.

Sánchez-Bayo, F., & Wyckhuys, K. A. (2019). Worldwide decline of the entomofauna: A review of its drivers. *Biological Conservation*, *232*, 8–27.

Sandin, M. 2017. Surface and subsurface transport pathways for pesticides to surface waters. https://pub.epsilon.slu.se/14474/.

Schneider, R., Cramp, A., Damuth, J., Hiscott, R., Kowsmann, R., Lopez, M., Nanayama, F., & Normark, W. (1995). Color-reflectance measurements obtained from Leg 155 cores. *Proceedings of the Ocean Drilling Program, 155 Initial Reports*, *155*, 697–700.

Schnurrenberger, D., Russell, J., & Kelts, K. (2003). Classification of lacustrine sediments based on sedimentary components. *Journal of Paleolimnology*, *29*(2), 141–154.

Schönenberger, U. T., Beck, B., Dax, A., Vogler, B., & Stamm, C. (2022). Pesticide concentrations in agricultural storm drainage inlets of a small Swiss catchment. *Environmental Science and Pollution Research*, *1*, 3.

Schuhmann, A., Klammler, G., Weiss, S., Gans, O., Fank, J., Haberhauer, G., & Gerzabek, M. H. (2019). Degradation and leaching of bentazone, terbuthylazine and S-metolachlor and some of their metabolites: A long-term lysimeter experiment. *Plant, Soil and Environment*, *65*(No. 5), 273–281.

Schymanski, E. L., Jeon, J., Gulde, R., Fenner, K., Ruff, M., Singer, H. P., & Hollender, J. (2014). Identifying Small Molecules via High Resolution Mass Spectrometry: Communicating Confidence. *Environmental Science & Technology*, *48*(4), 2097–2098.

Schymanski, E. L., Singer, H. P., Longrée, P., Loos, M., Ruff, M., Stravs, M. A., Ripollés Vidal, C., & Hollender, J. (2014). Strategies to Characterize Polar Organic Contamination in Wastewater: Exploring the Capability of High Resolution Mass Spectrometry. *Environmental Science & Technology*, *48*(3), 1811–1818.

Shang, Y., Beets, C. J., Tang, H., Prins, M. A., Lahaye, Y., van Elsas, R., Sukselainen, L., & Kaakinen, A. (2016). Variations in the provenance of the late Neogene Red Clay deposits in northern China. *Earth and Planetary Science Letters*, *439*, 88–100.

Sinninghe Damsté, J. S., & Schouten, S. (2006). Biological Markers for Anoxia in the Photic Zone of the Water Column. In *Marine organic matter: Biomarkers, isotopes and dna* (pp. 127–163). Springer-Verlag.

Sorrel, P., Jacq, K., Van Exem, A., Escarguel, G., Dietre, B., Debret, M., McGowan, S., Ducept, J., Gauthier, E., & Oberhänsli, H. (2021). Evidence for centennial-scale Mid-Holocene

episodes of hypolimnetic anoxia in a high-altitude lake system from central Tian Shan (Kyrgyzstan). *Quaternary Science Reviews*, *252*, 106748.

Srivastava, A., Jangid, N. K., Srivastava, M., & Rawat, V. (2019). Pesticides as Water Pollutants. In *Groundwater for sustainable development: Problems, perspectives and challenges* (pp. 1–19).

Staatsarchiv Kanton Bern. 1858. Atlanten 292 Lobsigensee: Entsumpfung, 1858 (Archiveinheit). http://www.query.sta.be.ch/detail.aspx?ID=431326. (Last accessed 15.02.2022).

Stehle, S., & Schulz, R. (2015). Agricultural insecticides threaten surface waters at the global scale. *Proceedings of the National Academy of Sciences of the United States of America*, *112*(18), 5750–5755.

United Nations. (2019). World Population Prospects 2019: Highlights. *Department of Economic and Social Affairs, Population Division*, (ST/ESA/SER.A/423).

Van Gemerden, H., & Mas, J. (1995). Anoxygenic Photosynthetic Bacteria. In R. E. Blankenship, M. T. Madigan & C. E. Bauer (Eds.), *Anoxygenic photosynthetic bacteria* (pp. 49–85). Springer Netherlands.

van Hateren, J., Prins, M., & van Balen, R. (2018). On the genetically meaningful decomposition of grain-size distributions: A comparison of different end-member modelling algorithms. *Sedimentary Geology*, *375*, 49–71.

Veit, H., & Gnägi, C. (2014). Die Böden des Berner Mittellandes. In *Die entwicklung im spiegel der forschung. jahrbuch geographische gesellschaft bern.* (pp. 267–292). Elisabeth Bäschlin, Heike Mayer, Martin Hasler.

Velisek, J., Stara, A., Koutnik, D., & Machova, J. (2014). Effect of Terbuthylazine-2-hydroxy at Environmental Concentrations on Early Life Stages of Common Carp (Cyprinus carpio L.) *BioMed Research International*, *2014*, 1–7.

von Büren, G., & Leiser, G. (1961). Der Lobsigensee. *Mitteilungen der Naturforschenden Gesellschaft Bern*, (19).

Weltje, G. J., & Tjallingii, R. (2008). Calibration of XRF core scanners for quantitative geochemical logging of sediment cores: Theory and application. *Earth and Planetary Science Letters*, *274*(3-4), 423–438.

Williams, P., Whitfield, M., Biggs, J., Bray, S., Fox, G., Nicolet, P., & Sear, D. (2004). Comparative biodiversity of rivers, streams, ditches and ponds in an agricultural landscape in Southern England. *Biological Conservation*, *115*(2), 329–341.

Woolway, R. I., & Merchant, C. J. (2019). Worldwide alteration of lake mixing regimes in response to climate change. *Nature Geoscience*, *12*, 271–276.

Zander, P. D., Żarczyński, M., Vogel, H., Tylmann, W., Wacnik, A., Sanchini, A., & Grosjean, M. (2021). A high-resolution record of Holocene primary productivity and water-column mixing from the varved sediments of Lake Żabińskie, Poland. *Science of the Total Environment*, *755*.

Zeh, M. 2003. Lobsigensee_Originalfoto.jpg. https://commons.wikimedia.org/wiki/File:Lobsigensee%7B%5C_%7Dcropped.jpg. (Last accessed 11.02.2022).

Appendices

Appendix A Subsampling Procedure and Measurement Data

Subsampling the core halves involves cutting the sediment at the chosen intervals using a stainless steel slicer tool, which allows for precise vertical sectioning. The samples are transferred to storage containers, of which the empty weight was recorded. The samples were then weighed and freeze-dried for at least 48 hours using a device consisting of a pump (Vacuubrand RZ 2.5) and a freeze-drier (Alpha 1-2LD). After freeze-drying, the samples are weighed again and subsequently homogenised using a mortar and pestle. It is crucial that all the tools used in this procedure are cleaned thoroughly with deionised water and ethanol after every sample to prevent sample carry-over and thus contamination.

From 60 cm to 110 cm, the resolution was decreased to 5 cm with an additional 2 cm sample taken from 110 cm to 112 cm yielding eleven additional samples. This approach ensures a reasonable temporal resolution for the timespan of interest while allowing for blank samples from the lower part containing no PPPs. In total 41 sediment samples were produced. For the eleven 5 cm thick samples, the material was distributed to two storage boxes due to volumetric limitations. The weighing of the material was then done on each box separately. For the water content and DBD calculations, the cumulative wet weight, dry weight and volume was determined by adding them together. After freeze-drying, each of the pairs were homogenised together and redistributed to two boxes. The samples were left in the freeze-drier for 55 hours. Some samples still showed some water content after this timeframe and so were refrozen and again freeze-dried for an additional 12 hours to be completely free of water.

To arrive at the dry bulk density (DBD) the sample can be described as a section from a cylinder with bottom and top area being a circle segment and its height being determined by the sample resolution. By measuring the sample sagitta h, the base area A of the sample can be determined. The volume V of each sample is then calculated by multiplying the base area with its thickness. The DBD of a sample is then described as the ratio of the dry sediment weight per volume. Equations 7 to 9 below are used in this procedure. Hereby, the circle radius R is the inner radius of the PVC tubes containing the core and according to the manufacturer and remeasured is $R = 2.95$ cm.

$$A = R^2 \arccos\left(1 - \frac{h}{R}\right) - (R - h)\sqrt{R^2 - (R - h)^2} \tag{7}$$

$$V = A \cdot \text{thickness} \tag{8}$$

$$\text{DBD} = \frac{\text{dryweight}}{V} \tag{9}$$

Sample ID	Core ID	Top [cm]	Bot [cm]	Segment Depth [cm]	Empty Box [g]	Wet + Box [g]	Dry + Box [g]	Wet Weight [g]	Dry Weight [g]	Water content [mass%]	Area segment [cm^2]	Vol segment [cm^3]	DBD [g/cm^3]
LOB21-3-1	LOB21-3B-1	0	2	2	13.13	31.15	15.84	18.02	2.71	84.96	8.16	16.33	0.17
		2	4	2	13.03	30.17	15.37	17.14	2.34	86.35	8.16	16.33	0.14
LOB21-3-2	LOB21-3B-2	4	6	1.9	13.02	31.37	15.53	18.35	2.51	86.32	7.61	15.22	0.16
		6	8	1.9	13.17	31.18	15.87	18.01	2.70	85.01	7.61	15.22	0.18
LOB21-3-3	LOB21-3B-3	8	10	2	13.15	32.7	16.24	19.55	3.09	84.19	8.16	16.33	0.19
		10	12	2	12.99	33.05	16.25	20.06	3.26	83.75	8.16	16.33	0.20
LOB21-3-4	LOB21-3B-4	12	14	2	13	32.89	16.21	19.89	3.21	83.86	8.16	16.33	0.20
		14	16	2	13.01	34.88	16.70	21.87	3.69	83.13	8.16	16.33	0.23
LOB21-3-5	LOB21-3B-5	16	18	2	13.17	35.5	17.18	22.33	4.01	82.04	8.16	16.33	0.25
LOB21-3-6	LOB21-3A-6	18	20	2.2	12.83	38.60	17.22	25.77	4.39	82.96	9.29	18.59	0.24
LOB21-3-7	LOB21-3A-7	20	22	2.3	12.88	37.87	17.52	24.99	4.64	81.43	9.87	19.73	0.24
LOB21-3-8	LOB21-3A-8	22	24	2.3	12.87	38.83	17.99	25.96	5.12	80.28	9.87	19.73	0.26
LOB21-3-9	LOB21-3A-9	24	26	2.3	13.99	40.87	18.88	26.88	4.89	81.81	9.87	19.73	0.25
LOB21-3-10	LOB21-3A-10	26	28	2.3	12.99	40.09	18.81	27.10	5.82	78.52	9.87	19.73	0.29
LOB21-3-11	LOB21-3A-11	28	30	2.3	12.91	41.60	18.67	28.69	5.76	79.92	9.87	19.73	0.29
LOB21-3-12	LOB21-3A-12	30	32	2.4	12.91	39.32	17.35	26.41	4.44	83.19	10.44	20.89	0.21
LOB21-3-13	LOB21-3A-13	32	34	2.4	12.91	41.00	17.6	28.09	4.69	83.30	10.44	20.89	0.22
LOB21-3-14	LOB21-3A-14	34	36	2.5	13.09	40.07	17.66	26.98	4.57	83.06	11.03	22.05	0.21
LOB21-3-15	LOB21-3A-15	36	38	2.5	12.88	41.53	17.77	28.65	4.89	82.93	11.03	22.05	0.22
LOB21-3-16	LOB21-3A-16	38	40	2.5	12.89	40.69	17.26	27.80	4.37	84.28	11.03	22.05	0.20
LOB21-3-17	LOB21-3A-17	40	42	2.6	12.89	42.49	17.32	29.60	4.43	85.03	11.61	23.22	0.19
LOB21-3-18	LOB21-3A-18	42	44	2.6	12.87	39.72	17.02	26.85	4.15	84.54	11.61	23.22	0.18
LOB21-3-19	LOB21-3A-19	44	46	2.7	12.99	41.54	17.79	28.55	4.80	83.19	12.20	24.39	0.20
LOB21-3-20	LOB21-3A-20	46	48	2.7	12.9	43.06	17.95	30.16	5.05	83.26	12.20	24.39	0.21
LOB21-3-21	LOB21-3A-21	48	50	2.7	13	42.30	18.03	29.30	5.03	82.83	12.20	24.39	0.21
LOB21-3-22	LOB21-3A-22	50	52	2.8	12.86	42.86	18.3	30.00	5.44	81.87	12.79	25.57	0.21
LOB21-3-23	LOB21-3A-23	52	54	2.9	13.01	43.51	18.33	30.50	5.32	82.56	13.37	26.75	0.20
LOB21-3-24	LOB21-3A-24	54	56	2.9	13	45.81	19.03	32.81	6.03	81.62	13.37	26.75	0.23
LOB21-3-25	LOB21-3A-25	56	58	3.0	12.99	44.91	19.53	31.92	6.54	79.51	13.96	27.93	0.23
LOB21-3-26	LOB21-3A-26	58	60	3.0	12.98	47.46	21.09	34.48	8.11	76.48	13.96	27.93	0.29
LOB21-3-27b	LOB21-3A-27	60	65	3.0	25.76	112.30	49.37	86.54	23.61	72.72	13.96	69.82	0.34
LOB21-3-28b	LOB21-3A-28	65	70	3.0	26	116.88	56.31	90.88	30.31	66.65	13.96	69.82	0.43
LOB21-3-29b	LOB21-3A-29	70	75	3.0	25.97	119.69	59.98	93.72	34.01	63.71	13.96	69.82	0.49
LOB21-3_6d	LOB21-3B-10	18	20	2.0	13.15	35.10	17.18	21.95	4.03	81.64	8.16	16.33	0.25
LOB21-3_8d	LOB21-3B-12	22	24	2.2	13.15	36.50	18.16	23.35	5.01	78.54	9.29	18.59	0.27
LOB21-3_11d	LOB21-3B-15	28	30	2.3	13.14	39.24	19.02	26.10	5.88	77.47	9.87	19.73	0.30
LOB21-3_14d	LOB21-3B-18	34	36	2.2	13.14	36.35	18.86	23.21	5.72	75.38	9.29	18.59	0.31
LOB21-3_16d	LOB21-3B-20	38	40	2.3	13.00	36.83	16.83	23.83	3.83	83.92	9.87	19.73	0.19
LOB21-3_18d	LOB21-3B-22	42	44	2.3	13.13	37.47	17.48	24.34	4.35	82.12	9.87	19.73	0.22

Table 5: Measurements taken during subsampling of the core for PPP Analysis.

Sample Serial No.	C %	N %	S %	C/N	Crucible empty	Sample weight	Cruc.+Sample wt. after 550	DW_550	Cruc.+Sample wt. after 950	DW_950	LOI_550%	LOI_950%	OC	IC	TC	CaCO3	CO3^2-
Nr	wt %	wt %	wt %		g	g	g	g	g	g	wt %	wt %	wt %	wt %	wt %	wt %	wt %
LOB21-3_1	17.549	1.729	1.001	10.152	15.0643	0.201	15.204	0.1397	15.1811	0.1168	30.50	11.39	14.32	3.11	17.55	25.91	15.53
LOB21-3_2	17.126	1.615	0.955	10.608	14.55	0.2064	14.6979	0.1479	14.6703	0.1203	28.34	13.37	13.31	3.65	17.13	30.41	18.23
LOB21-3_3	15.389	1.367	0.812	11.259	17.0902	0.2041	17.245	0.1548	17.2144	0.1242	24.15	14.99	11.34	4.09	15.39	34.10	20.44
LOB21-3_4	14.667	1.264	0.732	11.607	14.4895	0.2034	14.6469	0.1574	14.6154	0.1259	22.62	15.49	10.62	4.22	14.67	35.22	21.11
LOB21-3_5	14.209	1.134	0.760	12.525	13.6489	0.2027	13.8089	0.16	13.776	0.1271	21.07	16.23	9.89	4.43	14.21	36.91	22.13
LOB21-3_6	14.064	1.096	0.777	12.827	14.1531	0.2014	14.3132	0.1601	14.2794	0.1263	20.51	16.78	9.63	4.58	14.06	38.17	22.88
LOB21-3_7	13.512	1.022	0.724	13.218	15.2954	0.2043	15.4606	0.1652	15.4256	0.1302	19.14	17.13	8.99	4.67	13.51	38.96	23.36
LOB21-3_8	11.848	0.884	0.627	13.397	17.0447	0.2026	17.2103	0.1656	17.1764	0.1317	18.26	16.73	8.57	4.56	11.85	38.05	22.81
LOB21-3_9	12.943	0.973	0.723	13.304	16.7324	0.2014	16.8993	0.1669	16.8671	0.1347	17.13	15.99	8.04	4.36	12.94	36.36	21.80
LOB21-3_10	11.422	0.876	0.640	13.035	14.14	0.2007	14.3073	0.1673	14.2771	0.1371	16.64	15.05	7.81	4.10	11.42	34.22	20.51
LOB21-3_11	11.459	0.875	0.685	13.089	18.1787	0.2001	18.3456	0.1669	18.3148	0.1361	16.59	15.39	7.79	4.20	11.46	35.00	20.98
LOB21-3_12	13.879	1.019	0.834	13.627	15.0908	0.2056	15.2569	0.1661	15.2198	0.129	19.21	18.04	9.02	4.92	13.88	41.04	24.60
LOB21-3_13	13.923	1.043	0.893	13.350	15.5339	0.201	15.6947	0.1608	15.6603	0.1264	20.00	17.11	9.39	4.67	13.92	38.92	23.33
LOB21-3_14	13.815	1.033	1.087	13.376	20.3422	0.2038	20.5035	0.1613	20.4684	0.1262	20.85	17.22	9.79	4.70	13.82	39.17	23.48
LOB21-3_15	13.629	1.022	1.075	13.330	16.9068	0.2062	17.0702	0.1634	17.0342	0.1274	20.76	17.46	9.74	4.76	13.63	39.70	23.80
LOB21-3_16	15.658	1.102	1.197	14.214	20.6146	0.1827	20.7547	0.1401	20.7192	0.1046	23.32	19.43	10.95	5.30	15.66	44.19	26.49
LOB21-3_17	16.372	1.148	1.105	14.263	20.0238	0.2065	20.1845	0.1607	20.1418	0.118	22.18	20.68	10.41	5.64	16.37	47.03	28.19
LOB21-3_18	16.246	1.157	1.086	14.043	15.277	0.1885	15.4242	0.1472	15.3855	0.1085	21.91	20.53	10.29	5.60	16.25	46.69	27.99
LOB21-3_19	15.391	1.069	0.941	14.395	16.1768	0.2037	16.3379	0.1611	16.2965	0.1197	20.91	20.32	9.82	5.54	15.39	46.22	27.71
LOB21-3_20	16.038	1.078	0.901	14.875	14.2532	0.2005	14.4111	0.1579	14.3675	0.1143	21.25	21.75	9.98	5.93	16.04	49.45	29.65
LOB21-3_21	15.666	1.038	0.647	15.097	17.7092	0.203	17.8715	0.1623	17.8263	0.1171	20.05	22.27	9.41	6.07	15.67	50.64	30.36
LOB21-3_22	13.398	0.912	0.457	14.694	21.2951	0.2035	21.4645	0.1694	21.4205	0.1254	16.76	21.62	7.87	5.90	13.40	49.17	29.48
LOB21-3_23	12.831	0.916	0.297	14.008	16.9039	0.2013	17.07	0.1661	17.0302	0.1263	17.49	19.77	8.21	5.39	12.83	44.96	26.95
LOB21-3_24	11.007	0.853	0.267	12.908	15.4739	0.202	15.6415	0.1676	15.6105	0.1366	17.03	15.35	8.00	4.18	11.01	34.90	20.92
LOB21-3_25	9.091	0.757	0.199	12.002	14.5013	0.2014	14.6704	0.1691	14.6472	0.1459	16.04	11.52	7.53	3.14	9.09	26.20	15.70
LOB21-3_26	7.566	0.652	0.182	11.596	17.2357	0.204	17.41	0.1743	17.3905	0.1548	14.56	9.56	6.84	2.61	7.57	21.74	13.03
LOB21-3_27b	6.561	0.546	0.165	12.009	16.5534	0.203	16.7303	0.1769	16.7128	0.1594	12.86	8.62	6.04	2.35	6.56	19.61	11.75
LOB21-3_28b	4.564	0.443	0.111	10.292	17.5996	0.202	17.78	0.1804	17.7668	0.1672	10.69	6.53	5.02	1.78	4.56	14.86	8.91
LOB21-3_29b	3.450	0.387	0.082	8.908	16.5255	0.2002	16.704	0.1785	16.6972	0.1717	10.84	3.40	5.09	0.93	3.45	7.72	4.63
LOB21-3_6d	14.029	1.102	0.704	12.733	20.194	0.2066	20.3533	0.1593	20.3199	0.1259	22.89	16.17	10.75	4.41	14.03	36.77	22.04
LOB21-3_8d	12.648	0.940	0.689	13.456	16.9584	0.2043	17.1263	0.1679	17.0925	0.1341	17.82	16.54	8.36	4.51	12.65	37.62	22.56
LOB21-3_11d	11.032	0.822	0.544	13.420	16.4193	0.2006	16.5871	0.1678	16.5577	0.1384	16.35	14.66	7.68	4.00	11.03	33.33	19.98
LOB21-3_14d	13.503	1.008	1.034	13.393	16.3075	0.2042	16.473	0.1655	16.4385	0.131	18.95	16.90	8.90	4.61	13.50	38.42	23.03
LOB21-3_16d	16.030	1.128	1.241	14.216	17.3523	0.2028	17.5126	0.1603	17.4744	0.1221	20.96	18.84	9.84	5.14	16.03	42.84	25.68
LOB21-3_18d	16.078	1.130	1.079	14.231	18.185	0.2	18.3409	0.1559	18.3009	0.1159	22.05	20.00	10.35	5.45	16.08	45.48	27.27

Table 6: Measurements and calculations from LOI and CNS for the core LOB21-3.

Sample ID	Depth [cm]	Dry Weight	Age	DBD	Sed. Rate	MAR	Atrazine-desisopropyl	Azoxystrobin	Benzovindiflupyr	Boscalid	Carbendazim	Chlorantraniliprole	Chlorothalonil	Chlorpyrifos	Difenoconazole	Diflufenican	Diuron	Epoxiconazole	Fenpropimorph	Fludioxonil	Flufenacet	Fluopyram	Fluxapyroxad	Flupicolide	Fluquinconazole	Imazalil	Imazalil-ethyl	Pendimethalin	Prochloraz	Propiconazole	Propiconazole	Simazine	Terbuthylazine	Terbutylazine-2-hydroxy	Thiamethoxam
Nr	cm	g	yr	g/cm3	cm/yr	ng/m2	ng/m2	ng/m2	ng/m2	ng/m2	ng/m2	ng/m2	ng/m2	ng/m2	ng/m2	ng/m2	ng/m2	ng/m2	ng/m2	ng/m2	ng/m2	ng/m2	ng/m2	ng/m2	ng/m2	ng/m2	ng/m2	ng/m2	ng/m2	ng/m2	ng/m2	ng/m2	ng/m2	ng/m2	ng/m2
LOB21-3-1	0-4		2021.5	0.159	0.895	0.138	0	4.26505	0.6628	19.2153	7.0793	0	13.78095	248.92125	46.6638	0	15.8137	60.17595	0.7897	0	8.8911	3.8137	1.8371	1.797	0	18.5932	0	10.7375	41.4395	0	0	18.2898	6.5678
LOB21-3-2	4-8		2017.0	0.171	0.895	0.153	0	0.90155	0.8853	0	15.74895	16.17825	7.70115	62.1004	21.3743	0	4.78915	19.11565	0.6574	0	2.91855	8.5196	0.8185	2.88915	0	5.24815	0	11.1435	20.355	0	0	17.72625	3.92205
LOB21-3-3	8-12		2012.6	0.194	0.895	0.174	0	0.45725	0.6876	0	15.8415	14.4371	0	35.77065	9.0916	0	4.308	14.79835	0.4885	0	1.5837	11.9532	0	2.74	0	4.094	0	8.2495	10.3979	0	0	14.9035	2.7411
LOB21-3-4	12-16		2008.1	0.211	0.895	0.189	0	0	0.5208	0	18.0535	15.7938	0	16.13625	4.9401	1.1758	3.6037	9.09275	0.3913	0	0	23.2551	0	2.5429	0	0	1.1498	6.2935	7.0559	0	0	8.9005	3.3372
LOB21-3-5	16-18		2003.6	0.231	0.895	0.224	0	0	0	0	12.6068	10.8751	0	4.57725	3.3474	0	0	11.75275	0	0	0	25.8515	0	2.3375	0	0	1.5187	3.735	4.5756	0	0	4.7208	1.2344
LOB21-3-6	18-20		2001.4	0.236	0.895	0.211	0	0	0	0	20.3491	18.6601	0	6.80265	4.32625	0	0	12.5721	0	0	0	28.87135	0	2.81535	0	0	1.42295	0	4.4914	4.1418	0	0	7.3754	1.11255
LOB21-3-7	20-22		1995.2	0.235	0.895	0.210	0	0	0.3013	0	20.0851	31.6951	0	5.60055	4.3411	1.0832	0	16.57605	0	0	0	21.7727	0	3.4804	0	0	1.3891	0	3.8622	3.2846	0	0	7.9405	0
LOB21-3-8	22-24		1996.9	0.259	0.895	0.232	0	0	0	0	11.91601	25.61305	0	3.00815	2.13105	2.03475	0	10.1056	0	0	0	14.39185	0	2.03195	0	0	2.5052	4.819	2.83705	5.7425	0	0	8.5375	0
LOB21-3-9	24-26		1994.7	0.248	0.895	0.222	0	0	0	0	18.1975	35.1954	0	0	0	1.5401	0	12.68665	0	0	0	6.2737	0	2.342	0	0	3.8243	0	1.854	5.8635	0	0	10.7252	0
LOB21-3-10	26-28		1992.4	0.295	0.895	0.264	0	0	0	0	12.1647	36.8753	0	0	0	0.7044	0	6.05545	0	0	0	3.099	0	2.0761	0	0	4.722	0	0	7.1556	0	0	10.78	0
LOB21-3-11	28-30		1990.2	0.292	0.862	0.252	0	0	0	0	8.50015	27.4408	0	0	0	0.9424	0	3.412	0	0	0	1.8464	0	2.07275	0	0	1.8828	0	0	3.99765	0	0	6.18495	0
LOB21-3-12	30-32		1987.9	0.213	0.648	0.137	0	0	0	0	15.0091	22.8123	0	0	0	0	0	0	0	0	0	0	0	1.5393	0	0	0	0	0	6.2223	0	0	8.7919	0
LOB21-3-13	32-34		1984.8	0.225	0.648	0.146	0	0	0	0	6.6461	12.2633	0	0	0	0	0	0	0	0	0	0	0	1.5272	0	0	0	0	0	3.8671	0	0	5.2439	0
LOB21-3-14	34-36		1981.7	0.207	0.646	0.134	0	0	0	0	9.2961	23.8901667	0	0	0	0	0	0	0	0	1.61495	0	0	0	0	1.171	2.98116667	0	0	0	0	7.4153	9.19198333	7.57186667	0
LOB21-3-15	36-38		1978.6	0.222	0.646	0.143	0	0	0	0	15.8761	22.0947	0	0	0	0	0	0	0	0	3.87295	0	0	0	0	1.2276	8.9462	0	0	0	0	9.0621	13.6732667	8.826	0
LOB21-3-16	38-40		1975.5	0.108	0.697	0.120	0	0	0	0	7.7532	4.01965	0	0	0	0	0	0	0	0	3.39565	0	0	0	0	1.2581	8.2581	0	0	0	0	0	13.3819867	3.91535	0
LOB21-3-17	40-42		1972.2	0.191	0.572	0.109	0	0	0	0	12.2348	0	0	0	0	0	0	0	0	0	3.60145	0	0	0	0	1.3435	10.542	0	0	0	0	0	26.0503867	7.1805	0
LOB21-3-18	42-44		1968.7	0.179	0.572	0.102	0	0	0	0	10.2397	4.5137	0	0	0	0	0	0	0	0	6.9178	0	0	0	0	1.1118	18.08125	0	0	0	0	0	35.4279667	7.48075	0
LOB21-3-19	44-46		1965.2	0.197	0.572	0.112	0	0	0	0	6.3353	0	0	0	0	0	0	0	0	0	15.41445	0	0	0	0	1.4333	35.6991	0	0	0	0	0	94.3740667	12.7106	0
LOB21-3-20	46-48		1961.7	0.207	0.851	0.176	11.4317	0	0	0	8.5497	0	0	0	0	0	0	0	0	0	2.69915	0	0	0	0	0.9625	7.6009	0	0	0	0	0	11.2461667	4.0525	0
LOB21-3-21	48-50		1959.4	0.206	1.262	0.260	0	0	0	0	3.7908	0	0	0	0	0	0	0	0	0	2.35275	0	0	0	0	0.7387	5.2102	0	0	0	0	0	14.7052667	4.7259	0
LOB21-3-22	50-52		1957.8	0.213	1.053	0.224	0	0	0	0	7.1837	0	0	0	0	0	0	0	0	0	0	0	0	0	0	0.5008	0	0	0	0	0	0	2.02426667	0.9841	0
LOB21-3-23	52-54		1955.9	0.199	0.637	0.127	0	0	0	0	3.8151	0	0	0	0	0	0	0	0	0	0	0	0	0	0	0	0	0	0	0	0	0	2.6756667	0	0
LOB21-3-24	54-56		1953.7	0.215	0.596	0.128	0	0	0	0	5.4408	0	0	0	0	0	0	0	0	0	0	0	0	0	0	0	0	0	0	0	0	0	0	0	0
LOB21-3-25	56-58		1949.4	0.234	0.596	0.140	0	0	0	0	3.1883	0	0	0	0	0	0	0	0	0	0	0	0	0	0	0	0	0	0	0	0	0	0	0	0
LOB21-3-26	58-60		1946.9	0.250	0.596	0.173	0	0	0	0	0	0	0	0	0	0	0	0	0	0	0	0	0	0	0	0	0	0	0	0	0	0	0	0	0

Table 7: HPLC-MS Data from core LOB21-3.

Sample Serial No.	Depth [m]	Lat	Lon	DW_550 [g]	DW_950 [g]	LOI_550 w	LOI_950 wt%	Total N wt%	Total C wt%	Total S wt%	C/N	TOC wt%
LOB21surf-1	2.7	07°17'51.46"	47°01'48.47"	0.1294	0.098	37.94	15.06	1.655	22.140	1.966	13.37	17.81
LOB21surf-2	3.6	07°17'51.62"	47°01'48.86"	0.1458	0.1196	29.29	12.71	1.673	18.026	1.233	10.776	13.75
LOB21surf-3	3.8	07°17'52.96"	47°01'49.58"	0.149	0.1233	26.89	12.61	1.470	15.840	0.880	10.777	12.62
LOB21surf-4	3.9	07°17'53.45"	47°01'49.90"	0.1536	0.126	25.80	13.33	1.452	15.903	0.872	10.953	12.11
LOB21surf-5	3.7	07°17'54.01"	47°01'50.66"	0.1469	0.1172	27.95	14.57	1.607	17.699	1.349	11.012	13.12
LOB21surf-6	3.3	07°17'54.60"	47°01'51.56"	0.1387	0.1081	31.78	15.05	1.670	19.413	1.746	11.624	14.92
LOB21surf-7	2.4	07°17'54.49"	47°01'51.75"	0.1348	0.101	35.22	16.24	1.832	22.691	2.087	12.389	16.54
LOB21surf-8	2.4	07°17'55.29"	47°01'52.52"	0.1345	0.0999	34.39	16.88	1.741	21.937	1.954	12.603	16.15
LOB21surf-9	0.9	07°17'56.00"	47°01'50.84"	0.1331	0.1042	34.82	14.15	1.814	21.804	2.191	12.019	16.35
LOB21surf-10	2.5	07°17'55.13"	47°01'49.10"	0.1426	0.1135	32.06	13.86	1.688	20.490	1.598	12.14	15.05
LOB21surf-11	3	07°17'54.45"	47°01'49.11"	0.1446	0.1178	28.56	13.24	1.542	17.861	1.550	11.585	13.41
LOB21surf-12	3.8	07°17'52.84"	47°01'50.51"	0.1494	0.1224	28.17	12.98	1.570	17.087	1.057	10.886	13.23
LOB21surf-13A	2.4	07°17'51.76"	47°01'50.94"	0.1379	0.1108	33.89	12.99	1.703	20.774	1.546	12.201	15.91
LOB21surf-13B	2.4	07°17'51.76"	47°01'50.94"	0.1295	0.1048	35.60	12.28	1.655	20.109	1.434	12.147	16.72
LOB21surf-14	2.3	07°17'50.83"	47°01'50.47"	0.1308	0.0991	36.72	15.34	1.679	22.728	1.907	13.534	17.24
LOB21surf-15A	2.3	07°17'50.83"	47°01'50.47"	0.1406	0.1102	30.74	14.98	1.504	19.390	1.569	12.891	14.43
LOB21surf-15B	2.6	07°17'53.02"	47°01'48.12"	0.1398	0.1094	31.30	14.94	1.553	19.252	1.603	12.395	14.70
LOB21surf-16	0.8	07°17'55.66"	47°01'48.16"	0.1826	0.1793	10.67	1.61	0.496	5.383	0.212	10.853	5.01
LOB21surf-17	0.4	07°17'54.95"	47°01'47.44"	0.1797	0.1782	11.43	0.74	0.445	4.673	0.147	10.497	5.37
LOB21surf-18	0.5	07°17'56.40"	47°01'57.84"	0.1765	0.1731	15.02	1.64	0.758	9.937	0.196	13.101	7.05
LOB21surf-19	0.5	07°17'56.58"	47°01'58.87"	0.1943	0.1923	6.41	0.96	0.228	2.501	0.082	10.993	3.01

Table 8: Locations and measurements and calculations from LOI and CNS for the surface sediment samples.

Sample ID	Dry Weight	Azoxystrobin	Boscalid	Chloridazon	Chloridazon_2	Chlorpyrifos	Difenoconazole	Diflufenican	Diuron	Epoxiconazole	Fenpropimorph	Fluazinam	Fluopyram	Flusilazole	Fluxapyroxad	Isoproturon	Linuron	Metalaxyl	Metamitron	Metolachlor_OA	Napropamide	Propiconazole	Prosulfocarb	Tembotrione	Terbuthylazine	Terbutylazine-2-hydroxy
Nr.	g	microg/L	microg/L	microg/L	microg/L	microg/L	microg/L	microg/L	microg/L	microg/L	microg/L	microg/L	microg/L	microg/L	microg/L	microg/L	microg/L	microg/L	microg/L	microg/L	microg/L	microg/L	microg/L	microg/L	microg/L	microg/L
LOB21surf-1	4.0539	0	0	0	0	0	27.37715	18.6416	0	0	8.839	0	0	2.5613	0	0	0	0	0	0	0	6.9732	6.4671	0	0	42.11275
LOB21surf-2	4.0174	0	0	0	0	0	44.83865	10.4007	0	0	8.6252	0.2124	0	2.8278	0	0	0	0	0	0	0	10.2773	4.318	0	0	93.56945
LOB21surf-3	4.0164	0	0	0	0	0	49.86825	12.5499	0	0	9.756	0.1857	0	3.2445	0	0	0	0	0	0	0	0	3.8407	0	0	138.07465
LOB21surf-4	4.0062	1.7744	0	0	0	0	60.30615	14.21015	0	3.8745	8.3824	0.19015	0	3.14205	0	0	0	0	0	0	0	5.14085	3.64525	0	0	133.409
LOB21surf-5	4.0088	0	0	0	0	6.56625	46.00725	10.4936	0	0	6.4695	0.1794	0	2.962	0	0	0	0	0	0	0	4.8401	4.998	0	0	117.51335
LOB21surf-6	4.0049	0	0	0	0	0	52.22425	12.9995	0	0	8.1577	0.1567	0	2.221	0	0	0	0	0	0	0	9.2218	4.7632	0	0	149.80715
LOB21surf-7	4.0066	0	0	0	0	2.21305	40.68745	14.3404	0	0	7.3105	0.1207	0	0	0	0	0	0	0	0	0	6.3061	5.233	0	0	113.61515
LOB21surf-8	4.0028	0	0	0	0	2.21815	41.34455	12.5599	0	0	6.7811	0.1065	0	1.9448	0	0	0	0	0	0	0	7.1819	6.2379	0	0	109.97945
LOB21surf-9	4.0000	0	0	0	0	0	45.87775	20.6252	0	0	9.0117	0.1066	0	2.2215	0	0	0	0	0	0	0	8.6762	6.4176	0	0	161.71855
LOB21surf-10	4.0058	0	0	0	0	0	50.3719	17.9734	0	0	8.42155	0.1216	0	2.00695	0	0	0	0	0	0	0	7.77785	4.97665	0	0	134.41115
LOB21surf-11	4.0041	1.1506	0	0	0	0	67.76425	9.0297	0	0	5.6219	0.1382	2.3414	2.2461	0	0	0	0	0	0	0	5.6827	2.7868	0	0	123.67595
LOB21surf-12	4.0058	0	0	0	0	5.93255	70.68345	42.1454	0	0	10.1812	0.2197	0	0	0	0	0	0	0	0	0	7.168	6.068	0	0	224.37235
LOB21surf-13	4.0224	0	0	0	0	1.127375	28.92625	14.08255	0	0	8.9325	0.0543	0	1.29415	0	0	0	0	0	0	0	8.1524	4.775	0	0	162.72425
LOB21surf-14	4.0051	0	0	0	0	0	23.27705	26.8869	0	5.2601	5.595	0.1063	2.5163	0	0	0	0	0	0	0	0	4.8788	4.1684	0	0	99.21815
LOB21surf-15	4.0042	0	0	0	0	1.143725	49.85875	4.17435	0	0	4.9503	0.0683	0	2.3354	0	0	0	0	0	0	0	7.03095	4.91025	0	0	116.0341
LOB21surf-16	4.0052	2.1907	11.7495	0	0	0	22.54275	12.8037	0	15.9272	4.0466	0.1348	4.4623	0.5134	0	0	0	1.0001	0	0	0	0	0.8467	2.5675	5.1708	85.46645
LOB21surf-17	4.0385	2.4411	10.2704	3.6761	3.6761	0	14.25135	10.5886	0	15.9623	2.8575	0.1179	4.6302	0.4766	0	0	0	1.194	0	0	0	0	0.8307	2.243	5.1225	82.39205
LOB21surf-18	4.0080	1.1385	8.2894	4.0064	4.0064	0	2.38285	3.7288	1.1159	10.1979	1.1681	0	5.3735	0	0.6766	1.0152	0	2.1385	0	4.9493	2.6209	0	0.5359	1.7796	4.3635	178.20825
LOB21surf-19	4.0012	0	0	3.653	3.653	0	2.70705	3.5707	0.8509	17.0099	0.599	0	0.8527	0.5722	0.4452	1.505	1.7464	1.7086	6.1283	3.0851	0	0.9827	0.0841	0	0	45.45385

Table 9: HPLC-MS Data from surface sediment samples.

Appendix B Dating, MAR, Age-Depth Modelling, Code of Core Correlation

The age depth model of core LOB21-2 was built according to the description in the main text. Then the age-depth model was correlated to core LOB21-3 (which was used to measure PPPs) by linearly interpolating marker layers that have been correlated either visually or from HSI data.

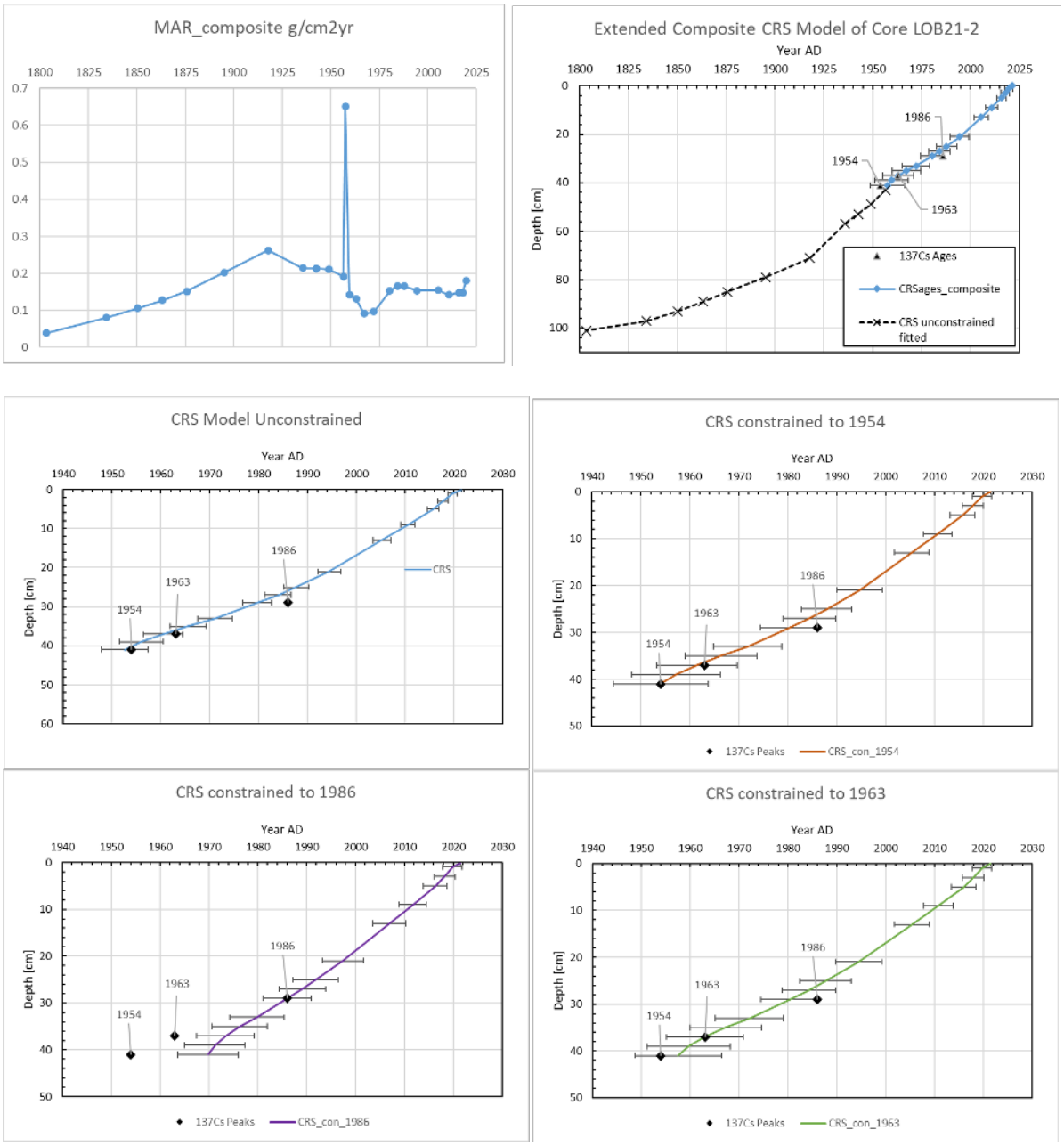

Fig. 35: MAR and definite CRS Models of core LOB21-2 with comparison of different constrained CRS models. Top left: MAR of composite model. Top right: Composite Age-depth model. Middle left: Unconstrained CRS model. Middle right: CRS model constrained to 1954. Bottom left: CRS model constrained to 1986. Bottom right: CRS model constrained to 1963.

```r
library(dplyr)
```

```
##
## Attache Paket: 'dplyr'
```

```
## Die folgenden Objekte sind maskiert von 'package:stats':
##
##     filter, lag
```

```
## Die folgenden Objekte sind maskiert von 'package:base':
##
##     intersect, setdiff, setequal, union
```

```r
library(readxl)

setwd("C:/Users/emman/OneDrive - Universitaet Bern/Master Thesis/04 Data/Dating and Correlation")
LOB21_AgeDepth_Modelling <- read_excel("C:/Users/emman/OneDrive - Universitaet Bern/Master Thesis/04 Da
                                       sheet = "AgeDepthAdjustmentToCore3",
                                       range = "A1:B27")
DepthMatching <- read_excel("LOB21 AgeDepth Modelling.xlsx",
                                       sheet = "AgeDepthAdjustmentToCore3",
                                       range = "J1:M12")
DepthMatching <- DepthMatching[complete.cases(DepthMatching[,3]),]

depth2_tointerpol <- LOB21_AgeDepth_Modelling$Depth_cm
age2_tointerpol <- LOB21_AgeDepth_Modelling$CRSages_composite
depth2 <- (0:1000) / 10


interpolation <- approx(x=depth2_tointerpol, y=age2_tointerpol, xout=depth2, method = "linear", rule=2)

plot(depth2_tointerpol, age2_tointerpol)
```

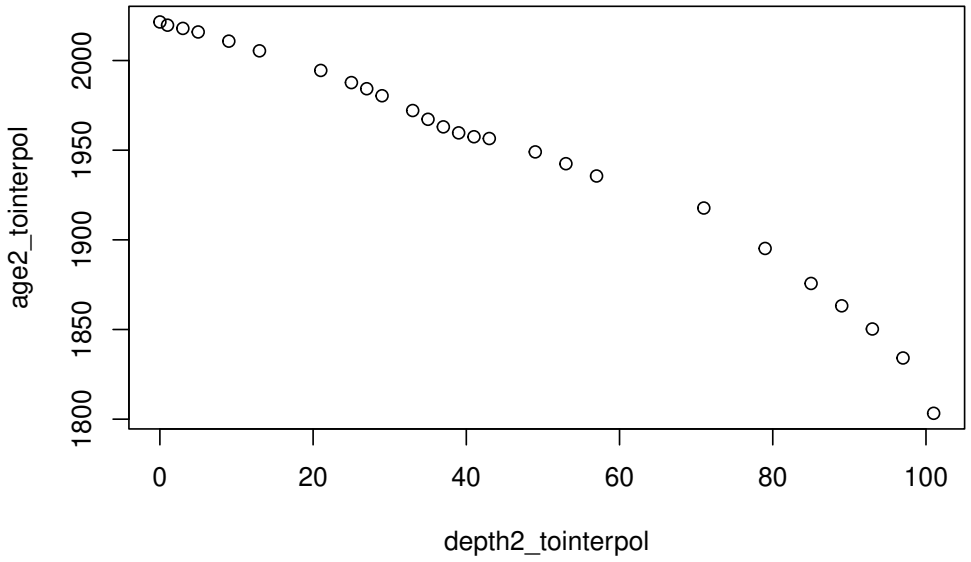


```
plot(interpolation$x, interpolation$y)
```

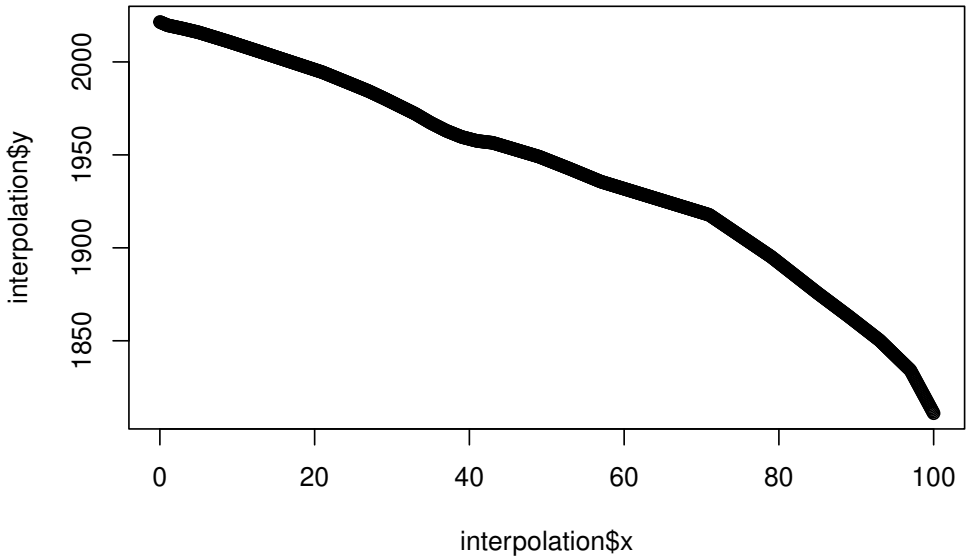


```
agedepthmodel2 <- cbind(interpolation$x, interpolation$y)
agedepthmodel2 <- data.frame(agedepthmodel2)
colnames(agedepthmodel2) <- c("depth2cm", "age2yr")

(agematched2 <- filter(agedepthmodel2, depth2cm %in% DepthMatching$`Depth Core2 cm`))
```

```
##    depth2cm   age2yr
## 1       0.0 2021.500
## 2      24.7 1988.199
## 3      32.1 1973.964
## 4      38.6 1960.320
## 5      42.5 1956.754
## 6      44.0 1955.263
## 7      56.0 1937.312
## 8      60.4 1931.260
## 9      66.3 1923.735
## 10     73.4 1910.980
## 11     91.1 1856.426
```

```
corecorr <- data.frame(agematched2, DepthMatching$`Depth Core3 cm`)
corecorr <- corecorr[,c(1,3,2)]
names(corecorr)[names(corecorr) == "depth2cm"] <- "DepthCore2cm"
names(corecorr)[names(corecorr) == "DepthMatching..Depth.Core3.cm."] <- "DepthCore3cm"
names(corecorr)[names(corecorr) == "age2yr"] <- "Age_yr"
corecorr
```

```
##    DepthCore2cm DepthCore3cm   Age_yr
```

```
## 1           0.0          0.0 2021.500
## 2          24.7         29.8 1988.199
## 3          32.1         39.0 1973.964
## 4          38.6         46.8 1960.320
## 5          42.5         51.3 1956.754
## 6          44.0         52.5 1955.263
## 7          56.0         63.2 1937.312
## 8          60.4         66.8 1931.260
## 9          66.3         74.3 1923.735
## 10         73.4         82.2 1910.980
## 11         91.1         97.8 1856.426
```

```
depthCore3allcm <- (0:1006.9) / 10
agedepthmodelCore3 <- data.frame(approx(x=corecorr$DepthCore3cm, y=corecorr$Age_yr, xout=depthCore3allcr

plot(agedepthmodelCore3)
```

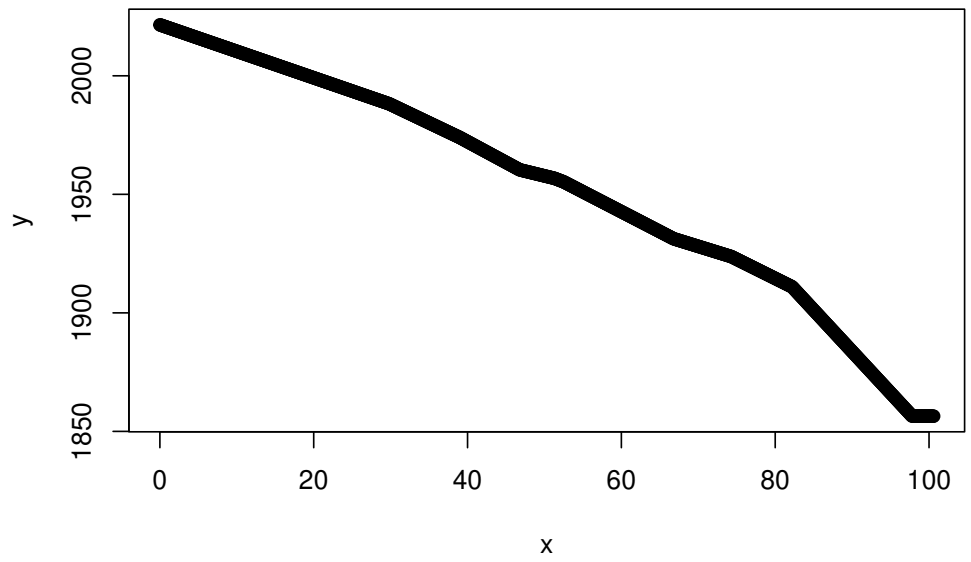


```
PPPs <- read_excel("C:/Users/emman/OneDrive - Universitaet Bern/Master Thesis/04 Data/PPPs Analysis/LOB
                                        sheet = "RtoCopy",
                                        range = "A1:AH30")
```

```
## New names:
## * `` -> `...5`
## * `` -> `...6`
## * `` -> `...7`
```

```
PPPs_agedepth <- filter(agedepthmodelCore3, x %in% PPPs$Depth)
```

Appendix C Dionex ASE 350 Extraction Accuracy

The VOA vials are weighed empty and then after extraction 1 and extraction 2. Extraction 1 uses solvent 1 consisting of 70:30 Ethyl-acetate:Acetone, while extraction 2 uses solvent 2 consisting of 70:30 Acetone: 1% Phosphoric acid. The densities are shown in Table 11.

ρ_{EthAc} [g/cm^3]	ρ_{Acetone} [g/cm^3]	$\rho_{\text{1\%PA}}$ [g/cm^3]	ρ_{Solvent1} [g/cm^3]	ρ_{Solvent2} [g/cm^3]
0.9020	0.7845	1.0080	0.86675	0.85155

Table 11: Solvent densities used for the calculation of extraction volumes.

$$\rho_{\text{Solvent1}} = 0.7 \cdot \rho_{\text{EthAc}} + 0.3 \cdot \rho_{\text{Acetone}} \tag{10}$$

$$\rho_{\text{Solvent1}} = 0.7 \cdot \rho_{\text{Acetone}} + 0.3 \cdot \rho_{\text{1\%PA}} \tag{11}$$

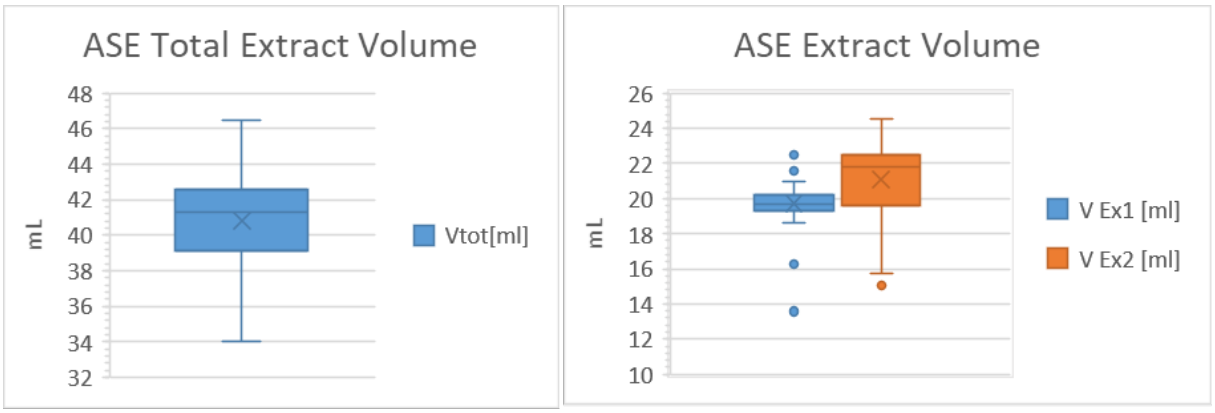

Fig. 36: Volume extract consistency of the Dionex ASE 350.

Sample ID	m vial [g]	m vial + Ex1 [g]	m vial + Ex1 + Ex2 [g]	m Ex1 [g]	V Ex1 [ml]	m Ex2 [g]	V Ex2 [ml]	Vtot[ml]
LOB21-3B-1+2	33.847	50.177	66.903	16.330	18.840	16.726	19.642	38.482
LOB21-3B-3+4	37.882	54.022	69.075	16.140	18.621	15.053	17.677	36.298
LOB21-3B-5+6	33.774	50.438	67.876	16.664	19.226	17.438	20.478	39.704
LOB21-3B-7+8	38.078	54.990	70.672	16.912	19.512	15.682	18.416	37.928
LOB21-3B-9	40.033	57.113	75.531	17.080	19.706	18.418	21.629	41.335
LOB21-3A-10	40.159	57.503	76.078	17.344	20.010	18.575	21.813	41.824
LOB21-3A-11	37.937	55.138	73.853	17.201	19.845	18.715	21.978	41.823
LOB21-3A-12	39.885	57.426	76.301	17.541	20.238	18.875	22.165	42.403
LOB21-3A-13	34.026	51.070	69.306	17.044	19.664	18.236	21.415	41.079
LOB21-3A-14	37.889	54.411	72.325	16.522	19.062	17.914	21.037	40.099
LOB21-3A-15	37.667	54.436	71.724	16.769	19.347	17.288	20.302	39.649
LOB21-3A-16	38.518	55.235	73.717	16.717	19.287	18.482	21.704	40.991
LOB21-3A-17	40.102	57.133	76.035	17.031	19.649	18.902	22.197	41.846
LOB21-3A-18	33.974	50.434	67.901	16.460	18.990	17.467	20.512	39.502
LOB21-3A-19	33.938	51.456	70.323	17.518	20.211	18.867	22.156	42.367
LOB21-3A-20	39.939	57.345	76.364	17.406	20.082	19.019	22.335	42.416
LOB21-3A-21	37.837	55.738	74.506	17.901	20.653	18.768	22.040	42.693
LOB21-3A-22	37.687	55.298	74.598	17.611	20.318	19.300	22.665	42.983
LOB21-3A-23	33.975	52.038	72.009	18.063	20.840	19.971	23.453	44.292
LOB21-3A-24	39.894	57.366	76.436	17.472	20.158	19.070	22.394	42.553
LOB21-3A-25	37.783	55.330	74.896	17.547	20.245	19.566	22.977	43.222
LOB21-3A-26	33.911	51.223	69.500	17.312	19.973	18.277	21.463	41.437
LOB21-3A-30	34.065	50.499	68.268	16.434	18.960	17.769	20.867	39.827
LOB21-3A-31	34.099	50.883	68.427	16.784	19.364	17.544	20.602	39.967
LOB21-3A-32	39.805	57.097	73.177	17.292	19.950	16.080	18.883	38.834
LOB21-3A-33	40.110	57.315	73.802	17.205	19.850	16.487	19.361	39.211
LOB21-3A-34	33.978	50.356	65.578	16.378	18.896	15.222	17.876	36.772
LOB21-3A-35	40.188	56.437	72.114	16.249	18.747	15.677	18.410	37.157
LOB21-3A-36	39.247	56.081	71.776	16.834	19.422	15.695	18.431	37.853
LOB21-3A-37	33.928	50.961	65.345	17.033	19.652	14.384	16.892	36.543
LOB21-3A-38	40.196	56.631	69.459	16.435	18.962	12.828	15.064	34.026
LOB21-3A-39	38.039	54.889	71.534	16.850	19.440	16.645	19.547	38.987
LOB21-3A-40	33.977	50.471	66.585	16.494	19.030	16.114	18.923	37.953
LOB21-3A-41	39.874	57.052	73.560	17.178	19.819	16.508	19.386	39.205
LOB21-3A-42	38.874	55.305	70.111	16.431	18.957	14.806	17.387	36.344
LOB21-3A-43	39.784	58.496	78.297	18.712	21.589	19.801	23.253	44.842
LOB21-3A-44	40.454	57.515	75.180	17.061	19.684	17.665	20.745	40.428
LOB21surf-1	40.325	57.247	75.745	16.922	19.524	18.498	21.723	41.246
LOB21surf-2	33.860	50.810	70.037	16.950	19.556	19.227	22.579	42.135
LOB21surf-3	33.966	50.883	70.042	16.917	19.518	19.159	22.499	42.017
LOB21surf-4	39.420	56.467	75.323	17.047	19.668	18.856	22.143	41.811
LOB21surf-5	38.318	55.582	75.363	17.264	19.918	19.781	23.229	43.147
LOB21surf-6	38.291	55.377	74.760	17.086	19.713	19.383	22.762	42.475
LOB21surf-7	37.910	55.038	74.499	17.128	19.761	19.461	22.854	42.615
LOB21surf-8	39.493	56.766	76.223	17.273	19.928	19.457	22.849	42.777
LOB21surf-9	37.630	54.339	72.951	16.709	19.278	18.612	21.857	41.134
LOB21surf-10	37.633	54.756	73.289	17.123	19.755	18.533	21.764	41.519
LOB21surf-11	33.979	51.484	71.518	17.505	20.196	20.034	23.527	43.723
LOB21surf-12	37.259	51.354	70.861	14.095	16.262	19.507	22.908	39.170
LOB21surf-13A	37.071	48.845	67.472	11.774	13.584	18.627	21.874	35.458
LOB21surf-13B	38.007	55.196	74.010	17.189	19.832	18.814	22.094	41.925
LOB21surf-14	40.589	58.253	75.243	17.664	20.380	16.990	19.952	40.331
LOB21surf-15A	38.553	56.739	75.894	18.186	20.982	19.155	22.494	43.476
LOB21surf-15B	33.902	51.626	70.656	17.724	20.449	19.030	22.347	42.796
LOB21surf-16	33.911	52.900	73.694	18.989	21.908	20.794	24.419	46.327
LOB21surf-17	34.245	53.256	74.143	19.011	21.934	20.887	24.528	46.462
LOB21surf-18	39.476	58.597	78.840	19.121	22.061	20.243	23.772	45.833
LOB21surf-19	37.673	57.165	70.537	19.492	22.489	13.372	15.703	38.192

Table 12: Weight measurements and calculated values of extraction volumes.

Appendix D Standard Operation Protocol: LOI

Standard Operation Protocol for sequential loss on ignition (LOI) measurements

Version number of SOP: 1

Typical application of the procedure:

LOI is a common method to estimate the organic matter (OM) and carbonate content of sediments. The word 'sequential' is used because in a first step organic matter is combusted to ash and carbon dioxide at a temperature of 550 °C. In a second step, the same sample is combusted at 950 °C CO2 is emitted from the carbonates leaving oxide. The weights of the sample before and after each combustion are used to calculate the OM content (or further organic carbon content) and carbonate content (or further inorganic carbon).

Reference to the original procedure:

Loss on ignition as a method for estimating organic and carbonate content in sediments: reproducibility and comparability of results. Oliver Heiri, André F. Lotter & Gerry Lemcke. *Journal of Paleolimnology* **25**: 101–110, 2001

Date SOP first issued: 2021-12-15

Person SOP issued: Emmanuel Schaad

Date SOP modified: -

Person who did the last modification: -

Contact person in the lab: Maarika Bischoff

Equipment needed

- Freeze-dried & homogenized samples
- Ceramic crucibles (found in the closet in Room n. 141, first floor Erlachstrasse)
  Note: Make sure you use crucibles of the same size for all your samples and that your crucibles are properly cleaned and baked before use.
- Sampling tools (spatulas etc.)
- Desiccator
- Muffle furnace capable of reaching 1000°C (Nabertherm B410, found in Room 151, first floor Erlachstrasse)
- Firebricks to place hot crucibles (found next to the muffle furnace)
- Balance weighing in grams (found in Room 141, first floor Erlachstrasse)

Safety

The most obvious hazard in LOI is being burned by hot samples fresh out of the furnace. Be patient and make slow movements. Use the high-temp gloves and mitts (usually found next to the muffle furnace). Keep in mind they are only good to about 350°C and can be awkward to use.

Basic operation of the furnace

- Power-on switch is located at the backside of the furnace.
- There are 4 buttons & a jog dial to select an input, see Figure 1. See Figure 2 for additional operation fields on the control board.
- Press MENU to scroll through the 7 different submenus using the jog dial: PROGRAM DISPLAY, PROGRAM START, ENTER PROGRAM, DELETE PROGRAM, COPY PROGRAM, EXTRAFUNCTION SELECT, SETTINGS. Only the first three will be necessary. The current selection can be confirmed by pressing the jog dial once.
- To check the setting of a program, press MENU, select DISPLAY PROGRAM, scroll to the desired program, and confirm it by pressing the jog dial. Then you can scroll through the setting pages of the program.
- Before starting a program, on the operation-temperature limiter always set the temperature to 30 °C above the max. temperature of the selected program. Use the small up- and down-arrows to adjust this temperature limit. This is a safety feature to make sure the furnace does not exceed this temperature.
- To start a program, press MENU, select PROGRAM START, press the jog dial to confirm DELAY NO, then press START
  If you want to delay the start of the selected program (e.g. you want it to start in 2 hrs, instead of immediately), select DELAY YES using the jog dial and then enter the desired delay-time. Then press START.
- To abort a running program, long-press START, the program will be terminated without additional input.

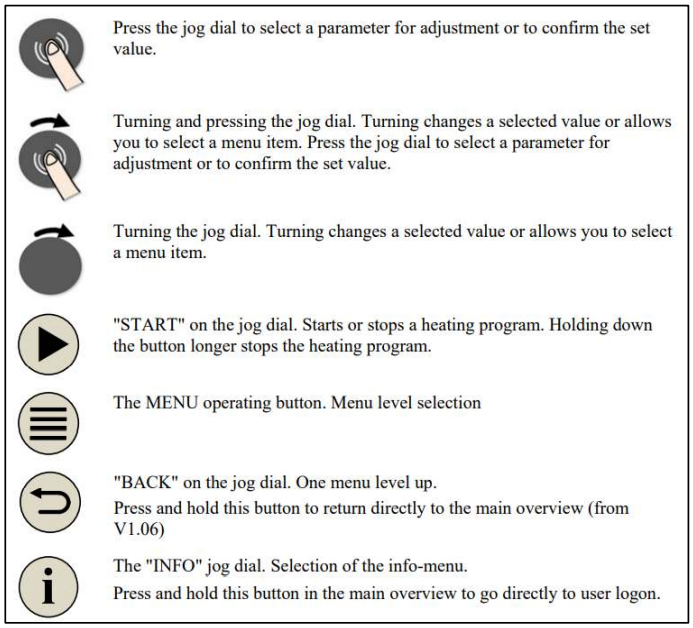

Figure 1: Operation Keys on the Furnace

B410/C450/P480

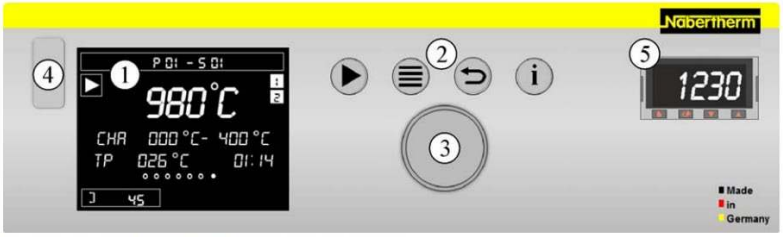

Fig. 2: Control field B410/C450/P480 (similar to picture)

No.	Description
1	Display
2	Control keys for "Start/Hold/Stop", "Menu" selection, "Back" function and information menu selection
3	Jog dial
4	USB interface for a USB stick
5	Over-temperature limiter with manual reset (optional)

Figure 2: Operation field

LOI procedure in detail

LOI 550

1. Select and weigh the number of crucibles you will need to use for your samples. Note the weight of the crucible in the spreadsheet (pdf and excel-sheet found in this folder).
   Note:
   - Use rubber gloves when weighing in the sediment
   - The crucibles are usually numbered with permanent marker. Check to see that they are still numbered and if not number them. To avoid problems in case numbering gets erased or is difficult to read, place the samples and take them out of the oven in a specific order.

2. Place ca. **0.2-0.5 g** of well-homogenized dried sediments in each crucible and weigh them. Note the weight of the crucible with the sediments in grams.
   Note:
   - try to keep the weight roughly the same for all samples. LOI 550 is dependent on the sample size so differences in the weight can affect the accuracy of the measurement.

3. Place the crucibles on the metal tray and place the tray in the oven. Do not place them too close to each other so you can easily remove them. Make a sketch on which position you put which crucible. This is done to avoid confusion if the number marking on the crucible is removed during ignition. Close the furnace door.

4. Set the temperature limit on the small display to 580 °C using the up- and down-arrow button.

5. Run the program *LOI 550 4H*:
   5.1. Turn the furnace on

5.2. Display the desired program by pressing MENU and selecting PROGRAM DISPLAY with the jog dial. Confirm by pressing the dial. The displayed program settings can now be viewed by turning the jog dial. When displaying a program, its settings are not changed. See Figure 3 for the correct settings of the program *LOI 550 4H*. If all settings are correct, proceed with 5.4.

Note:

- If different settings than in Figure 3 are displayed, the program must not be run but needs to be adjusted. See on how to edit a program.

5.3. Return to the overview by pressing the BACK button for 2 seconds.

5.4. Turn to the program *LOI 550 4H* using the dial and press it to confirm. Press to reject delayed start (NO). Press START to run the program.

6. After the ignition is done, open the door of the furnace halfway and wait until the furnace cools down to 30-50 °C (this usually takes 1-2 hours). Then take the samples out of the furnace (using a pair of tweezers for handling the crucibles) and place them on the firebrick or in the desiccator. **If the samples are still hot, do not place them in the desiccator!**
   Weigh them as soon as possible and note the weight in the spreadsheet ('Cruc.+sample weight (g) after 550').
   Note:
   - The crucibles may be stored in the desiccator until weighing if needed. For this the crucibles need to be cooled down (< 30 °C) and the plug of the desiccator must not be fully inserted.
   - When not burning or being weighed, the crucibles and the samples they contain must be stored in a desiccator. Make sure there is enough desiccator space for the number of samples you analyze. Wait until the samples are cool (< 30°C) before putting them in the desiccator. Check the silica gel if it needs to be dried again (blue color: still good, reddish color: needs to be dried). See further down how to prepare silica gel for the desiccator.

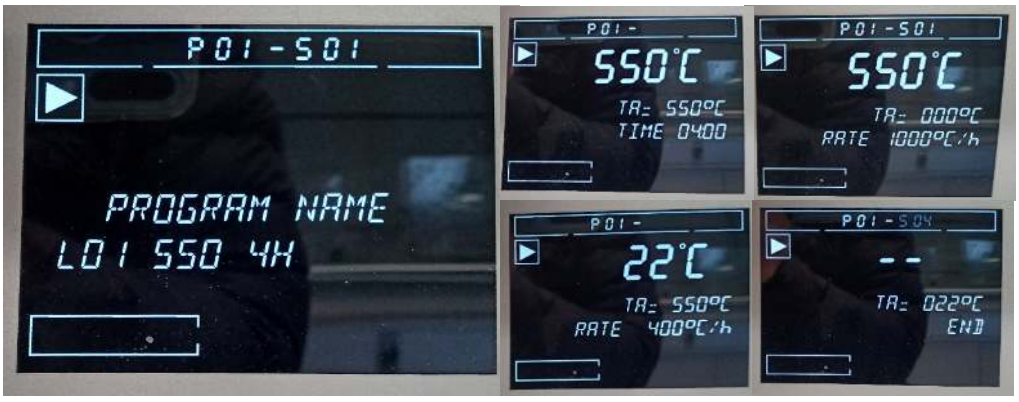

Figure 3: Program settings of LOI 550 4H

Figure 4: Over-temperature limiter setting for LOI 550

4

LOI 950

1. After weighing the crucibles, put them with the already ignited sample at 550°C in the furnace as explained above.
2. Set the temperature limit on the small display to 980 °C using the up- and down-arrow button.
3. Run the program *LOI 950 2H*:
   3.1. Check the program settings as described above. Crosscheck them with the settings for LOI 950 shown in below. If the settings are correct, proceed.
   3.2. Return to the overview by pressing the BACK button for 2 seconds.
   3.3. Turn to the program *LOI 950 2H* using the dial and press it to confirm. Press to reject delayed start (NO). Press START to run the program.
4. After the ignition is done, open the door of the furnace halfway and wait until the furnace cools down to 30-50 °C (this takes longer than LOI 550). Then take the samples out of the furnace as explained above and place them on the firebrick or desiccator. Weigh them as soon as possible and note the weight in the spreadsheet ('Cruc.+sample weight (g) after 950').

Cleaning of crucibles after usage

1. Remove any remaining residue and wash the crucibles with running water using a brush. Scrub the crucibles until all baked-on residue is gone. Some discoloration will remain.
2. Rinse the crucibles with DI water, shake and leave them to dry under the hood.
3. Place all washed crucibles in the furnace and bake them at **550 °C for 2 hours**. To do this, edit the program *LOI 550 4H* according to the description below.
4. When done, let the crucibles cool down, remove them from the furnace, cover with aluminum foil and store them.

Editing a program

1. Select "ENTER PROGRAM" and scroll to *LOI 550 4H*. The program name is flashing, press the dial to select it.
2. Edit the name by pressing the dial again. The first letter starts flashing to indicate it is selected to be edited. By clicking the dial you can change the position of the editable letter. Change the name *to LOI 550 2H*.
3. Exit the name-editor by pressing BACK. Scroll to the second page of the program and edit the time from 4:00 to 2:00 by selecting it (if selected, it starts flashing) and using the dial to set the time, see Figure 5.
4. Hit BACK until you are asked to save the program. Switch to YES using the dial and confirm by pressing the dial.

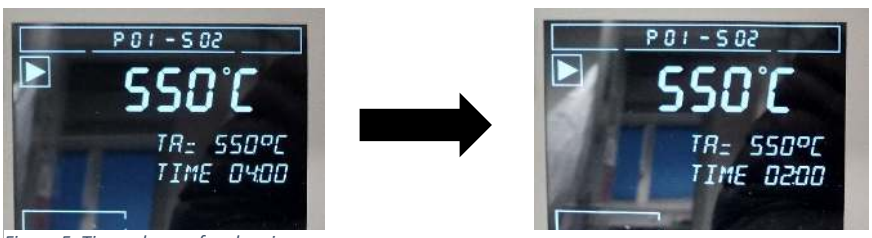

Figure 5: Timer change for cleaning program

Preparation of Silica Gel for Desiccator

If the silica gel in the desiccator shows a reddish color, it needs to be regenreated (baked) so that it can be used again. Distributed the silica gel onto a ovenproof container (e.g. aluminum). Make sure the silical gel layer is not too thick to ensure an even regeneration. Put the containers in the furnace and run the program SILICA GEL. The settings are 4 hrs at 120 °C.

After the program is finisehd, make sure the silica gel cooled down to room temperature before you fill it back into the corresponding labelled storage container.

Calculations

After ignition, we can use the weight from each step to calculate the percentage of LOI550 and LOI950 respectively.

- For LOI550 we use the following equation:

LOI550 (%) = ((DW – DW550) / DW) *100

Where

DW: dry weight of the sample before combustion in grams
DW550: dry weight of the sample after heating to 550°C in grams

LOI550 estimates the content of OM. Organic carbon (OC) content is calculated as approx. half of the LOI550 (Dean, 1974). So from this:

OC = LOI550/2.13

- For LOI950 we use the following equation:

LOI950 (%) = ((DW550 – DW950) / DW) *100

Where

DW: dry weight of the sample before combustion in grams
DW550: dry weight of the sample after heating to 550°C in grams
DW950: dry weight of the sample after heating to 950°C in grams

LOI950 represents the weight loss after 950°C that comes from the CO2 emitted during the combustion where solid CaO remains. In order to calculate inorganic carbon (IC) we assume that ignition follows a stoichiometric quantitative relationship (molecular weight for CO2 is 44, for CaO is 56, for CaCO3 it's 100 and for carbonate $CO3^{2-}$ it's 60). Hence, carbonate is given as 1.36 *LOI950 (Dean, 1974). From that, we can deduce that:
IC=0.273*LOI950
whereby 0.273 equals the quotient of the molar mass of C divided by the molar mass of CO2.

References

Dean, W.E., 1974. Determination of carbonate and organic matter in calcareous sediments and sedimentary rocks by loss on ignition; comparison with other methods. J. Sediment. Res. 44, 242–248.

Heiri, O., Lotter, A.F., Lemcke, G., 2001. Loss on ignition as a method for estimating organic and carbonate content in sediments: reproducibility and comparability of results. J. Paleolimnol. 25, 101–110.

Appendix E Standard Operation Protocol: CNS

Sample Preparation for CNS-Measurements and Description of the Measurement Method

No one is allowed to operate the CNS-analyser before being fully trained by a responsible person (technician, Adrien or Moritz).

1. General Information

Version number of SOP: 1

Typical application of the procedure
Measurement of the percentage content of nitrogen, carbon and sulphur in solid samples
(soil, sediments, plant materials)

Reference to the original procedure (paper or book chapter):

Date SOP first issued: 2020-04-02

Person SOP issued: Wienhues Giulia, Fischer Daniela

Date SOP modified (please specify why the method was modified in the comment below)

Person who did the last modification:

Contact person in the lab: Patrick Neuhaus

Other SOP related to this SOP:

SOP for the mills Retsch MM400 and Retsch PM200
SOP for the muffle furnace

2. Overview

The protocol describes the sample preparation for CNS analysis and further the principle of the measuring method.

3. Points which needs to be considered

The method is not capable to differentiate between organic and inorganic C. If the pH of the material is >6.5, inorganic C (e.g. $CaCO_3$) may occur in the soil. This can be tested by adding 10% HCl to the sample. If the acid reacts with the sample, it has inorganic C and needs to be analyzed twice. First the total sample is analysed (total C) and then the sample is ashed for 550°C for 2 h and analyzed (the organic C is burned and only the inorganic C is analyzed). The difference between total and inorganic C gives the organic C.

But note the C/N ratio always refer to **organic** C to N ratios.
Therefore the results of the two measurements are first used to calculate the proportion of organic carbon and, based on this, the C/N ratio need to be calculated.

The samples for CNS measurement should be very homogeneous. The more homogenous they are, the more reproducible are the results.
This means that samples should be **ground** (→ Retsch MM400 or Retsch PM200) if possible, at least, however, mortared

Triplicates of some of the samples need to be done

It is also recommended to measure some samples of a series in advance to see which sample quantity should be weighed in.

4. Reagents

5. Material for sample preparation

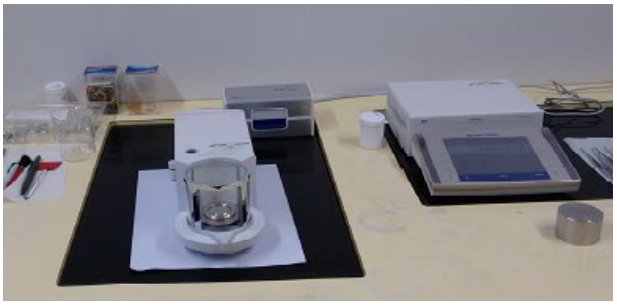

Material
Ceramic crucibels
Muffel furnance
Microbalance
Tweezers (special kind of) Elementar Prod.-No.: S03 001 248

Spatula
Tin foils 4x4x11 Säntis: SA 22 137 418
Tin foils 6x6x12 Säntis: SA 22 137 419
Metal block
Sample box

Standards
Glutamic acid 40.78%C; 9.52%N; C/N: 4.28 (Merck: 100291 0250)
Sulfanilic acid 41.61%C; 8.09%N; 18.5%S; C/N: 5.14 (Merck: 86090)
Low-Level_N and N 67.63%C; 0.73%N; 0.84 %S; C/N: 92.64
(Elementar: 05 000 959)

You have to measure standard samples with known amounts of N, C and S in every sequence. With the help of these you can calculate your daily factor.

6. Safety

10 % HCl is corrosive. Lab coat, gloves and safety googles need to be used!

7. Procedure

7.1 Sample Preparation

1. For samples with pH >6.5 a pretest with 10% HCl needs to be done to check for inorganic C. If the sample shows a visible reaction the sample need to be split and analyzed twice. First the total sample is analysed as described below (total C) and then the sample is ashed at 550°C for 2 h and analyzed again as described below (the organic C is burned and only the inorganic C is analyzed). The difference between total and inorganic C gives the organic C. If pH <6.5 or the HCl shows no reaction no ashing of the sample is necessary and one analysis is enough. In this case there is no inorganic C and the measured C corresponds to the organic C.

2. Samples are weighted into tin foil capsules using the micro balance.

We have 2 kinds of tin foils: a. 4x4x11 (small)
b. 6x6x12 (big)

Depending on the type of sample and its N and C content, different amounts of sample must be weighed in. For example, 3-5mg is sufficient for plant material, for mineral soil with very little organic matter you should weigh in up to 50mg.

3. First, tare the tin foil capsule. Then the sediment has to be carefully filled in with a little spoon spatula **(outside of the balance!).** After checking the sample weight with the balance, the tin capsule filled can be folded carefully to a little square package **(tin foil can rip easily!)** by using two tweezers. Make sure that the package is closed and no sediment material is leaking out.
   Leaking sample packages means you will get wrong results and the **ball valve** of the instrument is **damaged**

4. Weigh the final sediment package and note the weight with 3 digits after the decimal point (x.yyy mg) onto the sample table sheet. Later on, depending on the sample weight, the software will determine the percentage of C,N and S in the sample

5. The final sediment-tin packages are stored in a subdivided sample box.

7.2 Measuring CNS

The CNS analysis determines the total **N**itrogen, **C**arbon and **S**ulfur amount in solid (soil, sediment, plant etc.) samples and is based on the transformation of solids into gas phase by rapid and complete flash combustion of the sample material.
During combustion, compounds containing the elements C, H, N and S produce the gaseous combustion products CO_2, N_2, H_2O, NO, NO_2, SO_2, SO_3, as well as volatile halogen compounds if the sample contains halogens. The tin contained in the tin boat or tin capsule burns to SnO2 and is collected in the ash finger of the combustion tube.
With our instrument (Elementar vario EL cube) the amount of C, N and S in a **solid** sample can be measured.

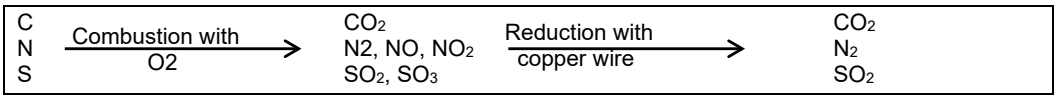

Measurement principle

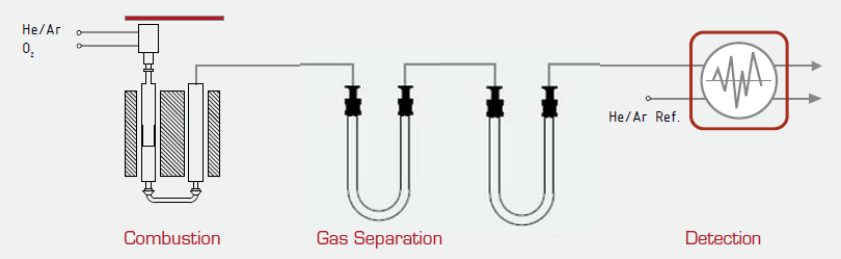

The Elemental Analyser consists of

1. sample feeding unit (sample holder (carousel) + ball valve)
2. sample digestion unit (combustion/reduction unit)
3. separation unit
4. detection unit
5. as a mobile phase you have He as the carrier gas

Sample combustion

With the help of the ball valve the sample is automatically transported from the sample carousel into the combustion tube. There an explosive combustion takes place at approx. 1150 °C in a helium atmosphere highly enriched with oxygen.
The gaseous combustion products are then transported with He as a carrier gas into the reduction tube. There combustion products like NO_x and SO_3 are reduced to N_2 and SO_2 respectively (. Additionally excessive oxygen is trapped by the reduced copper in the reduction tube. On top of the copper wires are some silver wool the trap the volatile halogenids.

Separation

After the gas left the reduction tube it contains N_2, CO_2 and SO_2 which we want to measure. Therefore we have to separate these compounds from each other. This is done by temporarily and reversibly binding of CO_2 and SO_2 in further tubes containing specific adsorbance material. In this way, the 3 combustion products can be fed to the detector one after the other.

Detection

We have two kinds of Detectors, a thermal conductivity detector (TCD) to measure Nitrogen and Carbon and an Infrared Detector (IR) to measure Sulphur.
First of all the N_2 is measured, which is not adsorbed anywhere. Then the the CO_2 is desorbed by heating the tube containing the specific adsorbing material for CO_2 and CO_2 is transported to the detector. At least the tube which adsorbed the SO_2 is heated and therefore the SO_2 is released and transported to the IR detector.
In that way you can measure N, C and S sequentially.

8. Quality control

With each measuring sequence of samples a sequence of standards need to be measured. The standards should be measured at the beginning, latest after every box (24pieces) and at the end of a sequence.
Additionally you should include blank values

One full sample box contains 24 samples
Depending on the sample weight, 2 or 3 full sample boxes can be measured in one sequence. Then the ash finger must be emptied again
If the sample weight is up to 10-12 mg one can measure 3 boxes in one run. If the sample weight is higher, the ash finger should be emptied after 2 boxes

Example of a measuring sequence:

1. 3-5 blank
2. 1x sulfanilic acid
3. 1xblank
4. 2x tin foils
5. 1xblank
6. 3xsulfanilic acid
7. 1xblank
8. 3xglutamic acid
9. 1xblank
10. up to **24** samples
11. 1xblank
12. 2xsulfanilic acid
13. 1xblank
14. 2xglutamic acid
15. 1xblank

9. Comments

about problems / limitation with the method / modifications done / new sample materials or new application the method was used for. Please give date and name together with your comment:

Appendix F Standard Operation Protocol: Extraction and Preparation of Samples for LC-MS/MS

1. Preparation of lake sediment samples for Accelerated Solvent Extraction (ASE) and
2. Cleaning procedure of the extraction cells

1. General Information

Version number of SOP: 3

Typical application of the procedure

1. Preparing lake sediment samples for pesticide extraction using an Accelerated Solvent Extraction (ASE 350)
2. Cleaning procedure of the extraction cells after usage

Reference to the original procedure

1. A high-resolution historical record of plant protection products deposition documented by target and nontarget trend analysis in a Swiss lake under anthropogenic pressure. Aurea C. Chiaia-Hernández, Paul Zander, Tobias Schneider, Sönke Szidat, Ronald Lloren, and Martin Grosjean
   Environ. Sci. Technol., 54 (20), pp 13090–13100. https://doi.org/10.1021/acs.est.0c04842

2. Correction to "A High-Resolution Historical Record of Plant Protection Products Deposition Documented by Target and Nontarget Trend Analysis in a Swiss Lake under Anthropogenic Pressure". Environ. Sci. Technol. 2021, 55, 4, 2707.
   https://doi.org/10.1021/acs.est.1c00623

Date SOP first issued: 2020-04-25. Modified SOP 2021-10-14

Person SOP issued: Dr. Aurea Chiaia-Hernandez

Date SOP modified (please specify why the method was modified in the comment below)

Person who did the last modification: Nayan Gosain, Emmanuel Schaad, and Aurea Chiaia-Hernández

Contact person in the lab: Maarika Bischoff

Other SOP related to this SOP:

ASE Pesticide extraction

2. Overview

This SOP describes the preparation of lake sediment samples for Accelerated Solvent Extraction (ASE) of pesticides.

Treatment of sediments

1. Freeze-dried and homogenized (mortar and pestle) sediment samples before pesticide extraction
2. Weight 4g of sediment into 20 ml glass containers previously cleaned, baked and labelled or into 20 ml glass containers completely new as illustrated in Figure 1. Record the exact weight of the sediment.

Figure 1. 20 ml glass containers for weighting and spiking of sediment samples

3. Spike each sediment sample with **70 µL surrogate solution of Carbamazepin-D10 (2.5 mg/L)** in acetronitrile. The spiking will give a final concentration in vial of 150 ng (300 µg/L) of Carbamazepin-D10. Do this under the hood.
4. Manually shake the samples for homogenization
5. Store the sediment samples at 4 °C in the fridge located in front of the -20 °C freezer overnight. Make sure everything is labelled with the name of the responsible/contact person and date. Only spike samples which are used in the ASE the following day due to possible degradation of the surrogate!

Note: In case that a surrogate is not added to the sediments, fill homogenized sediments directly to the ASE cells as described below. Please discussed this with your supervisor.

Preparation and transfer of sediments to ASE cells

- Each extraction cell consists of a middle part (cell body) and 2 end caps. Middle part and end caps are numbered by which they can be identified.
- It must be ensured that the 2 end caps are assigned to corresponding middle part.
- There is a list that can be used to assign the individual parts. See Table 1 for assigned top, bottom and cell body. Also, there is a direction to arm the cell. The cell body ID number should be in the right direction (up-side up, number should be readable)
- Cell end caps should **only** be disassembled if the PEEK seals or frits are replaced. If the end caps are disassembled, the PEEK seals can't be used again. Use a new PEEK seal to avoid leaks. In case the cells need to be opened, please contact the ASE responsible person. Figure 2 illustrates the assembly of the cell end caps. Dismantle the cells only if necessary (e.g., leak) and never do it without supervision.

Figure 2. Cell end cap assembly

Table 1. Cell number, body and end caps for each ASE cells

Cell	Cell-body	Cap 1 top	Cap 2 bottom
Cell nr.1	K7956	K08912E	K08909E
Cell nr.2	K7963	K08919E	K08920E
Cell nr.3	K7965	K08922E	K09377E
Cell nr.4	K8028	K06091E	K09376E
Cell nr.5	K8030	K08924E	K02119E
Cell nr.6	K8034	K08917E	K09373E
Cell nr.7	K8135	K01966E	K06082E
Cell nr.8	K8137	K08929E	K08926E
Cell nr.9	K8138	K06087E	K02124E
Cell nr.10	K8139	K01986E	K06066E
Cell nr.11	K8140	K08923E	K08916E
Cell nr.12	K8296	K06088E	K09372E
Cell nr.13	K8297	K02115E	K06070E
Cell nr.14	K8303	K06089E	K02111E
Cell nr.15	K8304	K06085E	K08476E
Cell nr.16	K8306	K02134E	K01979E
Cell nr.17	K8308	K02128E	K06069E
Cell nr.18	K8419	K08932E	K06090E
Cell nr.19	K8420	K09384E	K08927E
Cell nr.20	K8422	K01982E	K06093E
Cell nr.21	K8426	K06083E	K09071E
Cell nr.22	K8428	K09375E	K01975E
Cell nr.23	K8134	K08907E	K01970E

3. Material

Balance
Spatulas
Metal funnel (See Figure 3)
Big cellulose Filters (1, 5, 10, 22 mL ASE 350/150 Cell Filters; Product No: 068093) (See Figure 3 and 4)
Small Cellulose filters (10 mL ASE 100 Cell Filters; Product No: 060941) (See Figure 3 and 4).
Collection vials (VOA vials)

Black stick (See Figure 3)
Cleaned and baked collection vials (VOA vials)
Clean lids with Septa
Stainless steel extraction cells (10ml) consisting of 2 cell end caps and a middle part. The cells need to be armed according to the list provided in Table 1.

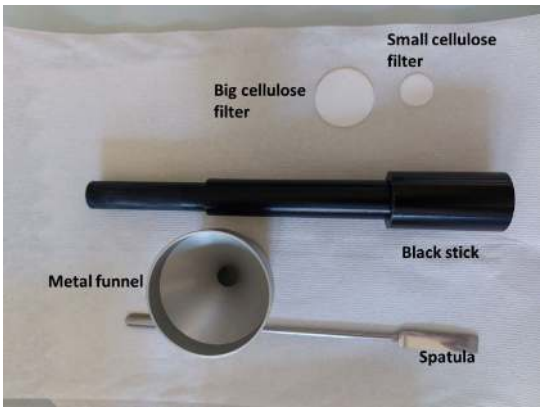

Figure 3. Selected material needed for the preparation of ASE cells

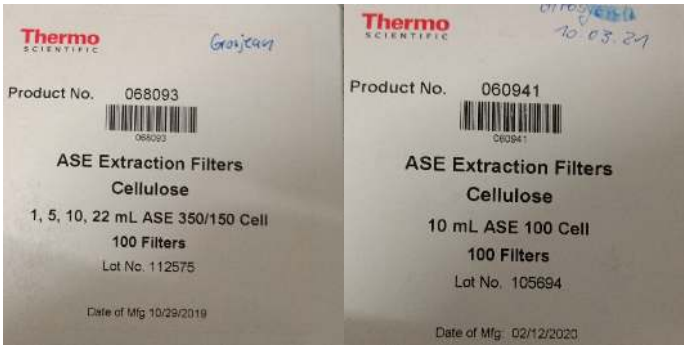

Figure 4. Big (left) and small (right) cellulose filters needed for the extraction of sediment samples

4. Safety

Wear gloves and lab coat at all times when you are working.

5. Preparation of Lake Sediment Samples for Accelerated Solvent Extraction

1. Insert very precisely and carefully, 1 big cellulose filter into the lower cell cap and screw the cell body (middle part). The filter has to fit inside the PEEK seal and not be on top of it.
2. Insert an additional small filter inside the cell body with the aid of a black stick (see Figure 3).

3. Place an assigned metal funnel on the cell body, tighten it hand-tight and put it on a balance. Make sure the balance range is big enough to measure the cell with sediment as illustrated in Figure 5.

Figure 5. Cell with metal funnel weighted in an analytical balance

4. Transfer the previously weighed and spiked sediment (~4g of sediment) directly into the cell
5. Weight the transfer sediment sample down to 3 decimal places.
6. Add 0.5g of Hydromatrix (diatomaceous earth) directly to the cell containing the sediment.
7. Mix well sediment sample and Hydromatrix with a small spatula. For preparation/treatment of hydromatrix before use see below.
8. Close the extraction cell with the appropriate cell cap and number the cell. **Note:** no filter is needed for the cell cap on the top. Please make sure there is not particles around the top of the cell or at the edges of where the cell is closed to avoid damaging the cell or leaking. In case is necessary, use a brush to clean these parts.
9. Place the extraction cell to the cell tray and put the previously labeled and weighted collection vials to the corresponding place in the collection tray
10. Run the ASE according to the SOP for "extracting sediment samples for pesticides"

ASE cell assembly are shown in Figure 6 and 7.

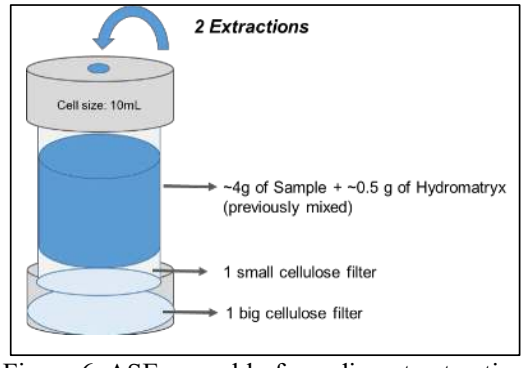

Figure 6. ASE assembly for sediment extraction

Figure 7. ASE assembly for sediment extraction with cell body and corresponding bottom and top covers. A big cellulose filter is placed in the bottom of the cell before closing.

Preparation of VOA vials

1. Take as many collection vials as ASE cells used, remove the aluminum foil covering the top
2. Into each cap, insert a small seal-plate with holes punched into them, see Figure 8 for correct assembly. The concave side of the seal-plate should be facing upwards. Note if the seal has too many holes and breaking to pieces, please discard it.
3. Label each vial at the bottom and record the empty weight of the vials

Figure 8: VOA vial cap with seal-plate inserted

Preparation of diatomaceous earth (Hydromatrix)

1. Use a clean glass bottle with a close cap (e.g., 1L or 500 ml Duran or Scotch bottle) as illustrated in Figure 9.
2. Fill half of the bottle with hydromatrix
3. Rinse the hydromatrix first with DI water and discard the content. Shake manually. Be careful not to lose too much material into the sink when discarding. If possible use a sieve.
4. Rinse a second time with 50:50 (%v/v) DI water: Ethanol (technical grade). Shake manually. Discard the rinsing content into the sink. Be careful not to lose too much material to the sink when discarding. If possible use a sieve.
5. Rinse a third time with 100% ethanol (technical grade). Shake manually. Discard the rinsing content into the sink. Be careful not to lose too much material to the sink when discarding. If possible use a sieve.

6. Cover the glass bottle with aluminum foil and bake over night at 290°C before use. Make sure all the plastic parts and labels are removed before baking, including plastic ring at the top of the bottle.
7. Let the hydromatrix cool down, remove the aluminum foil, place the previously removed plastic ring to the glass bottle, label, and close tide until future use.

Note: The hydromatrix will be very wet after rinsing but will be completely dry after baking

Figure 9. Glass bottle containing cleaned and baked hydromatrix

Cleaning the extraction cells

1. After the extraction is finished (after 2nd extraction with acetone:1%PA), let the cells cool down and open the cells under the hood until the sediment is dry.
2. Discard sediment in the garbage
3. Rinse cell body and caps first with tap water and brush them gently to get rid of any particles.
4. Rinse one more time with DI water and sonicate them in DI water for ~15min.
5. Let the cells dry under the hood or dry in the oven (~50°C) where all the clean glassware and plastic containers are dried. Do not use high temperatures to dry the cells (e.g. >60°C).
6. After the cells are completely dry, assemble the cells and transferred to the ASE for further cleaning. **Note: Assemble the cells according the description above. Meaning that the middle part is always assembled together with the corresponding cell caps**
7. Insert a used cellulose filter in the lower cap cell and screw the cell body (filters for cleaning can be reused)
8. Fill the cell with small glass beads. Make sure to not overfill the cells to avoid scratching the cell caps.
9. Screw the top cell cap on, tight the cells handtight and place the cells into the ASE carousel
10. Prepare collection vials to collect the extract.
11. Load Method 5 and extract the cells as illustrated in Figure 10.
12. Make a sequences with the correct method and number of samples to be extracted (cleaning)
13. Fill the solvent reservoir (Line A) with ethanol technical grade

Figure 10. Method 5 for additional cleaning of ASE cells.

14. After extraction unscrew the caps, collect the glass beads in a beaker and the filters. Discard the extracts into a yellow solvent waste canister
15. Sonicate cell bodies and caps (**assembled**) for 15min in ethanol tech grade followed by a further sonication for 15 min in Acetone.
16. Ethanol and acetone used for cleaning the ASE cells can be used repeatedly (up to 10 times or until visible particles are observed). In case new solvent is needed, discard the "used solvent" in a yellow solvent waste canister.
17. Dry the cells under the hood until they are completely dry. In case there is a need to dry the cells fast, it is possible to dry them in the oven at 50°C.
18. Storage the cells and bodies in the ASE room.

6. Quality control

1. For the QC of the extraction sequence please check the **corresponding SOP**: ASE-Pesticide-Extraction
2. Dummies are made to make sure that there are no contamination from materials, carry over from sample to sample and the to keep the system clean (extraction cells are filled with glass beads only)
3. Make Duplicates of ~20% of the samples analyzed

Prepare 1 or 2 "blank" samples. Blank samples can be taken from the lowest part of a sediment core (100 years), since they were not pesticides at that time. In case blank samples are not available fill 1-2 extraction cells only with Hydromatrix.

7. Products and suppliers

Product	Supplier	Prod._No.
Septa PTFE for 60ml collection vials	Thermo Fisher Scientific	055395
Septa PTFE for 60ml collection vials	BGB	24694
Collection vials, 60ml, clear	Thermo Fisher Scientific	048784
		RT26121
Cellulose Filter for ASE cells 1-22 mL	ThermoFisher Scientific	068093
Cellulose Filter for ASE cells 10 mL	Thermos Fisher Scientific	060941

Chemical	Formula	Supplier	Prod.-No.
Hydromatrix ISOLUTE HM-N		Thermo Fisher Scientific	9800-1000
Dionex™ ASE™ Prep DE		ThermoFisher Scientific	062819
Dionex™ ASE™ Prep MAP		ThermoFisher Scientific	083475

Extraction cells consisting of		
Cell end cap	ThermoFisher Scientific	068106
O-ring PTFE (within the cell end cap)	ThermoFisher Scientific	049457
stainless steel frit	ThermoFisher Scientific	056775
Seal PEEK	ThermoFisher Scientific	061687
Cap insert	ThermoFisher Scientific	
Snap ring	ThermoFisher Scientific	056778
sample cell body 10ml	ThermoFisher Scientific	068263

8. Comments

About problems / limitation with the method / modifications done / new sample materials or new application the method was used for. Please give date and name together with your comment

1. **Operate the ASE 350** (Accelerated Solvent Extractor)
2. **Extraction of Pesticides from Sediment Samples with the ASE 350**
3. **Cleaning procedure of the extraction cells**

No one is allowed to operate the ASE350 before being fully trained by a responsible person (technician or trained person).

1. General Information

Version number of SOP: 2 (upgraded from SOP 1 from 2020-04-25 created by Daniela Fisher and Aurea C. Chiaia-Hernández)

Typical application of the procedure

Extracting of pesticides from lake sediment samples

Reference to the original procedure

1. User manual ASE 350
2. A high-resolution historical record of plant protection products deposition documented by target and nontarget trend analysis in a Swiss lake under anthropogenic pressure. Aurea C. Chiaia-Hernández, Paul Zander, Tobias Schneider, Sönke Szidat, Ronald Lloren, and Martin Grosjean
Environ. Sci. Technol., 54 (20), pp 13090–13100.
https://doi.org/10.1021/acs.est.0c04842
3. Correction to “A High-Resolution Historical Record of Plant Protection Products Deposition Documented by Target and Nontarget Trend Analysis in a Swiss Lake under Anthropogenic Pressure”. Environ. Sci. Technol. 2021, 55, 4, 2707.
https://doi.org/10.1021/acs.est.1c00623

Date SOP first issued: 2021-09-30

Person SOP issued: Dr. Aurea Chiaia-Hernandez

Date SOP modified (please specify why the method was modified in the comment below)

Person who did the last modification: Nayan Gosain and Aurea C. Chiaia-Hernández

Contact person in the lab: Maarika Bischoff

SOP ASE_ACC_clean.docx

Other SOP related to this SOP:
This SOP has been adapted for the analysis of ~80 plant protection products (PPP) for more details look at cited publications

2. Overview

With the ASE- (Accelerated Solvent Extraction) System a broad range of compounds can be extracted from complex solid and semi-solid samples.
The automated extraction process uses elevated temperature and pressure. Compared to other extraction methods under less extreme conditions, ASE allows the extraction to be performed faster, more efficient and with less solvent.

The increased temperature increases the efficiency of the extraction for various reasons. Usually solubility of a compound in a solvent is temperature dependent. Therefore, solubility will increase with rising temperature. In general, interactions between and within different compounds are weakened by the application of thermal energy. Furthermore a higher temperature decreases viscosity of a liquid, allowing a better penetration of matrix particles.

Usually extraction temperature is above the boiling point of the solvent. By applying pressure, the solvent can be kept as a liquid in the extraction cell. Higher temperature combined with elevated pressure facilitates extraction of analytes trapped in matrix pores. Elevated pressure helps to force the solvent into pores.

Depending on the size of the extraction cell, between 1 and 100 ml solid or semisolid sample material can be extracted.
Commercially available cell sizes are 1, 5, 10, 22, 34, 66 and 100mL

The ASE method is used in many different areas (Environmental samples, Pharmaceutical samples, Polymer samples, Food samples, Consumer products like textile, detergents etc). An ASE illustration is shown in Figure 1.

In the GIUB the ASE is predominantly used to extract

- Pesticides and pigments from soil and sediment samples and
- microplastic from compost

here we describe the extraction of pesticides from sediment and soil samples

Instruments:
ASE 350 : Ser.-No.: 19050705

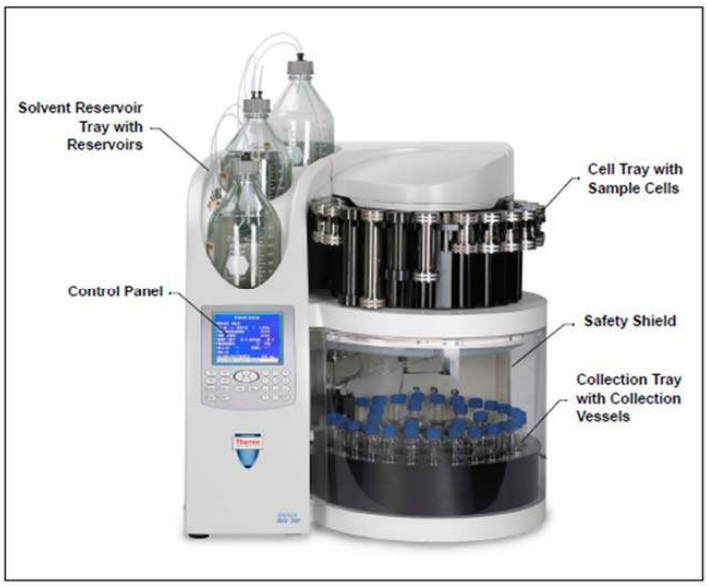

Figure 1. Accelerated Solvent Extractor - ASE 350

3. Points which needs to be considered

Make sure that everything is prepared before starting the ASE:

- Make sure artificial (pressurized) air bottle and N_2 bottles contain enough gas for planned extraction
- If you have to change the gas bottles you first **must** be trained by a responsible person (please ask Maarika B.). Once the tanks have been changed, adjust valves to 10 bar (N2) and 7 bar (pressurized air). Please make sure all the valves are open after the bottle exchange, including the brown knot located in the left size of the pressurize air (red circle in Figure 2). After bottle exchanged only open and close the main bottles without modification of the valves (yellow circle in Figure 2). Illustration of tanks are shown in Figure 2.

- 

Figure 2. Nitrogen tank (top) and pressurize air (bottom) with correct settings. Yellow circles illustrated the main tank opening. Red circle in pressurized air need to be open always except when the tank need to be change.

- Make sure that there is enough solvent for extraction and please only use pressurized bottles for solvent storage or for solvent extraction as illustrated in Figure 3.
- 

Figure 3. Pressurized bottles for ASE

- Collection vessels (VOA vials) need to be well labelled in the **middle/ lower** part otherwise it will interfere with the ASE laser scanner
- **Do not use amber** collection vessels. Amber vessels interfere with the laser scanner.
- **Never** force to move the cell tray or collection tray! Both trays can be moved easily if they are are unlock. **Unlock them by pressing "tray")** as illustrated in Figure 4**.**

- **Empty** rinse bottles R1 and R2 are located in the collection tray
- Make sure all extraction cells are hand tight and placed correctly in the cell tray
- Add additional dummies (Extraction cells only filled with glass beads) to avoid carry over or rinse the instrument between runs. Do this for ~10% of your samples

Figure 4. ASE 350 control panel. Press "tray" to unlock the collection and cell tray

4. Reagents

Ethanol ()	Chemistry shop
Methanol (HPLC grade)	Chemistry shop
Acetone (HPLC grade)	Chemistry shop
Ethyl acetate (HPLC grade)	Chemistry shop
Acetonitrile (HPLC grade)	Chemistry shop
Phosphoric acid 85% (ACS)	Merck Prod._No.:438081

Note: 1% phosphoric acid need to be made from the 85% Phosphoric acid.

Solvents

- **Methanol for rinsing**. Methanol is the solvent of storage and firt and last rinse of the instruments

- **Ethyl acetate : Acetone = 70:30 (%v/v)**. Extraction solvent mixture 1. To prepare 1L - add 700 ml of Ethyl acetate and 300 ml of acetone in a 1000ml volumetric flask. In case lower amounts are needed, please adjust accordingly

- **Acetone : 1% Phosphoric acid = 70:30 (%v/v).** Extraction solvent mixture 2. To prepare 1L - add 700 ml acetone, 300 ml Milli Q water and 3.52 mL of 85% phosphoric acid. In case lower amounts are needed, please adjust accordingly. **Always add acid to water and not water to acid** to avoid violent boiling or splashing concentrated acid out of the container.

- **Acetone : Methanol : Acetonitrile = 35:35:30 (%v/v) .**Cleaning solvent after extraction solvent mixture 3.To prepare 1L - add 350 ml acetone, 350 ml methanol and 350 mL of acetonitrile. In case lower amounts are needed, please adjust accordingly.

5. Material

Pressurized solvent bottles
10 mL extraction cells previously cleaned
Collection vessels (VOA vials) previously cleaned and baked
Rinse bottles (R1 and R2 position)

6. Safety

Wear safety goggle, gloves and lab coat at all times when you are working with the ASE.
Prepare and handle solvents always under the fume hood. After the end of the extraction, open extraction vessels under the fume hood. Be careful, the cells can be still hot
Solvent waste need to be disposed in corresponding canister labeled with the corresponding names and proportions of the used solvents. Yellow canister is for non-halogenated solvents and blue canister is for halogenated solvents.

7. Procedure

ASE Operation on 07.11.2019

Sequences and Methods have been already programmed
Note1: to move the carrousels for the ASE cells and vials, press "Trays"
Note 2: Sequences previously prepare/made to fit the description below
Note 3: Place vial labels at the middle of the vial, otherwise will interfere with the ASE scanner.

1. Open artificial/pressurize air and N_2 tank bottles
2. Turn on ASE (right side at the bottom)
3. Press, "Rinse" to rinse the system with the current Solvent (methanol/Solvent A). Solvent A is the default rinse line.

4. Fill desire solvent/solvents into coated/pressurized bottles
5. Verify that all the ASE cells are placed correctly, tight and in the right position as illustrated in Figure 5.

Figure 5. Loaded cells and extraction vials

6. **Weight extract vials (VOA vials) already labeled and record weight**
7. Check that each extraction cell correspond to the correct collection vial
8. Empty rinse bottles R1 and R2
9. Load needed sequence (e.g., Sequence, Number 7, Vial 1) and press “start”. For 12 samples + 2 dummies it will take around 4hrs. To create a sequences go to sequences on the main menu. Go to sequence and add your samples and press save. Do not override other sequences. To avoid confusion, always seve your sequences with the same number as your method. Before do it this make sure you get a proper introduction. An illustration is shown in Figure 6.
10. Check that all the vials have the **same amount of extract**. In case one vial is different, please record it and communicate to the responsible person. In most cases when the amount of extract is not correct, the samples will be extracted again. Check for leaks or damaging/open cells.
11. Weight extract vials (VOA vials) after extraction and record weight. Calculate the approximated amount of extract in each vial and record any differences. Use solvent densities to do this.

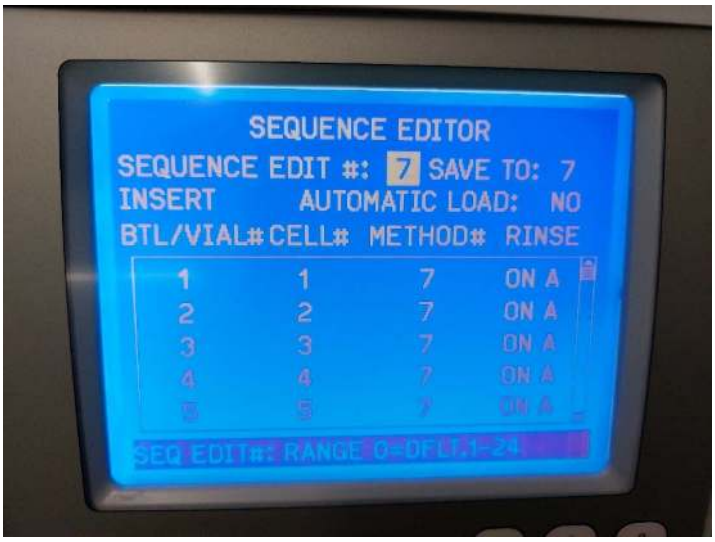

Figure 6. Exmaple of a seuqence using method 7.

********** Extraction Details **********

Extraction 1 - ASE method 7, 70:30 Ethyl acetate:Acetone

1. After rinsing the system with methanol, exchange the solvent with aa solvent mixture (mix 1) containing 70:30 Ethy lacetate : Acetone (%v/v) andconnect this bottle to Line A. rRnse the system by pressing “Rinse”. Use pressurized bottles only.
2. Load sequence 7 (previously prepared) and press, “start” as illustrated in Figure 7.
3. After the completion of the run, tight all the ASE cells again. The cells could be still hot so do it with gloves and carefully
4. Empty rinse bottles R1 and R2

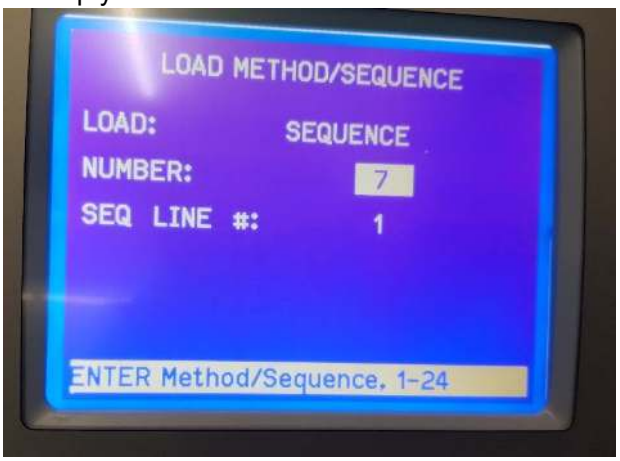

Figure 7. Sequence selection for sediment analysis. Note: in this case sequence 7 correspond to method 7 and starts at the cell number 1

Extraction 2 - ASE method 4, 70:30 Acetone:1%PA

5. Exchange the solvent bottle at Line A with a solvent mixture (mix 2) of 70:30 Acetone:1%PA (%v/v) and rinse the system by pressing “Rinse”. Only use pressurized bottles.

Note: The PA is 85% purity, so correction for the 15% is necessary. For details see below under solvents

6. Load Sequences 4 (Sequence, Number 4, Vial 1) and press “start”. For 12 samples + 2 dummies it will take around 4hrs.
7. After completion of the run, take away all the extract vials and ASE cells but **leave dummies**. Dummies are cells fill with glass balls and are only to clean the instrument between runs
8. Weight extract vials (VOA vials) after extraction and record weight. Calculate the approximated amount of extract in each vial and record any differences.

**********End of sediment extraction**********

9. **After extraction all the samples are spiked with 50µL of 2.5 mg/L mixture of 19 internal standards (absolute amount of 125 ng)**
10. Replace the septum caps in the extract vials with new ones (without any holes) and place the vials in the -20°C freezer until further evaporation. Add paraffin to the caps to prevent sample loss.
11.

Instrument Clean-up - ASE Method 5, 35:35:30 acetone:methanol:acetronitrile

1. Tight dummy cells left in the carrousel and empty the VOA vials. Dummy cells are cells fill with glass balls.

Collect all waste from the ASE. This waste should be disposed in the yellow waste containers. Please add to yellow containers the information of the waste (e.g methanol, ethanol)

2. Exchange the solvent bottle at Line A with a solvent mixture (mix 3)(of 35:35:30 Acetone:methanol:acetronitrile (%v/v)) and rinse the system by pressing “Rinse”. Only use pressurize bottles.
3. Load Sequence 5 (Sequence, Number 5, Vial 1) and press “start”. For 2 dummies it will take around 25 min or less. Rinse the system with a minimum of 2 dummies. Avoid leaving acid overnight (method 4) in the system because the acid can be corrosive and damage the instrument in the end.
4. At the end of the run, exchange the solvent bottle with Methanol (Bottle originally at the ASE) and rinse the system by pressing “Rinse”. Rinse twice.
5. Take away remaining cells (dummies) and vials and discard any solvent in the rinse bottles R1, R2 and in the dummy vials as explain before.
6. Turn off instrument, synthetic air and N2 tank bottles

**********Methods **********

SOP ASE_ACC_clean.docx

Note: At the new ASE (350), it is not possible to change the pressure, so ignore this value.

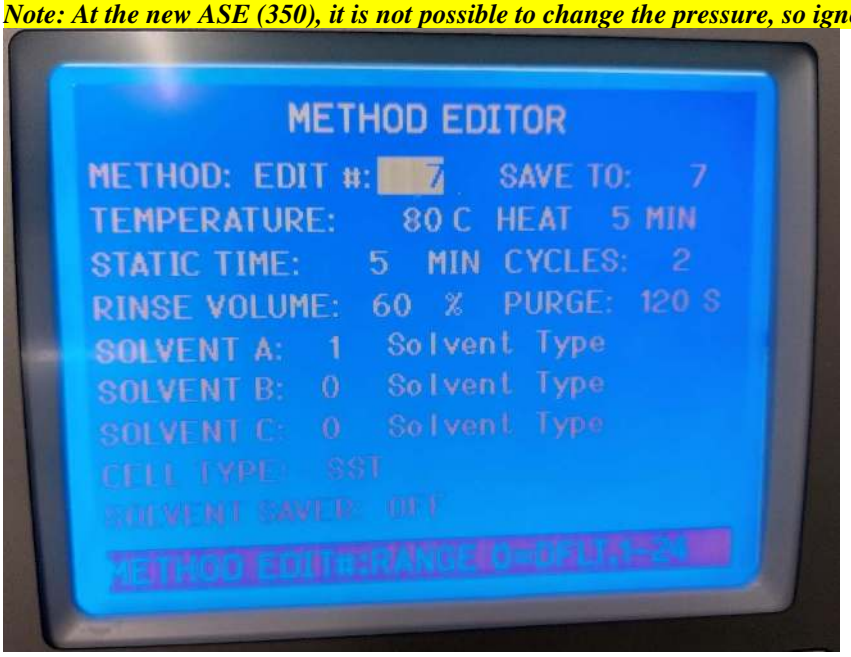

Figure 8. Method 7 as shown in instrument. Method 7 uses 70:30 Ethyl acetate: acetone (%v/v)

Figure 9. Method 4 shown in instrument. Method 4 uses 70:30 70:30 Acetone:1% phosphoric acid (%v/v)

Clean-up method

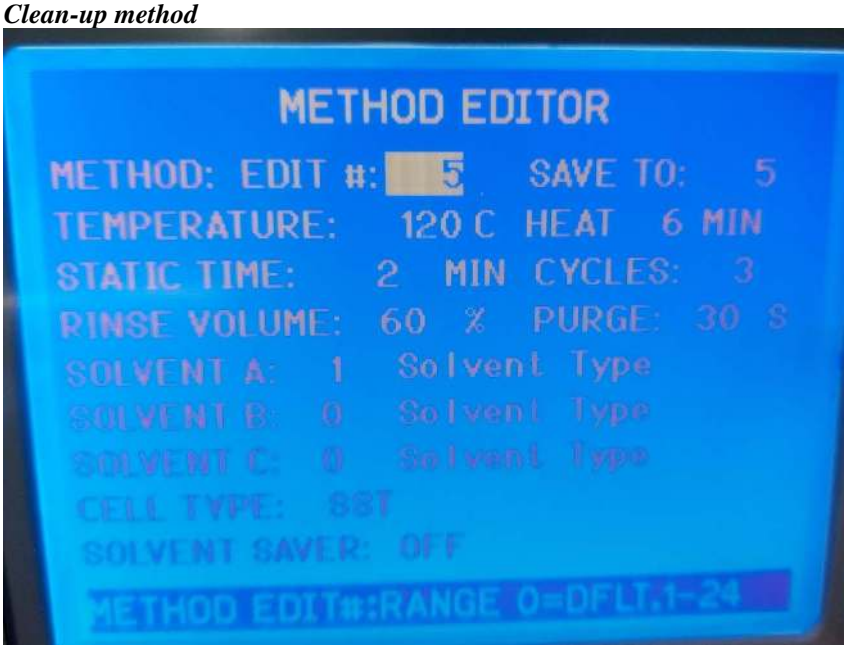

Figure 10. Method 5 shown in instrument. Method 5 uses 35:35:30 Acetone:methanol:acetronitrile (%v/v)

8. Quality control

1. Dummies are prepared to make sure that there are no contaminations from materials or the system used (extraction cells are filled with glass beads)
2. Quality controls are implemented during the whole extraction and clean-up procedures and consist in blank samples (sediment from >100 years or hydromatrix) and duplicates, making > 20% of the processed samples. In case the matrix of the sediment is evidently different from layer to layer, spiked samples are introduced to calculate recoveries.
3. In case sediment blank material is not available, replace blank sediment with Hydromatrix only
4. For quantification of pesticides, a calibration curve needs to be made. This can be by making an external calibration curve (in methanol) or a "matrix match" calibration curve with **final concentrations in vial** of e.g. 0.5, 1, 5, 10, 25, 40, 70, 100, 300 µg/L. Internal standard concentration should be identical as the samples (absolute amount of 125 ng). The range of the calibration curve depends on the expected sample concentrations; therefore, cal curve ranges can be change from analysis to analysis. However, this range can work well for sediment analysis in general.
5. For better results a "matrix match", calibration curve is recommendable but will involve additional work and consist in "blank sediment". "Matrix match" calibration curves are nt always possible due to the consistency of the sediment. For **"matrix match calibration curve**" blank sediment samples (sediments from >100 years) are extracted with methods 1 and 2 as described above. After extraction, samples are spike with internal standard (50 µL of 2.5 mg/L mixture of 19 internal standards) and with 2 different pesticide mixes. Mix 1

consist in a mixture of pesticides storage in methanol and Mix 2 contains a mix of pesticides storage in acetonitrile (sensitive pesticides). Both mixes containing a mixture of >70 pesticides and can be found at different concentrations (0.01, 0.1, 1 and 10 mg/L). The samples are then process as the rest of the samples.

For **external calibration curve**, make calibration curve in methanol and DI water (70:30 v/v) with final volume of 500 ml using Mix 1 and 2 as well as internal standard mix.

In addition, quality controls (QC) are used in the analysis to check for instrument performance. Therefore, spiked samples at 2 different concentrations (e.g. final concentration in vial 40 and 70 ug/L) are introduce in the analysis for instruments performance. This QC are spiked and processed as the samples from the calibration curves. The QC should be in the middle range of your calibration curve and in the range of the expected environmental samples.

Note: Do not do this alone. To create a calibration curve, please talk/discuss first with supervisor.

9. Comments

About problems / limitation with the method / modifications done / new sample materials or new application the method was used for. Please give date and name together with your comment:

1. **Evaporation of the lake sediment extracts after ASE Extraction and**
2. **Clean-up of the lake sediment extracts**

No one is allowed to operate the Turbovap before being fully trained by a responsible person (technician, Aurea).

1. General Information

Version number of SOP: 2

Typical application of the procedure

1. Evaporation of lake sediment extracts using the TurbovapII
2. Clean up of the lake sediment extract

Reference to the original procedure

1. A high-resolution historical record of plant protection products deposition documented by target and nontarget trend analysis in a Swiss lake under anthropogenic pressure. Aurea C. Chiaia-Hernández, Paul Zander, Tobias Schneider, Sönke Szidat, Ronald Lloren, and Martin Grosjean
   Environ. Sci. Technol., 54 (20), pp 13090–13100. https://doi.org/10.1021/acs.est.0c04842
2. Correction to "A High-Resolution Historical Record of Plant Protection Products Deposition Documented by Target and Nontarget Trend Analysis in a Swiss Lake under Anthropogenic Pressure". Environ. Sci. Technol. 2021, 55, 4, 2707. https://doi.org/10.1021/acs.est.1c00623

Date SOP first issued: 2020-04-25 and updated on 2021-06-05

Person SOP issued: Dr. Aurea Chiaia-Hernandez, Daniela Fischer

Date SOP modified (please specify why the method was modified in the comment below)

Person who did the last modification: Nayan Gosain, Emmanuel Schaad and Aurea C. Chiaia-Hernandez

Contact person in the lab: Maarika Bischoff

Other SOP related to this SOP:

ASE Pesticide extraction

2. Overview

In the first part of this SOP, the evaporation of the lake sediment extracts using the Turbovap II is described in detail. In the 2nd part, the SOP describes the clean-up of lake sediment extracts by Liquid-Liquid-Extraction (LLE) followed by **d**ispersive **S**olid **P**hase **E**xtraction (d-SPE) using the **Qu**ick, **E**asy, **Ch**eap, **E**ffective, **R**ugged, and **S**afe (QuEChERS) technique as illustrated in Figure 1.

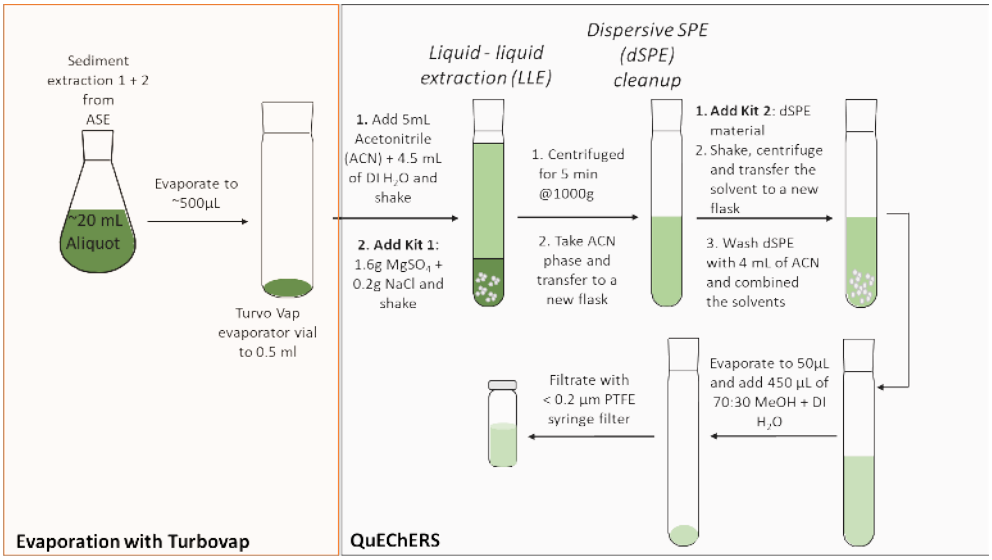

Figure 1. Overview of evaporation of ASE sediment extracts using a Turbovap evaporator follow by a clean-up technique using QuEChERS (, Easy, Cheap, Effective, Rugged, and Safe)

3. Points which need to be considered

Make sure the extracts contain internal standard (Pesticide-Mix) before evaporation. **This is extremely important step**

Never operate any instrumentation or open gas bottles before reading the instructions below or get fully trained

4. Procedure for evaporation of lake sediment extracts after ASE extraction

Material

Turbovap II evaporator
Turbovap 50ml vials previously cleaned and baked (see Figure 2)
Pipettes + tips
Labo vials (12ml) (see Figure 2)
Sample racks
Pasteur pipettes

Figure 2. Labco and Turbovap vials needed for the evaporation and clean-up of sediment extracts

4.1 Evaporation of ASE extracts with the Turbovap evaporator (step-by-step description)

1. Put the TurvoVap under the hood. The TurboVap is very heavy so never move it alone.

2. Fill the Turbovap with DI-water to a level until the metal rack with orange rings is completely immersed in water.

3. Add some drops of "Aquaresist" to prevent algae growth

4. Connect the gas inlet to a nitrogen tank as illustrated in Figure 3. **Do not turn on the nitrogen yet.** Please make sure that all connections look like Figure 3, including the exhaust port.

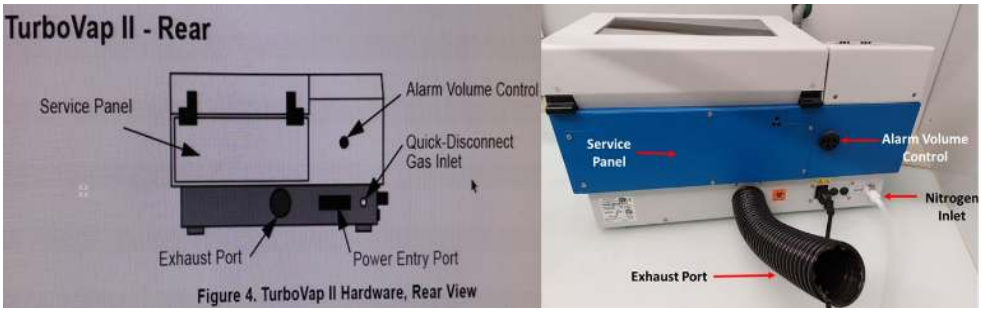

Figure 3. TurboVap evaporator with main connections

5. Connect the TurboVap to an electrical outlet and turn on the instrument

6. In the upper part of the front panel choose "Manual" with the "Endpoint select" button. See Figure 4 for illustration of TurboVap panel.

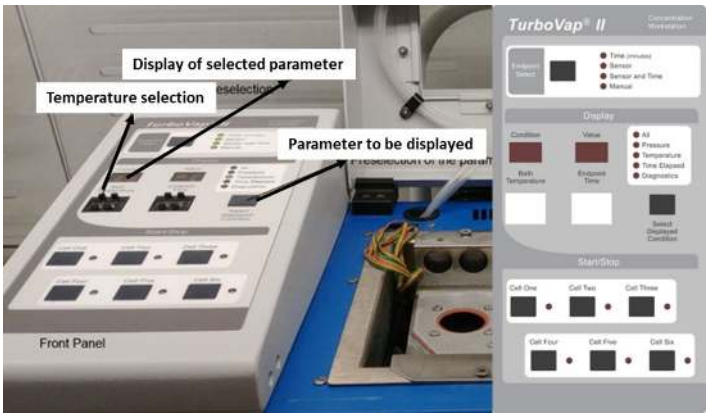

Figure 4. TurboVap display pannel

7. Set the "Bath Temperature" to 40°C (see figure 4). With the "Select Display condition" button, select "Temperature". The current temperature will be displayed. Note: To reach 40°C will take around 10 min so adjust the temperature in advance. Close the lid of the TurboVap while the water is reaching the desired temperature

8. When the desired temperature is reached (e.g., 40°C), switch the panel with the "Select displayed condition" button to “pressure” (see figure 4). The pressure will be displayed on the “Condition” display. Pull the regulator knob on the left side out and turn it fully counterclockwise to start at a pressure of zero. The regulator knob is illustrated in Figure 5.

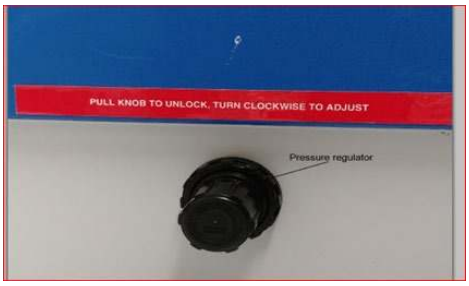

Figure 5. Turbo Vap pressure regulator knob

9. Before turning on the N2-gas bottle make sure all valves (1 to 3) are closed:
Valve 1 on the gas bottle can be closed by turning the valve clockwise ,
Valve 2 can be closed by turning the valve counterclockwise,
Valve 3 can be closed by turning the valve clockwise,
Note: Because there are many valves in the lab and the valves can change, please look always at the bottom of the valves’ knob for open and closing instructions.

10. Open Valve 1 (gas bottle). The remaining pressure in the gas bottle will be displayed. Then open valve 2 (to open turn valve clockwise) the pressure on the display 2 should not exceed 2.5-3bar. Finally, open valve 3 slowly/carefully to have nitrogen flowing. Figure 6 shows a nitrogen gas bottle and a valves for clarification.
Note: To avoid damage, supply inlet pressure to the instrument must not exceed 80 psi (5.52 bars) (Manual for Turbovap)

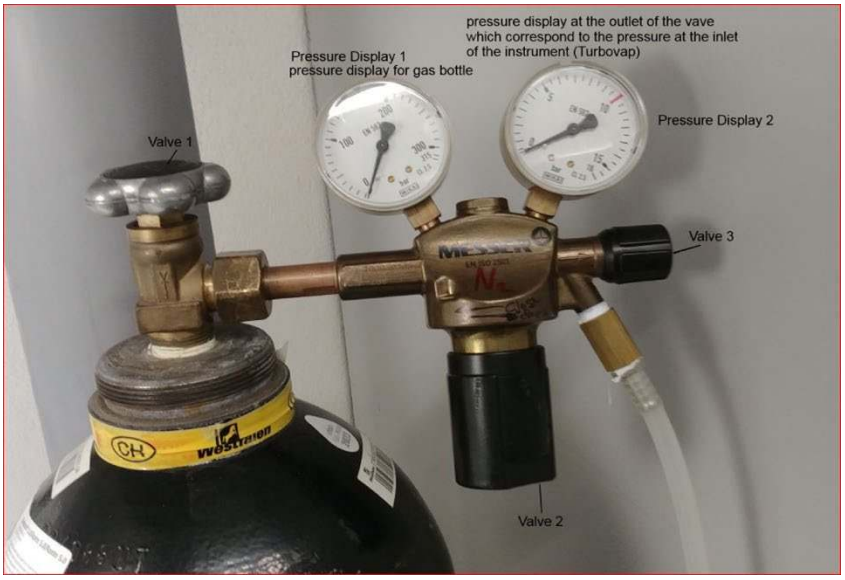

Figure 6. Nitrogen gas bottle with valve attached to regular the nitrogen flow.

11. Once the valve 3 is open and nitrogen is flowing to the TurboVap, pull the regulator knob out and turn it clockwise to adjust the inlet pressure. The TurboVap should be between 8 and 15 psi (0.6 and 1.0 bars). Once the pressure is adjusted, close the regulator knob by pushing the knob back in.

12. Test the nitrogen flow and stability by open the 6 cell inlets. The cell inlets can be open by pressing "Cell One" to "Cell six" bottoms under the display panel. A yellow light will be activated when the cells are running. Please see Figure 4 for clarification.

13. Once the cells are tested. Stop the nitrogen flow by pressing twice the cell bottoms. Yellow light will be off. Put the evaporation vials with the solutions to be evaporated into the chamber and "start" evaporating the occupied cells by pressing the corresponding button in the lower part of the front panel. Do not overfill the vials. Always fill maximum half of the vials. (If, i.e., 40ml should be evaporated, 2x20ml could be evaporated one after the other in the same vial)

14. Rinse the walls of the vials three times with 1mL acetonitrile during the evaporation process to avoid pesticide loss of the glassware: Rinse ASE vials once with 1 ml ACN, transfer it with pipette to turbovap-vial Then rinse turbovap 2x during evaporation process with 1 mL ACN each. → 3 mL ACN in total!

15. Extract should be evaporated until a remaining volume of maximum of 0.5mL. Do not dry completely the extract. If this occurs communicate it to your supervisor.

16. Transfer the ~0.5ml residue into a Labco vial with glass Pasteur Pipette. (It is also possible to also transfer precipitated, non-soluble components into the labco vials).

17. The TurboVap evaporation vials are then rinsed twice (2X) with 2.5 ml 100% acetonitrile each rinse. The solution (possibly also with solid, precipitated components) is then transferred into a Labco vial with Pasteur pipettes.

18. A total of ~5.5 ml extract (5 ml of which is 100% acetonitrile) is now in the Labco vials

19. Store the solution at -20°C until further clean-up or continue with further steps.

20. At the end of the evaporation with the Turbovap, clean the metal surface with Ethanol tech. If the evaporator won't be used for long periods of time, empty the water with the aid of a plastic hose and a bucket and store it in the cupboard under the hood.

4.2 Clean-up of lake sediment extraction solutions by using the QuEChERS method

Clean-up of extracts after Turbovap II evaporation

Prepare all the required material before starting the evaporation and clean-up procedure:

- For each extraction sample 1x QuEChERS -Kit 1 and 1x QuEChERS-Kit 2 must be prepared
- **2 Labco** vials are required for each sample (see Figure 1) previously cleaned and heated at 290°C for 12h before using

Preparation of Kit-1 + Kit-2:

- **Kit-1**: 1.6g $MgSO_4$ and 0.2g NaCl are weighted into a corning falcon tube (see Figure 7, tubes with orange caps). Record weight to 3 decimal places if possible
- **Kit-2:** 0.75g $MgSO_4$ and 0.125g SelectraSorb Clean-up (C18 irreg; 40-63µm)

are weighted in to a 5ml amber vial from Infochrom previously clean and baked (see Figure 7, vials with red caps). Record weight to 3 decimal places if possible

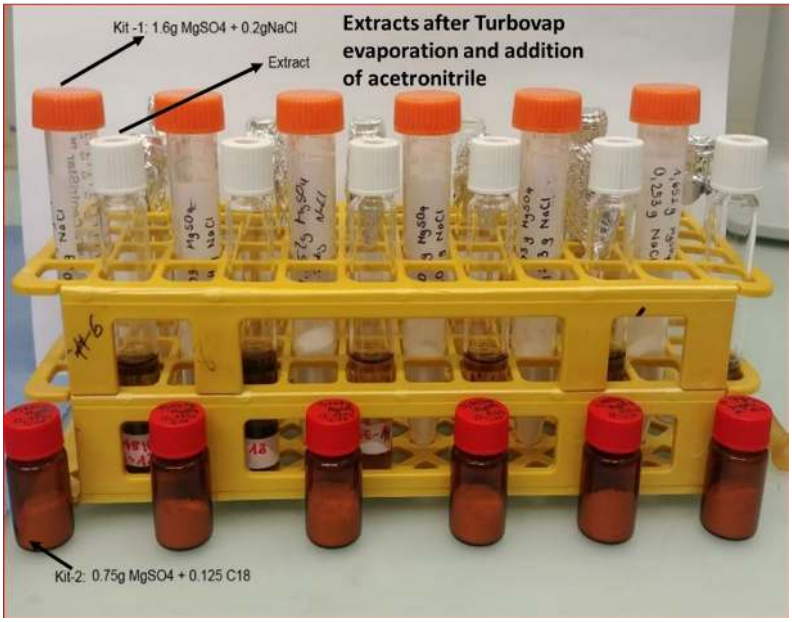

Figure 7. Preparation of kit 1 and kit2 for the clean-up of sediment extracts

Clean-up of extracts by QuEChERS

a. liquid-liquid partitioning (Kit 1)
b. d-SPE (dispersive solid phase extraction) (Kit 2)

Material

Centrifuge
Balance
Weighing pans
Corning tubes
Labco vials (12ml)
Spatula
Funnel (small one from ASE-Accessories)
PTFE syringe filter ø13mm; 0.22µm
1ml plastic syringe
Heater for evaporation
Equipment for Evaporation
HPLC vials and caps
Crimper
Boxes for HPLC vials

Liquid-Liquid-Partitioning

The extract is now further treated to reduce matrix effects that interfere with the identification and quantification of pesticides.

1. Add 4.5 ml MilliQwater to the 5.5ml sediment extract and shake by hand

2. Add the salt mixture **Kit 1** consisting of 1.6g MgSO4 and 0.2gNaCl in 2-3 consecutive portions. Each time a portion is added, shake the solution by hand or with the aid of a shaker.

3. Centrifuge the sample at 1000g for 5min (ACC/DEC=7/7)
   After centrifugation, a clear phase separation can be seen. See setting in Figure 8.
   Note: Because the Labco vials can break, place the Labco vial containing your extract inside a falcon tube for protection as illustrated in Figure 9. In case the vial breaks, collect the extract, centrifuge again in a new vial and proceed with the next step.

Figure 8. *Centrifuge settings for the clean-up of sediment extracts*

Figure 9. Labco vial inside of a Falcon tube use to proetct the glass vial and extract.

4. Transfer the supernatant (yellowish top layer) into a clean Labco vial (**Labco vial 2**) for further work up using a Pasteur pipette . The supernatant is illustrated in Figure 10
   The transferred supernatant contains the pesticides and can now be stored at -20°C if necessary until dSPE

Figure 10. Supernatant (yellowish top layer) from sediment extracts

Dispersive Solid-Phase-Extraction (d-SPE)

1. Kit 2 consisting of 0.75g $MgSO_4$ and 0.125g SelectraSorb Clean-up (C18 irreg; 40-63µm) is now added to the extract as illustrated in Figure 11.

2. Shake the sample by hand or using a shaker.

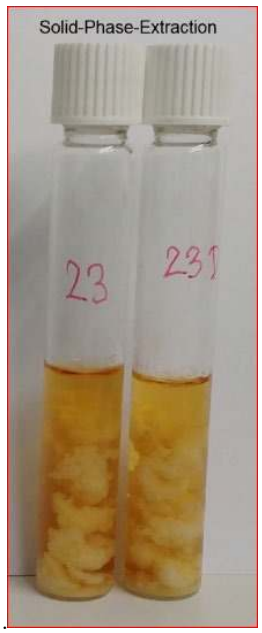

Figure 11. Addition of Kit 2 to sediment extracts for dSPE

3. Centrifuge the sample at 1000g for 5min (ACC/DEC=7/7) as previously described (see Figure 8)

4. Transfer the new supernatant to a new Labco vial (**Labco vial 3**)

5. Wash the dSPE with 4.0 mL of 100% Acetonitrile by shaking the vial. Centrifuge at 1000g for 5 min (ACC/DEC=7/7) as previously described (see Figure 8) and combine the supernatants in Labco vial 3.

6. Store the Labco vials at -20ºC until N_2 evaporation.

4.3 Further evaporation of extracts

Material
Evaporation tray with 10 lines
Metal holders (see Figure 11)
Pasteur pipettes
Nitrogen (N_2) tank
Heating plate
Metal sample rack with 10 holders

1. Prepare the N_2 station with Pasteur pipettes as illustrated in Figure 12.

2. Set heating plate at 45ºC under the N_2 tray

3. Place metal rack on top

4. Open all the lines that will be used as illustrated in Figure 13 and set the N_2 flux. The N_2 flux should have a very slow flow (~ 3 bar pressure). Once the N2 flux is set, closed the N_2 using only valve 3 (see Figure 6)

5. Upload your open extracts and place them under each station. The Pasteur pipettes should be very close to the top of the vial or even inside the vial as illustrated in Figure 12. Make sure there is enough space between the extract and the pipette, otherwise, the extract will spill.

6. Evaporate the final extract under a stream of N_2 to 50µl

7. Rinse during evaporation process 2 times with 70:30 MeOH:H_2O

8. Once the extract has reach ~50µL, reconstitute the extract with 450µl of 70:30 MeOH:H_2O (%v/v). Because it is difficult to measure 50 µL, use a reference vial containing 500µL of µL. **The final volume is very important so please, always use a reference vial!**

9. The final extract is then filtrated through a 0.22µm PTFE filter directly into an amber HPLC vial and capped with a crimper tool.

   Note: Keep an eye on the evaporation process especially at the end it can go very fast.
   Do not evaporate until dryness. If evaporated until dryness, then please record, reconstitute with 500 µL of 70:30 MeOH:H_2O (%v/v) and shake very well using a shaker**.**

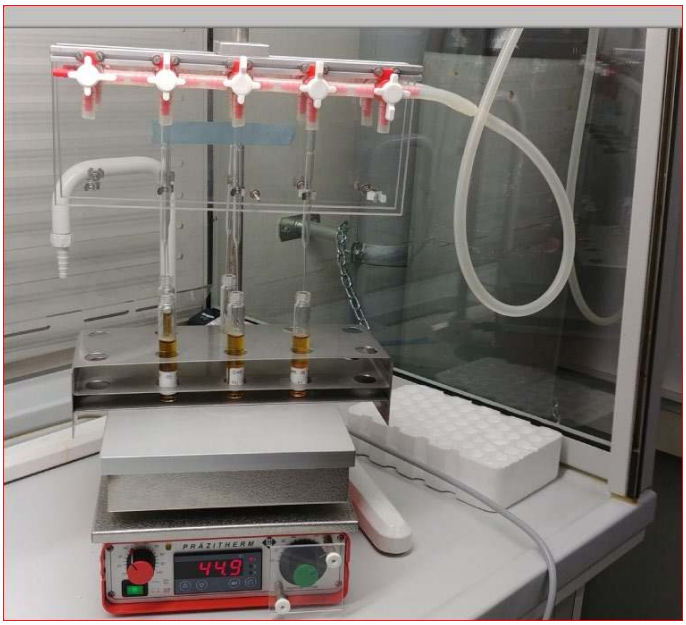

Figure 12. Nitrogen try set up for the evaporation of sediment extract.

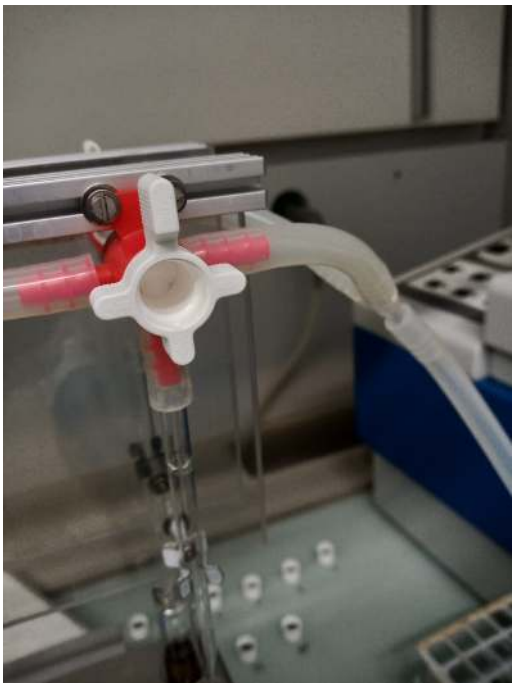

Figure 13. Nitrogen station with open N2 valve

5. Safety

Wear safety goggle, gloves and lab coat at all times when you are working.

Solvent waste need to be disposed in a yellow canister labeled with the corresponding names and proportions of the used solvents

6. Quality control

1. Quality controls are implemented by adding internal standards to the soil/sediment extracts after ASE extraction.

7. Reagents and chemicals

Gas
Nitrogen gas-bottle for evaporation. Please announce in advance to technical staff the number of glass bottle needed for evaporations.

Solvent	**Supplier**	**Prod.-No.**
Acetonitrile HPLC Grade	Fisher Scientific / Chemikalienausgabe	A/0627/17
Methanol HPLC Grade (HiPerSolv)	VWR /Chemikalienausgabe	83638.320
Milli-Q water		

Chemicals	**Formula**	**Supplier**	**Prod.-No.**
Magnesium sulfalte	MgSO4	Brenntag Schweizerhall AG / Chemikalienausgabe	81783-330
Sodium Chlorid Ph.Eur	NaCl	Schweizer Rheinsalinen	7731
SelectraSorb Clean-up; C18 irreg; 40-63µm, 10g	C18 Material	BGB	UCT-CEC1800X

Material	**Supplier**	**Prod.-No.**
TurboVap vials/ 50ml-0.5ml endpoint	Biotage	C 128 508
Labco vials with Septum, soda glas for Kit-2	Labco Lampeter UK	736W
Pasteur Pipettes	Chemikalienausgabe	

Material	**Supplier**	**Prod.-No.**
Corning tubes 15ml	Sigma-Aldrich	CLS430790
Labco vials with Septum, soda glas for Kit-2	Labco Lampeter UK	736W
pasteur pipettes	Chemikalienausgabe	

PTFE Filters; 0.22µm, 13mm; hydrophobic	BGB	SF1304-1
plastic syringes	Chemistry shop	
HPLC vials	BGB	11BW
crimp caps	BGB	11030101
labels		

Solvent	**Supplier**	**Prod.-No.**
Acetonitrile HPLC Grade	Fisher Scientific / Chemikalienausgabe	A/0627/17

8. Comments

About Problems / limitation with the method / modifications done / new sample materials or new application the method was used for. Please give date and name together with your comment:

Appendix G Standard Operation Protocol: Grain-Size Distribution

Grain size analysis*

*updated version by Giulia Wienhues (Dec 2019), original version by Tobias Schneider (Jan 2016)

This very brief manual shall focus on the steps needed in order to measure grain size distribution in lake sediments. It is a summary of older versions of the manual. It is not meant to be 'the' solution. Please read through carefully different literature before starting with the procedure. In case you want combine the analysis of biogenic silica (BSi) with grain size analysis, please check the BSi extraction protocol as well.

The first part summarizes the Sample preparation using chemicals and the second part summarizes the use of the Malvern Mastersizer (Hard- and Software).

(1) Sample preparation

Needed material:

- 12 ml PP-tubes with the double-klick lid (round-bottomed centrifuge tubes)
- Hydrogen peroxide 30% (H_2O_2)
- NaOH-leaching solution
- Dispersion-solution: $(NaPO_3)_6$ + $(Na_2CO_3)_6$
- 100 mg freeze-dried, homogenized (**not ground!!!**) sample material*
- vortex
- water bath and drying oven

* To be most accurate the 'optimal' sample weight can be tested before starting the series

I. Depending on your sediment properties weigh in (or different):
   a. 1 sample 100mg
   b. 1 sample 150mg
   c. 1 sample 200mg

II. Follow the procedure explained below (the same way as we do for the grain size series)

Chemicals:

NaOH
750 ml of NaOH (1.25M): add 37.5 g NaOH into a resistant bottle (PE, PP, avoid glass!) and fill it up to 750 ml with mili-Q water

Dispersion
500 ml of dispersion: add 16.5 g of Sodium-hexametaphosphate $(NaPO_3)_6$ and 3.5 g Sodium Carbonate (Na_2CO_3) fill it up to 500 ml with mili-Q water and use a magnetic steering-tool to homogenize it.

Chemical procedure:

1. Weigh in the right amount of sample material which was determined with the sample test (explained above) into 12 ml- PP-tubes (round bottom)
2. Digest the organic matter using H_2O_2 (30%):
   a. Depending on the organic content of the sample, the H_2O_2 has to be added slowly and carefully. In organic rich samples: put in 0.5 ml of H_2O (mili-Q) and 0.5 ml H_2O_2, and prepare a cooling-bath (in order to slow down the reaction). In samples with little amount of OM, put in 1 ml Peroxide (H_2O_2) directly.
   b. Add more Peroxide (H_2O_2), always carefully observe the reaction (might be delayed ~10-15 mins!) and be ready to cool the samples down)
   c. Heat the samples in the water bath. Until they do not react any longer (=OM removed), this can take few days up to weeks!
3. Wash the samples 3 times in briefly explained order:
   a. Fill up the tubes to the 10ml-mark with mili-Q water
   b. Use the Vortex again to shake them up
   c. Put them into the centrifuge (tare them) at 4500 rpm for ~10 minutes
   d. Decant them to the 2 ml-mark (using the vacuum-water-pump)
   e. Fill the samples up again, use the Vortex and go on with this step for 3 times
4. ONLY IF YOU HAVE TO DO THIS STEP!
   Leach the BSi (you want to remove Diatoms and Chrysophytes from your samples in order to avoid clastic grain size-alteration; if you want to measure the BSi-content, please follow first the BSi- standard protocol, if not follow the following steps a-e):
   a. Add NaOH (1.25M) up to 10 ml
   b. Put the samples into the ultrasonic bath for about 1min
   c. Use the Vortex to shake the sample again
   d. Heat the samples in the oven for about 3 hours at 90°C (the lid in the first-click, loose position)
   e. Centrifuge (4500rpm ~10 min) the sample and decant it to 1ml.
5. If you do not have to do STEP 4: you have to decant the sample down to 1 ml after the last washing!
6. Add the dispersion (Sodium-hexametaphosphate $(NaPO_3)_6$ and Sodium Carbonate (Na_2CO_3)) up to 5ml
7. Use the Vortex (2 to 3 times) in order to shake the sample (repeat this step after 30 minutes again)

(2) Measurement with Malvern Mastersizer

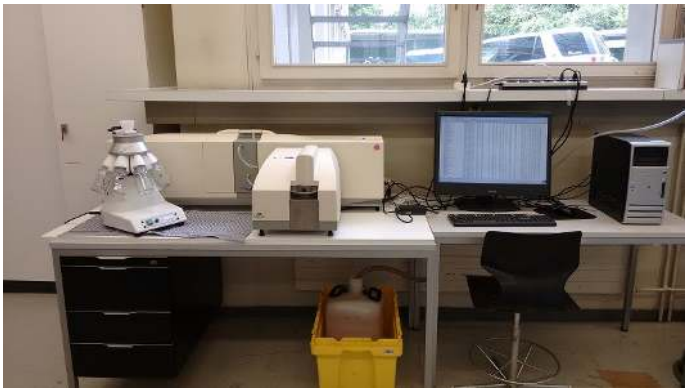

This is a very brief manual to handle the Malvern Mastersizer for the "standard procedure" we do in lake sediments. Follow each step carefully.

0. Have all your samples ready (standard preparation procedure, see the Grain Size Manual).

1. **How to turn on the Mastersizer:** (press 2 buttons: blue light lamp and hydro 2000s), turn on computer and open the Mastersizer 2000 software, then wait for 20-30 minutes until the light has its full intensity and is ready.

2. Always make sure that the water tank on top of the shelf is filled with normal water and the waste water tank (below the Mastersizer table) is not too full (it is easier to empty it when it is not filled to the top).

3. **How to start the measurements:** Measure -> Start SOP -> Choose SOP Unibern -> choose soil_sediments_1. There you can enter your sample name and start the measurement.

4. **How to get the right sample amount:** Wait until the background-signal is measured, when there is the noisy 'peep' appearing, put in the entire sample. Make sure that the blue bar stays in between the optimal boundaries (green area). Add some distilled water in case that the blue bar is reaching over the green area, add more sample when it does not reach the lower limit. Make sure that the input area is clean of sample (wash it in with distilled water).

When to use the sample divider: If your test sample is too concentrated (blue bar is over the green area when you put in the whole sample) you have to use the sample divider and add only a part of it. If you have to split the samples with the sample divider you should make some triplets from time to time to guarantee the quality.

5. **During the measurement:** One measurement takes about 9 minutes. Meanwhile you can get started with cleaning the bottles of the sample divider. When the measurement is

done, the software asks you to run the SOP again. Say yes if you want to make more measurements, say no if you want to finish your measurement series.

6. **How to rinse the Mastersizer after doing measurements:** Go to Configure -> Accessories, then first press 'Clean' (it cleans the tank), then press 'Empty' (it empties the tank).

7. **How to clean the lenses (needs to be done after your series):** Open the part of the Mastersizer where the lens sits. Find the Mastersizer kit on the right side of the room on the bottom. Take out kind of a screwdriver. You can take out the lens with it. Clean both lenses with distilled water and dry them with special towels you find in the Mastersizer kit. Never touch the lenses with your hands and never rub it on the towel when drying (only dab it softly). Put the lenses back into the machine and make another cleaning procedure (Configure -> Accessories -> Clean). Open the lens part again to make sure that nothing spilled out. Empty it.

8. **Switch off** the Mastersizer (blue light lamp and hydro2000s)

9. If you want to export your results: Mark them all, copy and paste them in a new MS Excel file. Do not forget to shut down the computer as well.

Appendix H R Code HCA, Flux Plots and Risk Assessment

PPP Temporal Fluxes, HCA and RQ Analysis

Emmanuel Schaad

2022-04-12

```
# use this line from GIUB PC
#setwd("C:/Users/eschaad/OneDrive - Universitaet Bern/Master Thesis/04 Data/PPPs LCMSMS HRMS ASE")
#  use this line from home
setwd("C:/Users/emman/OneDrive - Universitaet Bern/Master Thesis/04 Data/PPPs Analysis")
library(readxl)
library(reshape2)
library(ggplot2)
library(jcolors)
library(scales)
library(data.table)
```

```
##
## Attache Paket: 'data.table'
```

```
## Die folgenden Objekte sind maskiert von 'package:reshape2':
##
##     dcast, melt
```

```
library(dplyr)
```

```
##
## Attache Paket: 'dplyr'
```

```
## Die folgenden Objekte sind maskiert von 'package:data.table':
##
##     between, first, last
```

```
## Die folgenden Objekte sind maskiert von 'package:stats':
##
##     filter, lag
```

```
## Die folgenden Objekte sind maskiert von 'package:base':
##
##     intersect, setdiff, setequal, union
```

```
load("ppp.fluxes.RData")
load("ppp.RQ.RData")


# unscaled plots sorted by PPP type, Fungicides as example
p.fungicide <- ggplot(subset(ppps, type %in% "Fungicide"),
aes(x=depth.cm, y=flux, colour=name)) +
  geom_line(size=1) +
  geom_point(shape = 18) +
  facet_grid(~ name, scales = "free") +
  labs(x = "Depth [cm]", y = expression(paste("Flux [pg/", cm^2, "yr]"))) +
```

```
  coord_flip() + scale_x_reverse() +
  scale_color_jcolors(palette = "pal12", name = "Compound" ) +
  theme_bw() +
  theme(axis.text.x = element_text(angle = -90, hjust = 1, vjust = 0.5),
        panel.spacing.x  = unit(1, "lines"),
        legend.position = "none")


#Risk Assessment
# RQ Plots
RQ.colors <- c("darkgreen", "green", "gold1", "orange", "red")
rects <- data.frame(ystart = c(0,0.1,1,2,10), yend = c(0.1,1,2,10,200),  col = letters[1:5])

# summing up RQ values by type
setDT(ppps)
RQ.sums <- ppps[, sum(RQ), by = list(depth.cm, age.yr, type)]
names(RQ.sums)[4] <- "RQ.sum"

ggplot(na.omit(RQ.sums), aes(x=depth.cm, y=RQ.sum, colour = type)) +
  annotate("rect", xmin=0, xmax= 60, ymin = 0, ymax = 0.1, alpha = 0.2, fill = "darkgreen") +
  annotate("rect", xmin=0, xmax= 60, ymin = 0.1, ymax = 1, alpha = 0.2, fill = "green") +
  annotate("rect", xmin=0, xmax= 60, ymin = 1, ymax = 2, alpha = 0.2, fill = "yellow") +
  annotate("rect", xmin=0, xmax= 60, ymin = 2, ymax = 10, alpha = 0.2, fill = "orange") +
  annotate("rect", xmin=0, xmax= 60, ymin = 10, ymax = 25, alpha = 0.2, fill = "red") +
  geom_line(size=1) +
  labs(x = "Depth [cm]", y = "RQ Sum", color="Type") +
  theme(axis.text.x = element_text(angle = 0, hjust = 1, vjust = 0.5),
        panel.spacing.x  = unit(1, "lines"),
        legend.position = "right") +
  coord_flip() + scale_x_reverse() +
  theme_bw()
```

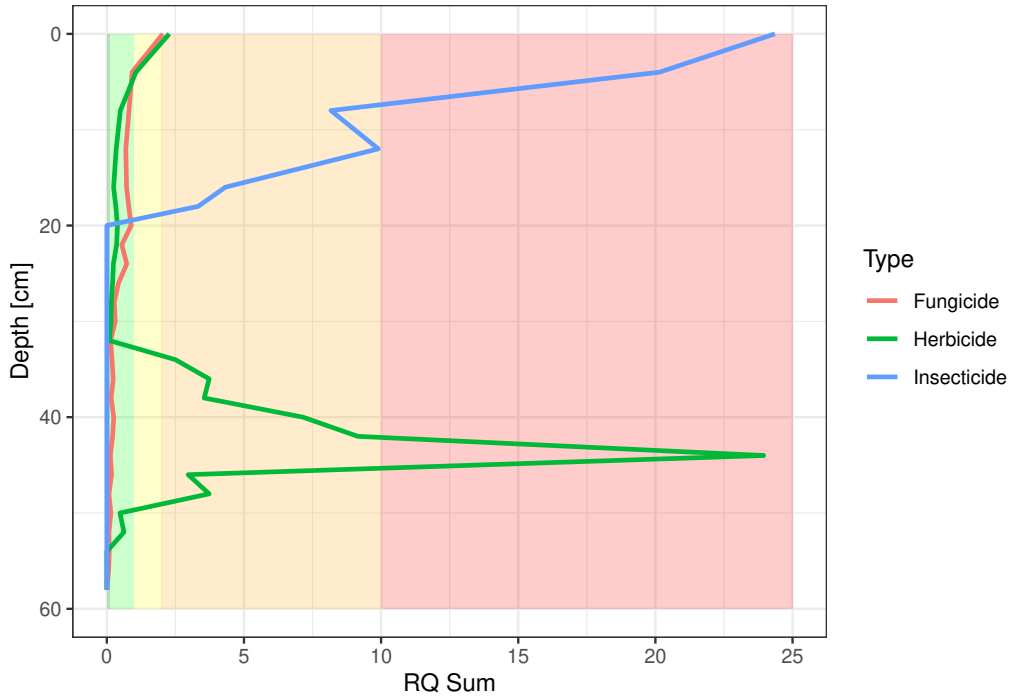


```
#HCA

library(dplyr)
library(data.table)
library(tidyverse)  # data manipulation
```

```
## -- Attaching packages --------------------------------------- tidyverse 1.3.1 --
```

```
## v tibble  3.1.6     v purrr   0.3.4
## v tidyr   1.2.0     v stringr 1.4.0
## v readr   2.1.2     v forcats 0.5.1
```

```
## -- Conflicts ------------------------------------------ tidyverse_conflicts() --
## x dplyr::between()    masks data.table::between()
## x readr::col_factor() masks scales::col_factor()
## x purrr::discard()    masks scales::discard()
## x dplyr::filter()     masks stats::filter()
## x dplyr::first()      masks data.table::first()
## x dplyr::lag()        masks stats::lag()
## x dplyr::last()       masks data.table::last()
## x purrr::transpose()  masks data.table::transpose()
```

```
library(cluster)    # clustering algorithms
library(factoextra) # clustering visualization
```

```
## Welcome! Want to learn more? See two factoextra-related books at https://goo.gl/ve3WBa
```

```
library(gridExtra)
```

```
##
## Attache Paket: 'gridExtra'
```

```
## Das folgende Objekt ist maskiert 'package:dplyr':
##
##     combine
```

```
ppps.norm <- ppps %>%
  group_by(name) %>%
  mutate(flux.norm = (flux - min(flux)) / (max(flux) - min(flux))) %>%
  ungroup()

ppps.scaled <- as.data.frame(scale(importfluxes))
ppps.scaled <- as.data.frame(t(ppps.scaled))
colnames(ppps.scaled) <- rownames(importfluxes)
rownames(ppps.scaled) <- colnames(importfluxes)

dist_mat_euc <- dist(ppps.scaled, method = 'euclidean')
dist_mat_euc <- hclust(dist_mat_euc, method = 'ward.D2')

fviz_nbclust(ppps.scaled, pam, method = "silhouette") + theme_classic() #skeleton plot
```

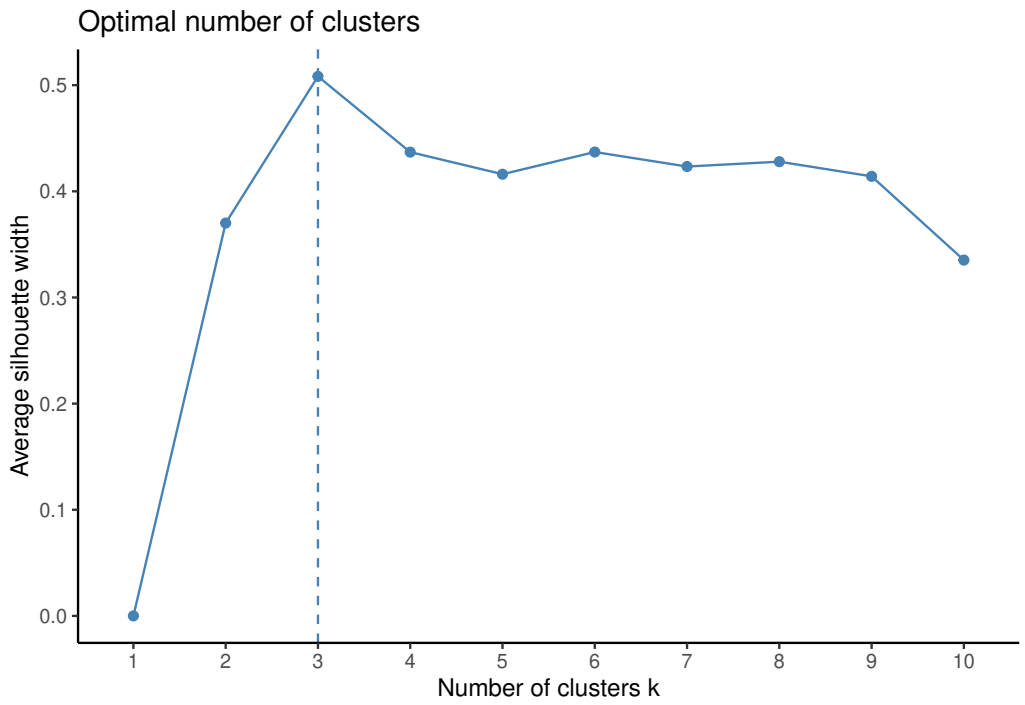


```
sub_grp <- cutree(dist_mat_euc, k = 3)

plot(dist_mat_euc, main = "PPP Cluster Dendrogram", xlab = "Distance Matrix of Compounds") #dendrogram
```

```
rect.hclust(dist_mat_euc, k = 3, border = 2:5) #adding significant cluster
```

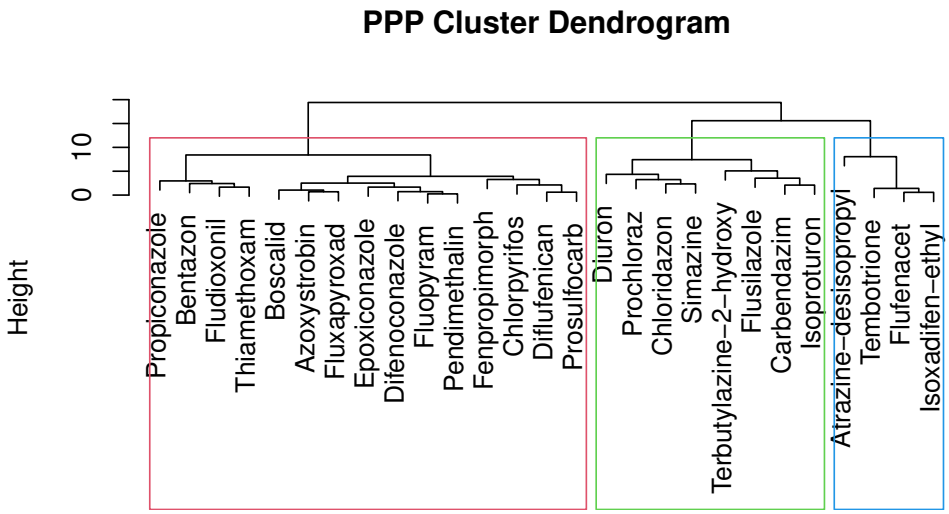


```
fviz_cluster(list(data = ppps.scaled[,1:25], cluster = sub_grp)) #cluster plot
```

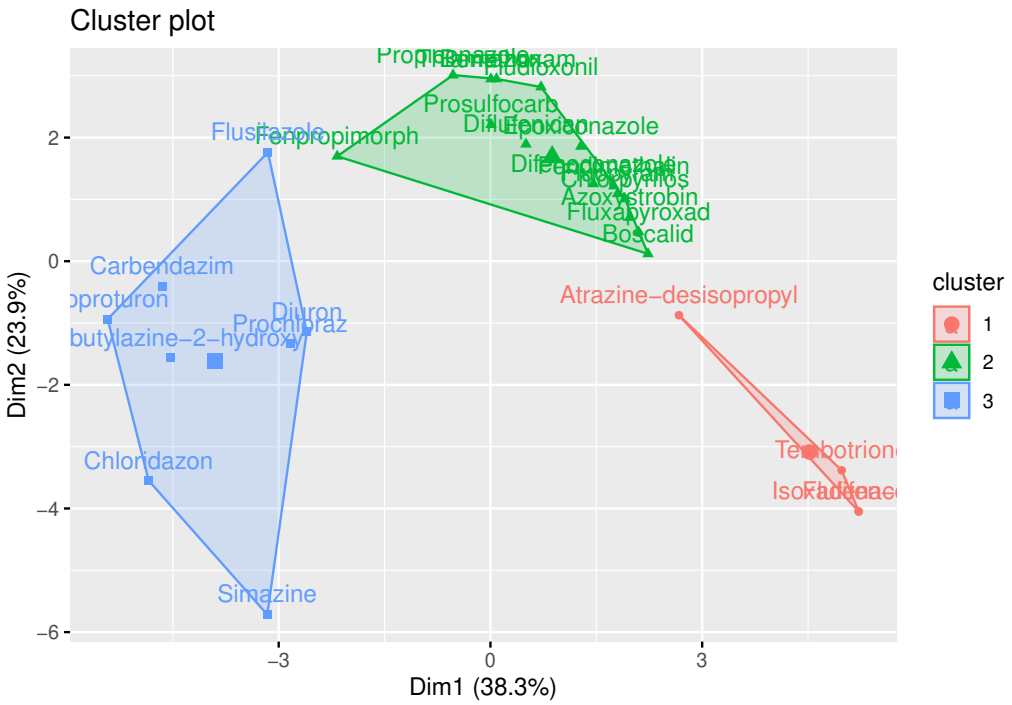
Cluster plot
Fludioxonil
Prosulfocarb
Fenpropimorph
Azoxystrobin
Fluxapyroxad
Boscalid
Carbendazim
Diuron
Atrazine–desisopropyl
Chloridazon
Simazine
Dim2 (23.9%)
Dim1 (38.3%)
2
0
−2
−4
−6
−3
0
3
cluster
1
2
3

Declaration of consent

on the basis of Article 30 of the RSL Phil.-nat. 18

Name/First Name: Schaad Emmanuel Jona

Registration Number: 17-105-388

Study program: Master in Climate Sciences

Bachelor ☐ Master ☑ Dissertation ☐

Title of the thesis: Plant Protection Products in Sediments of a Swiss Pond: Breaking down PPP Contamination in Lobsigensee, Switzerland

Supervisor: Prof. Dr. Aurea C. Chiaia-Hernández R.

I declare herewith that this thesis is my own work and that I have not used any sources other than those stated. I have indicated the adoption of quotations as well as thoughts taken from other authors as such in the thesis. I am aware that the Senate pursuant to Article 36 paragraph 1 litera r of the University Act of 5 September, 1996 is authorized to revoke the title awarded on the basis of this thesis.

For the purposes of evaluation and verification of compliance with the declaration of originality and the regulations governing plagiarism, I hereby grant the University of Bern the right to process my personal data and to perform the acts of use this requires, in particular, to reproduce the written thesis and to store it permanently in a database, and to use said database, or to make said database available, to enable comparison with future theses submitted by others.

Bern, 18.07.2022

Place/Date

Emmanuel Schaad

Signature

Digital signiert von Emmanuel Schaad
DN: C=CH, CN=Emmanuel Schaad, E=emmanuel.schaad@hotmail.ch
Grund: Ich bin der Verfasser dieses Dokuments
Ort: hier den Ort der Signierung ein
Datum: 2022.07.18 17:47:35+02'00'
Foxit PhantomPDF Version: 10.1.1